DOCUMENT RESUME

ED 206 451 SE 035 475

AUTHOR Rogers, Dana B.: And Others
TITLE BIOCONAID System (Bionic Control of Acceleration Induced Dimming). Final Report.
INSTITUTION Dayton Univ., Ohio.
SPONS AGENCY Air Force Human Resources Lab., Brooks AFB, Texas.
REPORT NO AFHRL-TR-81-3
PUB DATE Jul 81
CONTRACT F33615-77-C-0080
NOTE 112p.

EDRS PRICE MF01/PC05 Plus Postage.
DESCRIPTORS *Aerospace Education: *Aircraft Pilots: Military Training: *Physiology: Postsecondary Education: *Simulation: Technical Education: *Vision: Visual Acuity: Visual Impairments
IDENTIFIERS *Flight Simulation

ABSTRACT

The system described represents a new technique for enhancing the fidelity of flight simulators during high acceleration maneuvers. This technique forces the simulator pilot into active participation and energy expenditure similar to the aircraft pilot undergoing actual accelerations. The Bionic Control of Acceleration Induced Dimming (BIOCONAID) System consists of an electromyographic subsystem and software for four physiological models: cardiovascular model, g-suit model, straining model, and visual field model. Experimental results indicate that the system can realistically simulate visual dimming with straining during high accelerations. (Author/WB)

AFHRL-TR-81-3

AIR FORCE HUMAN RESOURCES LABORATORY

BIOCONAID SYSTEM
(BIONIC CONTROL OF ACCELERATION INDUCED DIMMING)

By

Dana B. Rogers
David L. Quam
Jack G. Crouch
Andrew Higgins
School of Engineering
University of Dayton
Dayton, Ohio 45469

OPERATIONS TRAINING DIVISION
Williams Air Force Base, Arizona 85224

July 1981

Final Report

AIR FORCE SYSTEMS COMMAND
BROOKS AIR FORCE BASE, TEXAS 78235

NOTICE

When U.S. Government drawings, specifications, or other data are used for any purpose other than a definitely related Government procurement operation, the Government thereby incurs no responsibility nor any obligation whatsoever, and the fact that the Government may have formulated, furnished, or in any way supplied the said drawings, specifications, or other data is not to be regarded by implication or otherwise, as in any manner licensing the holder or any other person or corporation, or conveying any rights or permission to manufacture, use, or sell any patented invention that may in any way be related thereto

This final report was submitted by the School of Engineering, University of Dayton, Dayton, Ohio 45469, under Contract F33615-77-C-0080, Project 6114, with the Operations Training Division, Air Force Human Resources Laboratory (AFSC), Williams Air Force Base, Arizona 85224. Robert L. Makinney was the Contract Monitor for the Laboratory.

This report has been reviewed by the Office of Public Affairs (PA) and is releasable to the National Technical Information Service (NTIS). At NTIS, it will be available to the general public, including foreign nations.

This technical report has been reviewed and is approved for publication.

MILTON E. WOOD, Technical Director
Operations Training Division

RONALD W. TERRY, Colonel, USAF
Commander

Unclassified

SECURITY CLASSIFICATION OF THIS PAGE (When Data Entered)

REPORT DOCUMENTATION PAGE

READ INSTRUCTIONS BEFORE COMPLETING FORM

1 REPORT NUMBER: AFHRL-TR-81-3	2 GOVT ACCESSION NO
3 RECIPIENT'S CATALOG NUMBER	
4 TITLE (and Subtitle): BIOCONAID SYSTEM (BIONIC CONTROL OF ACCELERATION INDUCED DIMMING)	5 TYPE OF REPORT & PERIOD COVERED: Final
6 PERFORMING ORG REPORT NUMBER	
7 AUTHOR(s): Dana B. Rogers, Jack G. Crouch, David L. Quam, Andrew Higgins	8 CONTRACT OR GRANT NUMBER(s): F33615-77-C-0080
9 PERFORMING ORGANIZATION NAME AND ADDRESS: School of Engineering, University of Dayton, Dayton, Ohio 45469	10 PROGRAM ELEMENT PROJECT, TASK AREA & WORK UNIT NUMBERS: 62205F, 61141909
11 CONTROLLING OFFICE NAME AND ADDRESS: HQ Air Force Human Resources Laboratory (AFSC), Brooks Air Force Base, Texas 78235	12 REPORT DATE: July 1981
	13 NUMBER OF PAGES: 108
14 MONITORING AGENCY NAME & ADDRESS (if different from Controlling Office): Operations Training Division, Air Force Human Resources Laboratory, Williams Air Force Base, Arizona 85224	15 SECURITY CLASS (of this report): Unclassified
	15a DECLASSIFICATION DOWNGRADING SCHEDULE

16 DISTRIBUTION STATEMENT (of this Report)

Approved for public release; distribution unlimited.

17 DISTRIBUTION STATEMENT (of the abstract entered in Block 20, if different from Report)

18 SUPPLEMENTARY NOTES

19 KEY WORDS (Continue on reverse side if necessary and identify by block number)

acceleration induced dimming
biocontrol
electromyographic subsystem
flight simulation
mathematical modelling
psychophysiolical factors
visual scene dimming

20 ABSTRACT (Continue on reverse side if necessary and identify by block number)

The BIOCONAID System represents the development of a new technique for enhancing the fidelity of flight simulators during high acceleration maneuvers. This technique forces the simulator pilot into active participation and energy expenditure similar to the aircraft pilot undergoing actual accelerations. The system consists of an electromyographic (EMG) subsystem and the software implementation of four physiological models: Cardiovascular Model, G-Suit Model, Straining Model, and Visual Field Model. The EMG subsystem is required for signal processing of muscular straining signals used in the Straining Model. The EMG subsystem and all software except the Visual Field Model have been carefully checked-out to yield results consistent with experimental data and known physiology. Consequently, the BIOCONAID System has the potential of providing a very realistic simulation of visual

DD FORM 1 JAN 73 1473 EDITION OF 1 NOV 65 IS OBSOLETE

Unclassified

SECURITY CLASSIFICATION OF THIS PAGE (When Data Entered)

Item 20 (Continued)

dimming with straining during high accelerations. It is recommended that the system be implemented and evaluated in an Air Force simulator with experienced pilots.

SUMMARY

Objective

The objective was an improved system for simulating pilot "grayout" or "blackout" in an aircraft flight simulator

Background

During a coordinated steep turn or pull-up, pilots experience an acceleration that tends to pull them tighter against the aircraft seat This acceleration reduces the blood pressure to the eyes and the pilot may experience grayout or blackout if the turn or pull-up is maintained To counteract the effects of these acceleration forces, the pilot may perform straining maneuvers (M-1 or L-1 maneuvers) to increase the eye-level blood pressure. Such straining represents expenditure of energy that leads to fatigue The "G-suit" is a protective garment that inflates to decrease the pooling of blood in the lower extremities during high-acceleration maneuvers and thereby increases the pilot's tolerance to acceleration.

Some modern flight simulators, which are widely used for combat crew training, provide visual scene dimming as the simulated G-load increases. They may also provide G-suits that realistically react to the G-load. Missing, however, is the pilot's need to perform the beneficial straining maneuver with its attendant energy expenditure. Also missing is the characteristic loss of vision progressing from the peripheral field inward The purpose of the system described in this report is to provide the means to simulate both of these missing elements.

Approach

Four integrated software models and an electro-myographic (EMG) subsystem were developed The software models are as follows

1 The Cardiovascular Model which predicts the effect of G-level on the unprotected pilot's eye-level blood pressure.

2 The G-suit Model which predicts the beneficial effect of the protective garment on the eye-level blood pressure

3 The Straining Model which predicts the beneficial effect of straining on the eye-level blood pressure

4 The Visual Field Model which predicts the visual scene brightness and the limits of the visual field under acceleration

Specifics

The cardiovascular model is a linear second-order transfer function relating dynamic G-loading to eye-level blood pressure response The transfer function coefficients are selected so that the dynamic characteristics approximate available experimental results The cardiovascular model output then represents the eye-level blood pressure of an unprotected pilot under acceleration

The G-suit model uses an actual G-suit worn by the pilot and inflated according to a schedule based on the input G-level The difference between the actual suit pressure and the standard suit fill schedule is used as an input to the model The model then provides full protection if the suit pressure is equal to or greater than that called for by the standard pressure schedule The protection provided drops off linearly if the suit pressure is below standard and when a deficiency of 80 mm Hg exists no protection is provided

The output of the G-suit model is a pressure increment that is added to the unprotected eye-level blood pressure calculated in the cardiovascular model

The straining model provides another pressure increment that is added, along with the G-suit model output, to the predicted eye-level blood pressure. The protection afforded by the M-1/L-1 straining maneuvers is dependent both on the straining level and on the repetition rate of the maneuver. The straining model simulates this situation by providing a protection value that is related to these two factors.

The EMG subsystem senses and processes the electrical signals (from the pilot's skin) that result from M-1/L-1 muscular activity. Either the Latissimus Dorsi (back) or External Oblique (abdomen) muscle sites are suitable for electrode placement. The raw EMG signal is filtered, magnified, rectified, and smoothed for presentation to the digital software.

The visual field model simulates the retinal blood supply and a simple expression is obtained for the retinal limit of vision as a function of eye-level blood pressure. The two eyes are considered together to generate the binocular external field of view for the pilot. Brightness and contrast are also taken to be linearly related to eye level blood pressure so that signals are available to control the projection of field of view and the cockpit lights that the pilot sees.

In the integrated system, the pilot controls the aircraft, thereby generating a G-signal that provides an input to the cardiovascular model and to the G-suit model. The cockpit lights and visual scene dim with predicted decreases in eye-level blood pressure, augmented by the G-suit. When the pilot executes a straining maneuver, he thereby recovers some of the visual loss.

Although the integrated system has not been demonstrated, the software has been carefully checked out and several experiments have been conducted on the EMG subsystem. These experiments have shown that the EMG subsystem provides a smoothed, usable response to straining maneuvers, not corrupted by physical motions.

Conclusions/Recommendations

This study demonstrates the feasibility of an improved system for simulating pilot grayout and blackout in flight simulators. It is recommended that the proposed integrated system be developed and evaluated in an Air Force simulator with experienced pilots.

PREFACE

The BIOCONAID System was developed by the University of Dayton under Contract No. F33615-77-C-0080 from the Air Force Human Resources Laboratory, Brooks AFB, Texas 78235. Dr. Dana B. Rogers, the original Principal Investigator, addressed this problem in his doctoral dissertation which was partially supported under the contract. This support is gratefully acknowledged. This dissertation (Rogers, 1978) is the fundamental reference for the development of the various models.

TABLE OF CONTENTS

TABLE OF CONTENTS (continued)

LIST OF FIGURES

LIST OF FIGURES (continued)

LIST OF FIGURES (continued)

LIST OF TABLES

LIST OF SYMBOLS

a_1	a constant in cardiovascular model transfer function, P(s)
b_1, b_2	constants in cardiovascular model transfer function, P(s)
d	degrees offset of the optical disc from the horizontal axis (Figure 2.11)
EMG	electromyographic signal taken from skin surface
G(t) or G_z	usually dynamic acceleration loading (z-directed). Z-component of lift and thrust forces divided by the weight of the aircraft minus one. Positive upward. Sometimes total acceleration.
G(s)	Laplace transform of G(t)
K_1	cardiovascular model gain constant
$K_2(t_R)$	function which modifies straining protection value according to repetition rate
K_4	outer circulation limit of the retina corresponding to the ora serratta
ℓ	length of tube simulating blood vessel
n	set point variation (to account for pilot variations)
PV	simulated eye level blood pressure under acceleration
PV_c	protection value output from cardiovascular model
PV_G	protection value output from protective garment model
PV_s	protection value output from straining model
PV_m	maximum value multiplier in straining protection value
P(s)	linear transfer function relating $PV_c(s)$ to G(s)
P_R	effective retinal artery pressure differential
P_{ae}	eye level supply pressure
P_{IO}	interocular pressure differential required for eyeball rigidity (10-20 mm Hg)

$P_r(x)$	retinal pressure differential at x degrees from optic disc
P_{CRIT}	transmural pressure differential in retina
P1, P2	levels of eye-level blood pressure
Q	blood flow, kg/sec
r	degrees visual limit measured from optical axis (Figure 2.11)
r	radius of tube simulating blood vessel, meters
r_d	degrees offset of optical disc from optical axis (Figure 2.11)
s	the Laplace variable
t_R	repetition period of M-1 or L-1 maneuver
T_1, T_2	filter time constants, sec
x	Appendix D, dynamic G-level
x	Figure 2.14 dummy variable used in wiring diagram
x	distance in degrees along arteriolar bed in retina
x_L	visual limit in degrees measured from optic disc
x	axis forward
y	Appendix D, output, PV_c, of cardiovascular model
y	axis to the right
y	Figure 2.14, dummy variable used in wiring diagram
z	axis downward
z	Figure 2.14, smoothed EMG signal

Greek Symbols

θ	seat-back angle, degrees
ΔP_G	suit pressure minus standard curve pressure, mm of Hg

σ	EMG standard deviation
ΔP	pressure differential in tube of length ℓ, N/m^2
Ψ	degrees of angular position measured counterclockwise about the optical axis (Figures 2.11 and 2.12)
η	kinematic coefficient of viscosity, m^2/sec

SECTION 1

INTRODUCTION

This report presents the development of a new technique for enhancing the fidelity of flight simulators. The name given to the technique and to the system which applies the technique is BIOCONAID, an acronym for Bionic Control of Acceleration Induced Dimming.

When an aircraft is subjected to a change in its velocity vector an acceleration is experienced by the occupants. The common situation is that of a pilot changing the direction of motion of the aircraft through a steep turn or pull-up. Then, if the maneuver is coordinated, the pilot experiences an acceleration tending to pull him tighter against his seat as if he weighed more. This acceleration also affects the blood pressure distribution in his body. The blood pressure supplying the eyes and the brain is reduced and the pilot may experience gray-out or black-out if the turn is continued or the pull-up becomes steeper.

In a combat situation, the pilot needs to continue the turn or pull-up and retain his vision. He may perform straining maneuvers (described in Appendix C) to increase the eye-level blood pressure and fight the black-out tendency. Such straining represents expenditure of energy which leads to fatigue. The "G-suit" is a protective garment which exerts pressure on the lower extremities, thereby restricting the pooling of blood to the lower extremities during high-acceleration maneuvers. Pilots of high performance aircraft wear this garment to increase their tolerance to acceleration.

Modern flight simulators, which are widely used for combat crew training, provide visual scene dimming as the simulated G-load increases. Also provided are G-suits which realistically react to the G-load. Missing, however, is the pilot's need to perform the beneficial straining maneuver with its attendant energy expenditure. Also missing is the characteristic

loss of vision progressing from the peripheral field inward. The BIOCONAID System provides the means to simulate both of these missing elements.

The BIOCONAID System consists of four integrated software models plus hardware which senses and processes pilot straining information for input to the computer. The computer software models are:

- Cardiovascular Model (predicts effect of G-level on eye-level blood pressure)
- G-suit Model (predicts beneficial effect of G-suit at the input G-level)
- Straining Model (predicts the beneficial effect of straining)
- Visual Field Model (predicts the visual scene brightness and the limits of the visual field under acceleration)

The complete system also includes an electromyographic (EMG) subsystem (signal processor).

Section 2 of this report includes a discussion of the development of each of the models mentioned above plus the EMG Subsystem (EMG straining signal). Also treated is the integration of the entire system. Sections 3 and 4 cover development and documentation of the algorithms and straining experiments.

Section 5 gives conclusions and recommendations. Briefly, the BIOCONAID System performs as planned. A usable, smoothed EMG signal is produced by pilot straining. Either the abdomen (external oblique) or the back (latissimus dorsi) muscles are suitable as electrode sites. Neither extraneous motions nor electronic noise seems to affect the system adversely. All software algorithms perform satisfactorily. Full implementation of the Visual Field Model was not accomplished during the contract period due to equipment limitations.

Because possible detrimental cardiovascular effects of sustained straining in a 1-G environment may exist, it is recommended that some

medical research be conducted to identify system limitations or restrictions. It is also recommended that the BIOCONAID System, with possible limitations or restrictions, be evaluated in an Air Force simulator with experienced pilots.

Appendix A gives a test plan for system evaluation which might be accomplished in the F-4 simulator at Luke Air Force Base. Appendix B gives a complete listing of the computer programs developed during this effort. Appendix C gives a discussion of the M-1/L-1 straining maneuvers and Appendix D describes the special Tustin solution method used for the cardiovascular model.

SECTION 2

THEORY

The human organism is a highly complex system of interconnecting and interdependent systems. Its responses, in general, must be considered non-linear and extremely difficult to model. However, by restricting the number and levels of variables in a specific situation, it is often possible to model complex systems successfully.

The purpose here is real-time modelling of the human response to G-loading. To simplify the problem, it is assumed that only z-directed (normal) acceleration will be considered and that the only variables influencing acceleration are G-level, G-suit protection, and pilot straining. The complex human system can then be partitioned into four tractable models: the cardiovascular model, the protective garment model, the straining model and the visual scene model. The relationship between these models is shown in Figure 1. The result of each of these blocks is a contribution to the pseudo blood pressure variable called "protection variable" (PV). In all cases, the contribution to this blood pressure variable is either derived directly from the acceleration profile or is a secondary result of that profile and the operation of life support equipment. Note that a set-point value (one-G blood pressure at eye level) is summed with the PV values (see Figure 1). A normally distributed random variation, labeled "n" is also included to account for variations with pilots on different days.

The cardiovascular response model is represented by a linear transfer function which corresponds to the acceleration response of the pilot's blood pressure. One prime governing factor in pilot response to acceleration is the onset of grayout and blackout. These visual problems are directly related to the blood pressure at eye level. This model output provides a dynamically correct signal which is equivalent to the nominal loss in eye level blood pressure for an unprotected human undergoing any acceleration profile, G(t).

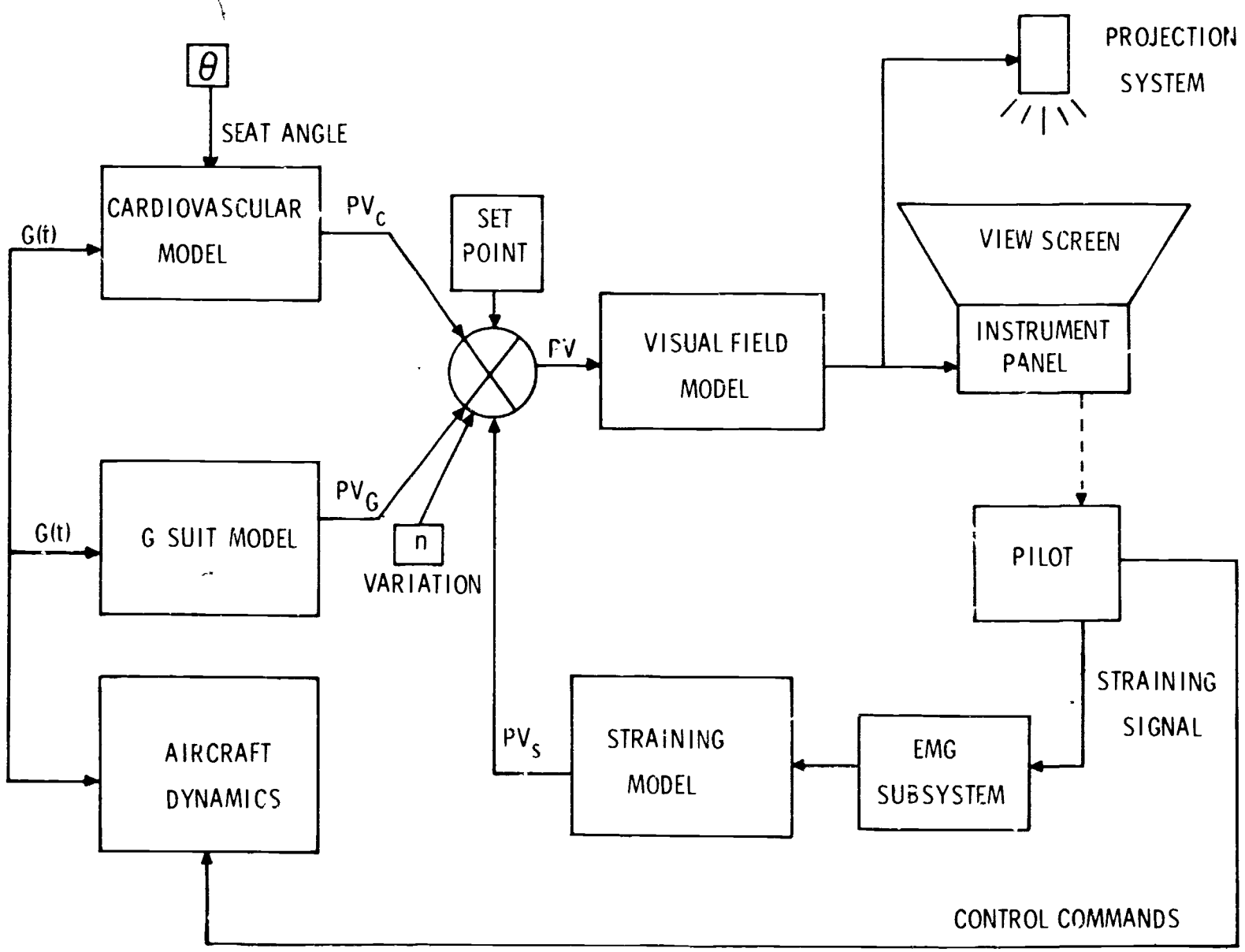

Figure 1. System Design Plan

The straining simulation model accounts for the G tolerance enhancement which is afforded by a properly executed M-1 or L-1 straining maneuver. The purpose of these straining maneuvers is to increase the eye level blood pressure in order to maintain vision. Proper performance of the maneuvers requires that the abdominal and upper torso muscles be tensed isometrically and that expirations should be made against a closed glottis. The result is an increased intrathoracic pressure and increased blood pressure at the eye. Proper application of the straining maneuvers also results in the appearance of myoelectric signals on the skin surface. These low voltage electric signals are directly associated with muscle contraction (Bigland and Lippold, 1954; Brody, Scott, and Balasubiramanian, 1974). These biologically derived signals are then processed by the model to generate a straining contribution to the protection variable, PV_s, which represents the increased blood pressure due to the M-1 or L-1 maneuver.

The pressurized G suit is a protective garment used to increase the individual's tolerance to $+G_z$. The suit uses pressurized bladders to press against the legs and lower abdomen. The external pressure inhibits pooling of the blood volume in the lower extremities, thus insuring a better supply to the heart during acceleration. The suit must be inflated by the G valve to a predetermined level for the suit to be effective. The simulation model accounts for the required pressure level and uses the actual suit to provide the necessary dynamics. The suit pressure is compared with the normal flight pressure schedule and a protection variable contribution is generated by the model.

The dynamic visual field model was developed to be readily implemented in a simulation system. The visual field model uses the eye level blood pressure predicted from the simulated G profile and the other protection variable contributions as inputs to produce dynamically responsive signals which predict the expected visual field of a pilot undergoing that G profile.

The system presented on the following pages represents the results of partitioning this complex physiological system into models. Each

model is explored and developed in detail based on a common protection variable, PV, which is related physiologically to system blood pressure. The blood pressure models are then finally combined in a systematic paradigm which provides the driving values for the visual field response model.

2.1 THE CARDIOVASCULAR RESPONSE MODEL

Human tolerance to long term $+G_z$ acceleration is normally measured in terms of visual loss (blackout) and unconsciousness. Both of these tolerance end points are related to the ability of the cardiovascular system to deliver oxygenated blood at adequate pressure to the retinal and cerebral regions. The acceleration causes a changing blood pressure profile in the human such that the effective pressure vertically above heart level is decreased and the pressure below heart level is increased. There is therefore a lower perfusion pressure at eye level. The distribution of the blood in the body also changes as the acceleration pools blood in the lower parts of the body and lungs. There is therefore less available blood to circulate and a lower oxygen content because the lungs do not operate as efficiently.

There are two cardiovascular systems which are dynamically involved in the process of blood pressure maintenance while the human is undergoing $+G_z$ acceleration. The hydrostatic system is responsible for the reduced retinal perfusion pressure at the eye and eventual loss of pressure at the cerebral level. The orthostatic system is related to blood pooling in the lower body with a concomitant reduction of venous return to the heart.

The cardiovascular system has feedback systems which are affected by blood volume and pressure. The feedback systems attempt to regulate the pressure and flow characteristics of the cardiovascular system. One of the primary pressure sensors for this system is located in the carotid artery. Any change in pressure at the sensors results in a regulatory operation which attempts to return the pressure to a preset value. For

example, a pressure drop at the carotid sinus initiates a neurologic reflex action which changes the heart rate and output so as to increase the overall pressure level. This section develops the rationale for a cardiovascular transfer function model which describes the G_z acceleration response of the blood pressure delivery system.

A radically new model for the cardiovascular system was not the intent of this system. Rather a reasonably accurate transfer function based on physiological and physical principles as well as experimental observation was sought. The major requirements were that the transfer function model retain the major response characteristics of the cardiovascular system, be implementable in a real time digital simulation system, and retain factors which are identifiable with measurable physiological factors.

A number of models of the cardiovascular system have been developed (Gillingham, Freeman, and McNee, 1972; Knapp, Randall, Evans and Marquis, 1978; Koushanpour and Spickler, 1975; and Miller and Green, 1973). The model developed by Gillingham (Gillingham, et al., 1972) is used in the present effort. This linear model uses a transfer function of the form:

$$P(s) = \frac{K_1(1 + a_1 s)}{1 + b_1 s + b_2 s^2} = \frac{PV_c(s)}{G(s)} \qquad (1)$$

Values selected for a_1, b_1 and b_2 are compromise values from the literature and Gillingham's response curves. The break frequency for the lead compensator factor, $(1 + a_1 s)$, was selected at 30 mHz (millihertz). The denominator factor $(1 + b_1 s + b_2 s^2)$ was selected to give complex roots with a natural frequency of 70 mHz and a damping ratio of 0.7. These characteristics result in time responses and Bode plots which agree reasonably well with experimental measurements. To obtain these characteristics we find that $a_1 = 5.31$, $b_1 = 3.23$ and $b_2 = 5.17$.

In order to evaluate the system gain constant, K_1, Rogers, 1978, treated the artery from the aortic arch to the eye as a column of blood under the hydrostatic action of the G-loading. This column is offset from the Z-axis by an angular displacement of θ degrees due to the angular inclination of the pilot's seat. The system gain determined in this way $K_1 = -21.4$, compares very closely with the gain derived from experimental blackout results (Burton, Leverett and Michaelson, 1974). When the seat inclination is included, K_1 becomes $-21.4 \cos \theta$. The final transfer function is shown in Figure 2. (Note that G(t) here is dynamic G-loading = $G_z - 1.$) The solution technique used for generating PV_c from G(t) is described in Appendix D.

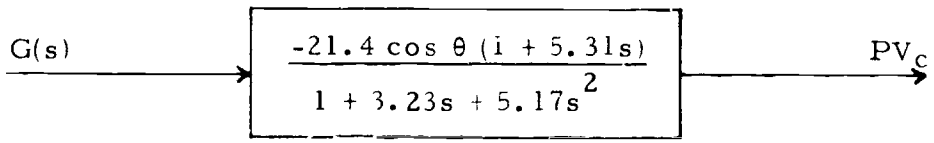

Figure 2. Block Diagram of Cardiovascular System Response

2.2 THE PROTECTIVE GARMENT MODEL (G-SUIT MODEL)

The history of G-suits dates from World War II and has been well reviewed in recent monographs (Burton, et al., 1974; Fraser, 1966; Gaur and Zuidema, 1961; and Howard, 1965). The wrap-around CSU-3/P cutaway-type of anti-G suit, presently used by the U.S. Air Force, improves blackout tolerance in the $+G_z$ direction by about 2G above resting tolerance (Leverett, Whitney and Zuidema, 1961). However, the mechanism by which this beneficial effect takes place is not entirely understood. Investigations have shown that the protection afforded by the suit is not associated with any increase in cardiac output (Lindberg and Wood, 1963) nor with any increase in eye-level blood pressure (McCally, 1970). The G-suit attempts to prevent pooling of the blood in the lower extremities of the body during plus-G maneuvers (Leverett,

et al., 1961). Thus, it is not possible to model the physiological system dynamics pertaining to the G-suit until more knowledge is gained about the system.

The approach taken in the present research effort is to use an actual valve plus a G-suit on the pilot to provide the suit dynamics and to model only the known beneficial effect -- the 2G improvement in blackout tolerance with a properly operating suit. The valve will be activated by the computer-generated G signals.

The normal suit pressure versus G-loading schedule is shown in Figure 3. If the actual suit pressure, at a given G-level, falls in the cross-hatched area labeled "Acceptable Region", then partial protection is being provided. Full 2G protection is afforded when the suit pressure reaches the right-hand edge of the "Acceptable Region". At higher suit pressures no additional protection is provided and at suit pressures to the left of the "Acceptable Region" no protection is provided.

A linear variation of protection within the acceptable region is assumed which has a width of approximately 80 mm Hg. The simulation procedure is to obtain the difference between the actual suit pressure and the standard curve pressure (right hand edge of acceptable region, Figure 3). This difference is labeled ΔP_G. Then the protective garment protection value contribution is generated as follows:

$$\text{if } \Delta P_G < -80 \quad \text{then } PV_G = 0 \tag{2}$$

$$\text{if } -80 \leq \Delta P_G < 0 \quad \text{then} \quad PV_G = \left(\frac{42.8}{80.}\right) \Delta P_G + 42.8 \tag{3}$$

$$\text{if } 0 \leq \Delta P_G \quad \text{then} \quad PV_G = 42.8 \text{ mm Hg} \tag{4}$$

Note that 42.8 mm of Hg is equivalent to 2G protection since the cardiovascular system gain is -21.4. The simulation model is presented in block diagram form in Figure 4.

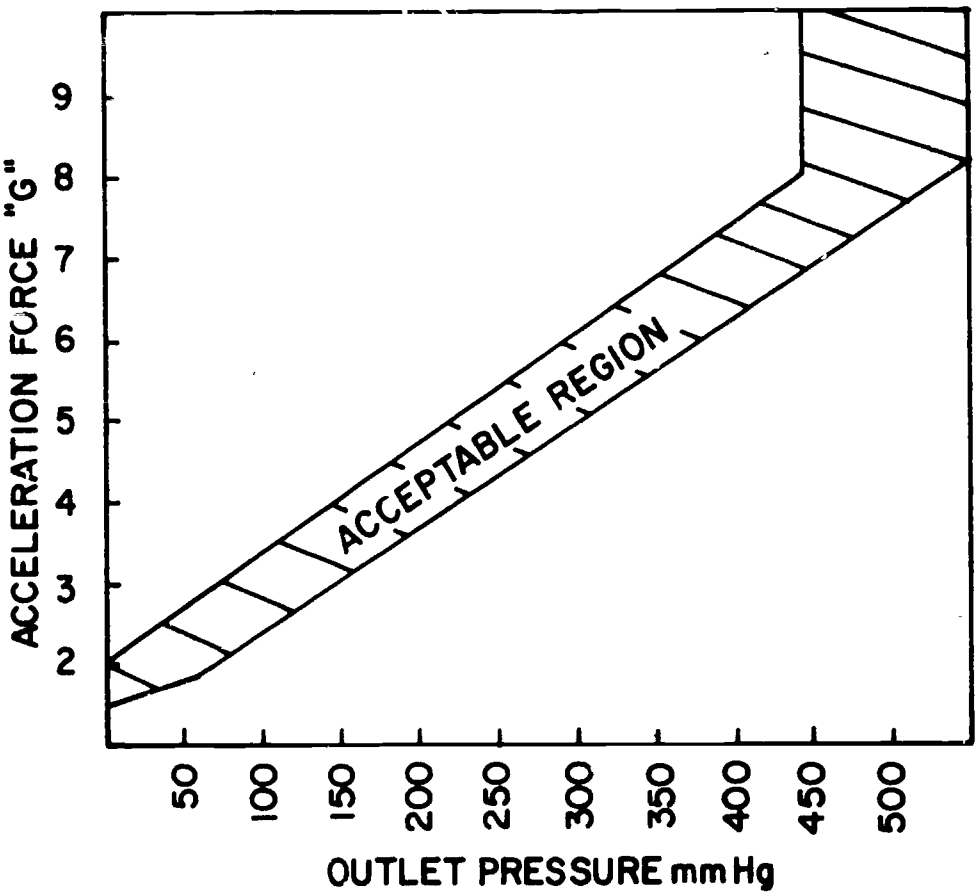

Figure 3. Standard Pressure Suit-Valve Fill Schedule

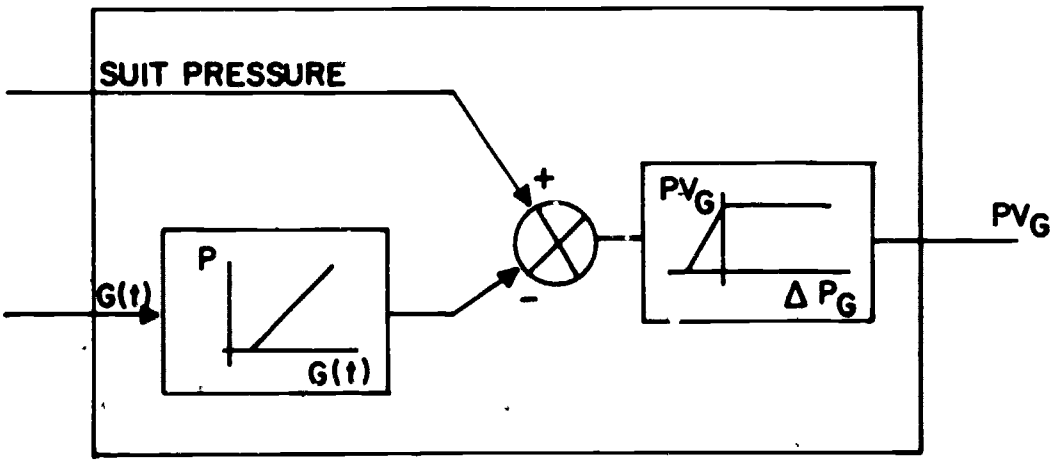

Figure 4. G-Suit Model for Generation of Protection Value PV_G

2.3 THE STRAINING MODEL

Human tolerance of acceleration may be improved by the use of protective measures and devices. Straining and grunting in tight turns was practiced by German pilots prior to World War II to improve their tolerance. This technique gradually evolved into the M-1 maneuver. At the same time it was discovered that bending forward also improved the tolerance of pilots in high acceleration maneuvers. The effects of posture, restraint, and body position on G tolerance have been well worked out and have been reviewed in detail (Davson, 1969; Fraser, 1966; and Gaur and Zuidema, 1961).

Since the early days of flying, the value of muscular straining as protection against the effects of $+G_z$ acceleration has been recognized. Pilots observed that blackout or grayout could be postponed if they grunted or screamed and tensed the skeletal musculature during acceleration. The M-1 maneuver, defined as muscular straining with expiration against a partially closed glottis (see Appendix C) is a most effective voluntary protection against the circulatory effects of $+G_z$ acceleration (Lindberg, Sutterer Sutterer, Marshall, Headley, and Wood, 1960; White, 1958). The physiological basis for this protection has been ascribed to its effect on increasing the arterial pressure at eye level during acceleration. As forced expiration is instituted the resulting increase in intrathoracic pressure is transmitted directly to the aorta. There is an immediate increase in peripheral arterial pressure which is only slightly less than the increase in intrathoracic pressure. This maneuver affords up to 2.4 G protection against blackout (Burton, et al., 1974). The circulatory mechanisms described were identified by Rushmer in 1946. The "pressure raising" approach has theoretical difficulties in that blood pressure is controlled within rather narrow limits by a number of effective servomechanisms, the baroreceptor system being the best known. As a matter of course the elevated intrathoracic pressure can result in a decreased venous return, lowered cardiac output and therefore a lower blood

pressure at the eye. The carotid sinus reacts to the initially increased blood pressure and also attempts regulation. Both of these effects are minimized by a cyclic application of the M-1 or L-1 procedure with a repetition period of 4-5 seconds.

The skeletal muscle is controlled by signals which are transmitted to selected motor units of a muscle through the motor neurons. The force generated by the muscle is the result of both the frequency of firing of motor units and the number of motor units which are recruited. The muscle tension is accompanied by electrical signals (EMG) which can be detected by suitable electrodes on the skin surface. The electrical signal exhibits the characteristics of its primary source in that it represents a weighted sum of motor unit activations (Shannon, 1975). There is therefore a correspondence between the EMG and muscle force (Bigland and Lippold 1954).

The EMG signal can be considered to be the summation of a large number of individual potential waveforms each resulting from the firing of a motor unit. Thus we can assume that the EMG signal is Gaussian with a mean of zero. If such a signal is the input to a full wave rectifier, it has been shown (Davenport and Root, 1958) that the mean output is proportional to the standard deviation of the input. Furthermore, the standard deviation has been shown (Shannon, 1975) to be the appropriate measure of the EMG signal to use for control purposes. This reasoning leads to selection of the rectified, smoothed EMG signal for determining a straining protection value.

The simulator model requires the presence of two signals to generate the straining protection value, PV_s. The two signals represent the prime factors which are present in a properly executed straining maneuver. The EMG signal is generated by the straining subject and processed to provide an intermediate protection value PV_m. The protection afforded by muscle straining is then modified by the effects of the breathing maneuver (M-1). The protection factor generated by the breathing pattern is critically

controlled by the straining and breathing rate. An improperly performed M-1 can actually reduce protection and result in a detrimental pressure drop.

We assume the thoracic cavity to be represented by a flexible cylinder surrounded by a muscle girdle. The muscle straining signal representing muscle force around the thoracic volume is then assumed to bear a linear relation to the internal pressure increase at low straining levels. At higher levels a maximum pressure is achieved and increases in muscle straining are no longer effective. The pressure straining relationship used in the model is shown in Figure 5 as a curve with a saturation level related to the maximum pressure rise in the thoracic cavity.

The effectiveness of the straining maneuver is also governed by the repetition rate. The straining protection value PV_m is therefore modified by a function dependent upon maneuver repetition period $K_2(t_R)$. Experimentally, $K_2(t_R)$ is maximum at 3-5 seconds according to Gillingham

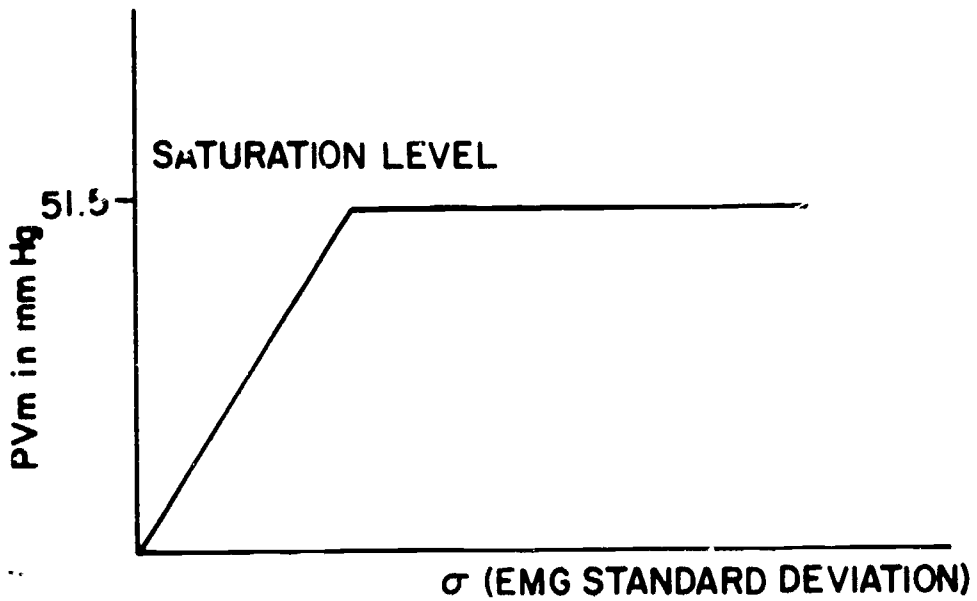

Figure 5. Pressure-Straining Relationship Based on EMG Statistical Properties

(Appendix C). Shorter time periods do not allow sufficient time for the internal pressure to rise and longer time periods involve countering responses due to baroreceptor feedback and reduced venous return to the heart. The function representing the variation of K_2 with maneuver repetition rates is shown in Figure 6. The straining simulation block diagram is shown in Figure 7.

2.4 THE VISUAL FIELD MODEL

Rogers, 1978 discusses the structure and functioning of the eye as it forms the basis for a usable model of the visual field under acceleration. The effect that acceleration has on the visual apparatus is observed in terms of tunnel vision, greyout and blackout. During the periods of grayout there are also decreases in visual acuity and brightness contrast detection ability. Tunnel vision means that loss of visual perception occurs first in the peripheral areas of the visual field and progresses inward. Although there are many factors related to the anatomy, psychology and physiology of the human which are responsible for these effects, the structure of the eye is a primary factor, and it provides a suitable model for the effects of acceleration on the visual field.

The primary cause of the effects of accelerationoon vision is believed to be the reduction of blood supply to the rods, cones and cells in the retinal layers. This has been confirmed by various investigators (Lewis and Duane, 1956; Newsom, Leverett and Kirkland, 1968). The eye is supplied by the opthalmic artery which has two branches in the eye itself. One branch, the retinal artery, enters the eye through the optic nerve and provides the primary source of blood to the retinal layers. The other branch, the ciliary artery, supplies the outer layers of the eye and the ciliary processes. Figure 8 shows the retinal artery entering through the optic disc and branching out to supply the entire retina.

The structure at the retina is idealized as a network of cylindrical hydraulic pipes with a central supply at the entrance of the optic nerve,

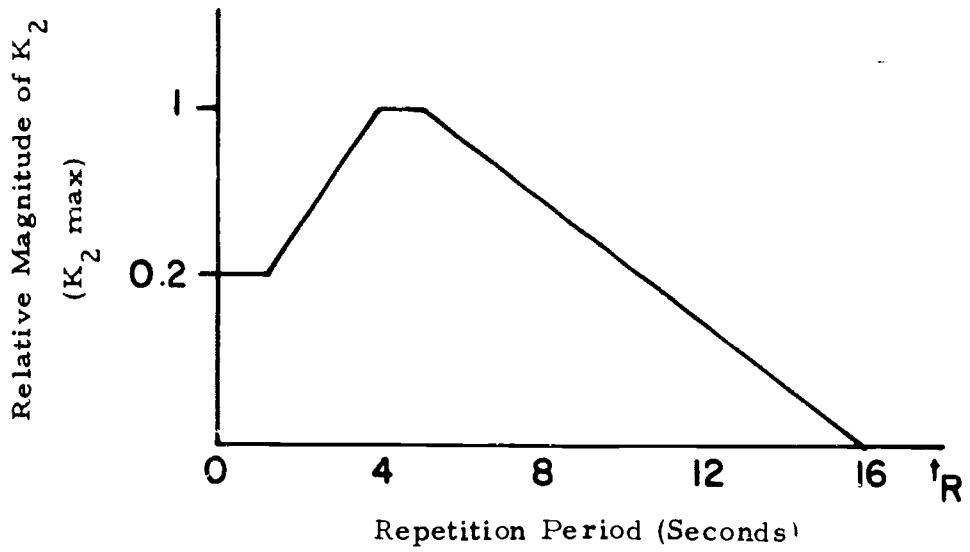

Figure 6. Effect of Repetition Period on Straining Protection Values

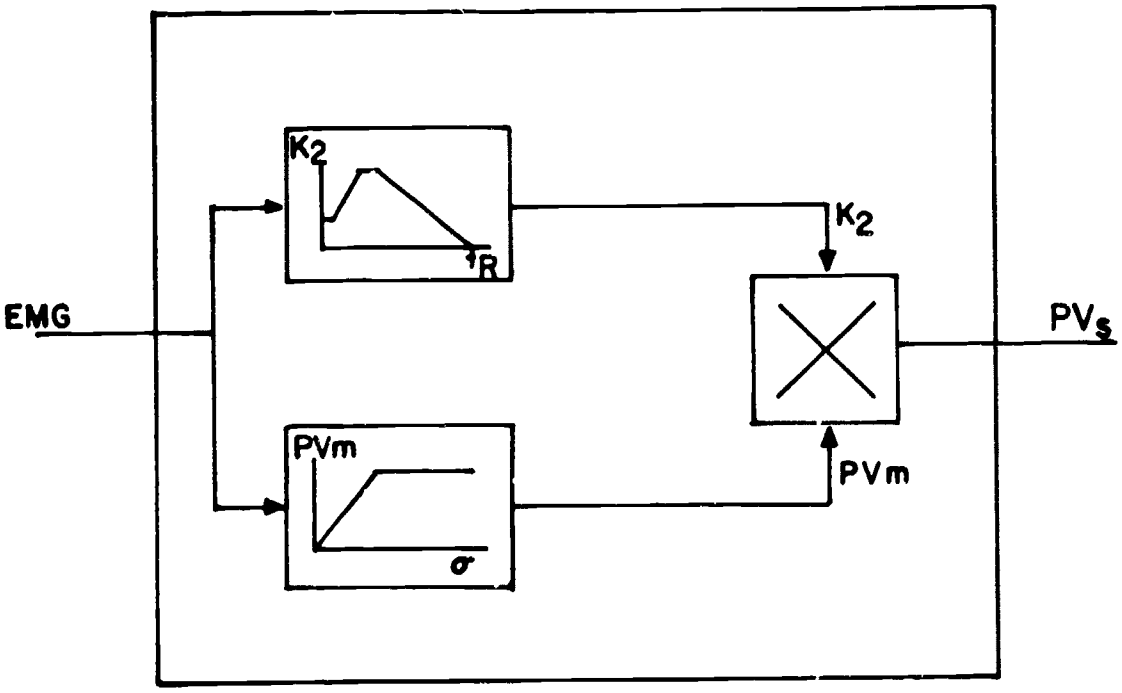

Figure 7. Straining Model for Generation of Protection Value (PV_s)

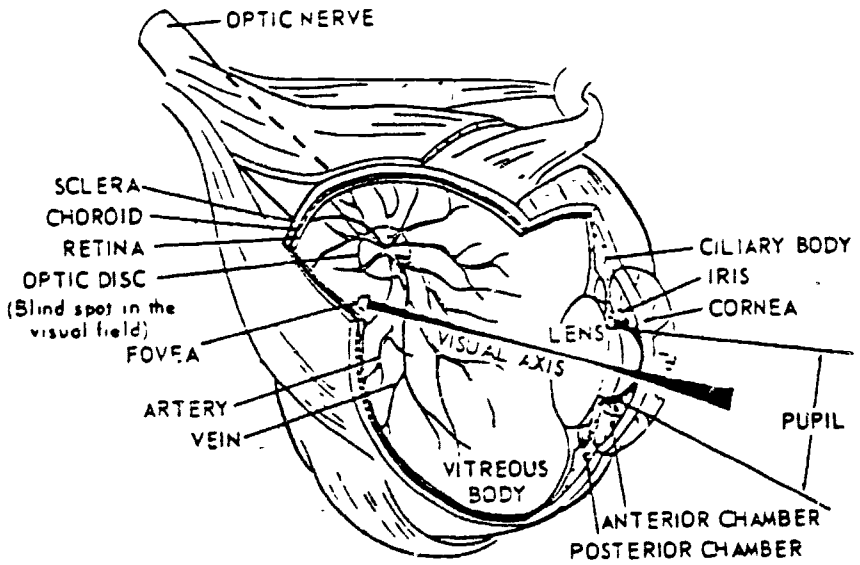

Figure 8. Topography of the Eyeball
from W. J. White in Reference 26

Figure 9. If a steady laminar flow is assumed through a cylindrical tube the flow, Q, will vary with the 4th power of the radius of the tube and the pressure differential ΔP. Also the flow will vary inversely as the length ℓ of the tube and the kinematic viscosity of the fluid η. This is stated in Poiseuille's law as:

$$Q = \frac{\pi r^4 (\Delta P)}{8 \eta \ell} \qquad (5)$$

The blood pressure drop across the cardiovascular system is mostly across the arterioles (Berne and Levy, 1972). At higher levels of pressure the retinal arteries supply the arterioles with sufficient pressure that the entire retina is perfused with a continuous flow of freshly oxygenated blood. As the pressure at the retinal artery drops, the flow must decrease in accordance with Poiseuille's Law, and less blood, therefore less oxygen, is available to replenish the retina.

The effective pressure (P_R) in the retinal artery is the difference between supply pressure P_{ae} and the interocular pressure P_{IO} (a pressure differential of 10-20 mm Hg is required to maintain eyeball rigidity).

$$P_R = P_{ae} - P_{IO}$$

As an initial approximation, the retinal supply network is assumed to be a network with the supply pressure distributed linearly across the network. That is at any point along the supply.

$$\frac{dP_r}{dx} = \text{constant}$$

where x is the distance in degrees along the arteriolar bed, P_r is the corresponding differential pressure along x, and the slope is a function of the supply pressure at the optic disc.

The family of curves describing the pressure gradient across the retina is a series of straight lines with slope

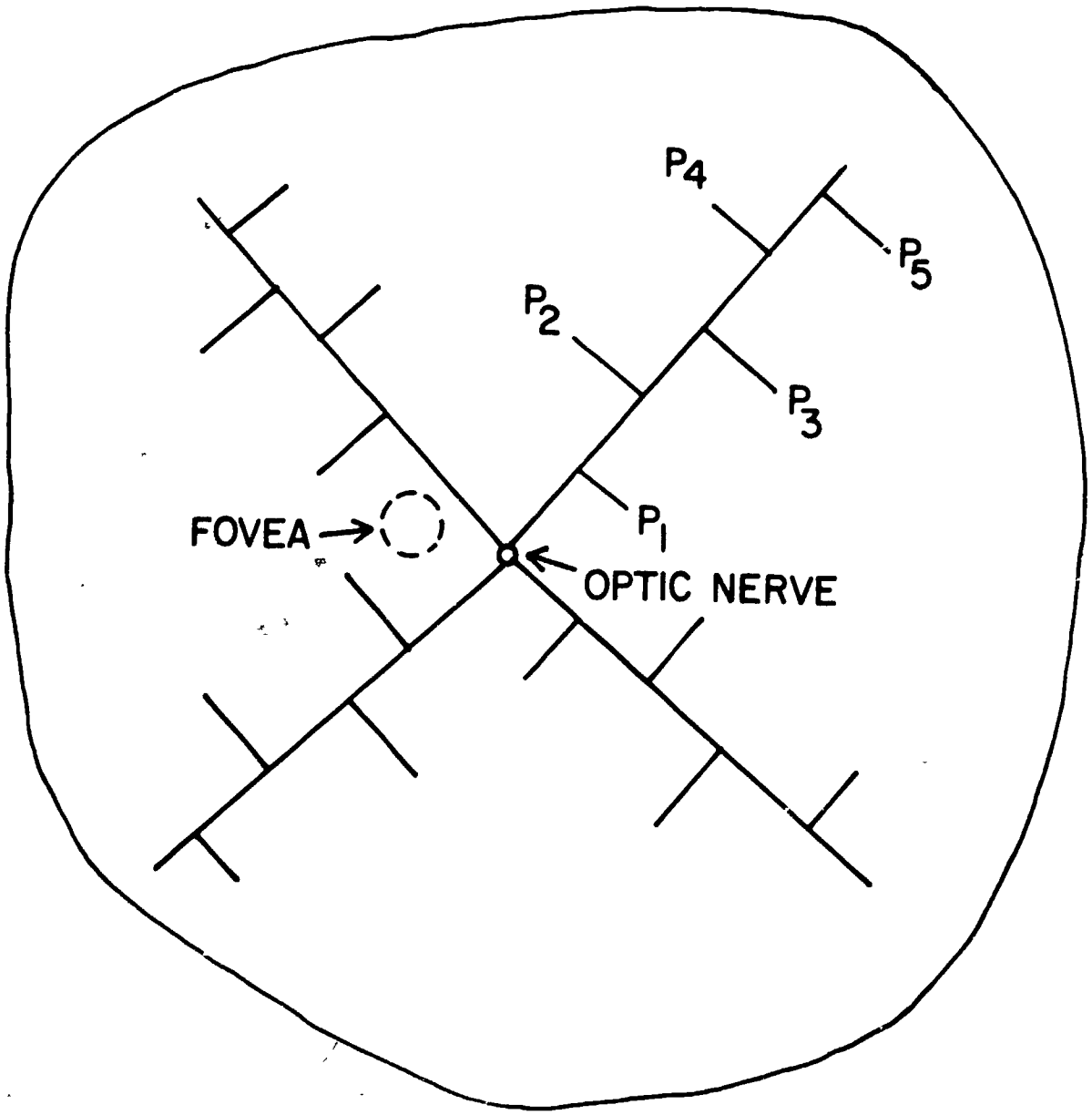

Figure 9. Linearized Representation of Blood Supply to the Retina

$$-\frac{P_R}{K_4}$$

where P_R represents the current retinal arterial pressure at the disc and K_4 is the outer circulation limit of the retina corresponding with the ora seratta. For any value of P_{ae} the retinal pressure as a function of degrees from the disc is given by:

$$P_r = -\frac{P_R}{K_4} x + P_R \tag{6}$$

In a small blood vessel a pressure differential of about 15-20 mm Hg across the vessel wall is required to maintain an open flow channel (Berne and Levy, 1972). When this transmural pressure is not maintained, the vessel collapses, and the blood supply is cut off to all points beyond. This critical pressure differential is now labeled P_{CRIT}.

The threshold value for any x (called x_L) in Figure 10 occurs when P_r falls below P_{CRIT}. Solving for x_L in terms of P_{ae} at the P_{CRIT}:

$$P_{CRIT} = -\left(\frac{P_{ae} - P_{IO}}{K_4}\right) x_L + (P_{ae} - P_{IO}) \tag{7}$$

$$x_L = K_4\left(\frac{P_{ae} - P_{IO} - P_{CRIT}}{P_{ae} - P_{IO}}\right) \tag{8}$$

For a nominal value of $K_4 = 110^\circ$ representing the outer circulation limit, x_L is given by: (let $P_{IO} = 20$ mm Hg, $P_{CRIT} = 17$ mm Hg)

$$x_L = \frac{110(P_{ae} - 37)}{P_{ae} - 20} \tag{9}$$

The quantity x_L represents arc length measured from the center of the optic disk. The optic disk is located on a visual field map approximately 10° to the right of the optical axis and 10° below the horizontal right eye and to the left and below for the left eye. The peripheral edge of the model

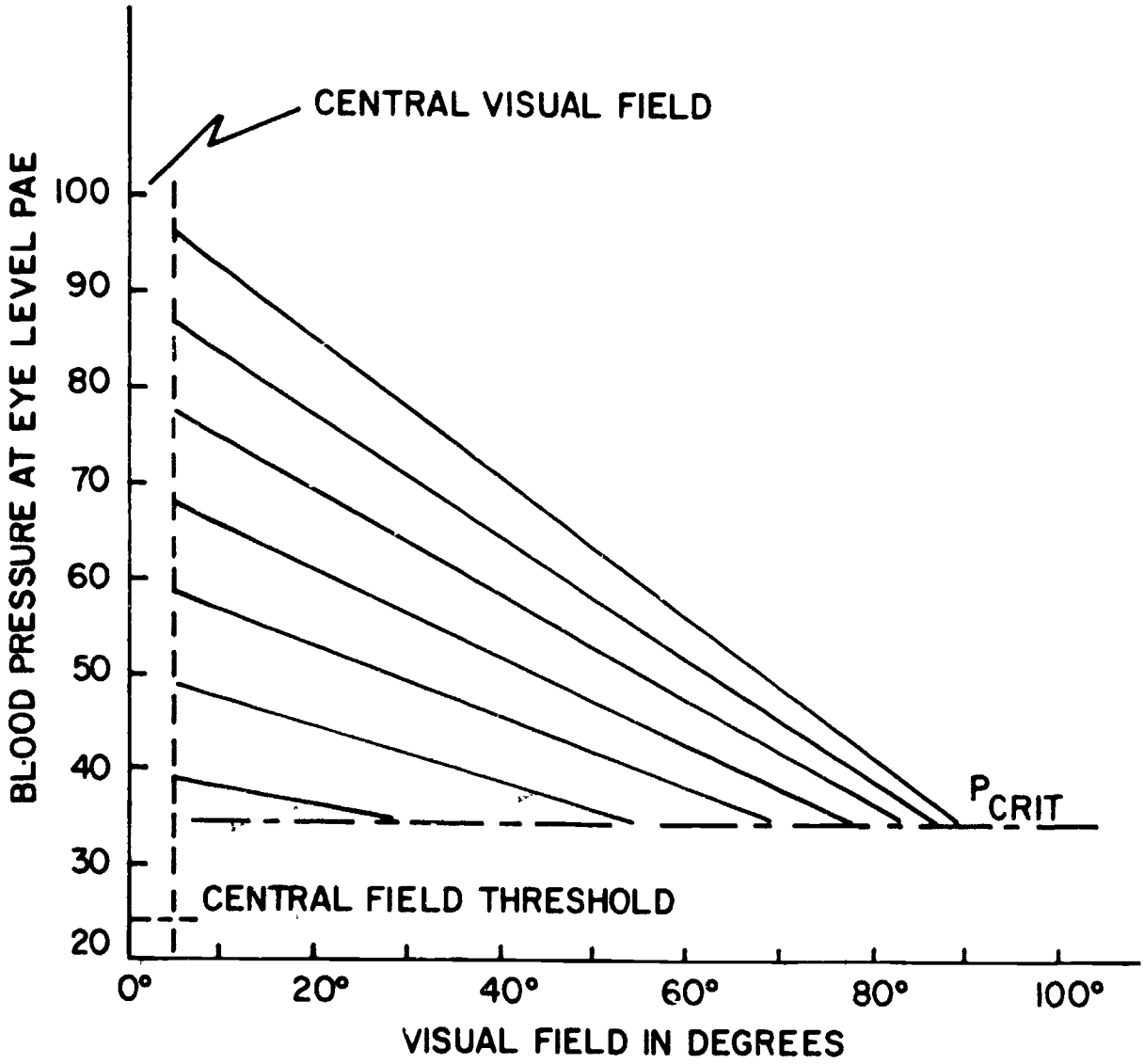

Figure 10. Poiseuille's Law Applied to the Retina (where $dP/dx = K_i$ for Various P_{ae})

is determined by a polar projection of the retinal field. The coordinate origin of the polar map is taken as the visual axis and the optic disc is taken as the flow center. Defining Ψ as degrees of angular location measured counterclockwise about the optical axis (Figure 11), the field contribution of the right eye under acceleration is then given by the solution of:

$$r^2 - 2r_d r \cos(d + \Psi) + r_d^2 = x_L^2 \qquad (10)$$

where r (degrees) is the sensed visual limit at Ψ, r_d is offset distance (degrees) of the disc from the visual axis and d is the angular offset (degrees) of the disc from the horizontal axis. A similar expression is found for the left eye.

The visual field model can now be extended to a binocular field. Figure 12 is a binocular field map showing the coincident foveal areas as the visual center, and the optic disc for each eye in a manner that depicts the observed field from inside out. The outer lines depict the outer edges of the peripheral vision. Lowered blood pressure supply in each of the modeled retinas causes the field to collapse as concentric circles with centers at each of the optic discs as shown by the dashed lines. Thus the visual field collapses toward a somewhat oval shape with the vertical field having a smaller visual angle than the horizontal field. This shape is in agreement with Gillingham's experimental results (Gillingham and McNaughton, 1972).

At some point after the visual field has collapsed, the central vision is lost. Gillingham, et al., 1972, shows that central vision remains after the peripheral field has collapsed. The operating model is therefore modified to allow for central vision by incorporating a central visual cone which is responsive to the eye elevel protection value. Mechanization of the model utilizes a binary decision to determine presence of the central field. The decision point is chosen at a nominal 10 mm Hg below that of the peripheral field critical point.

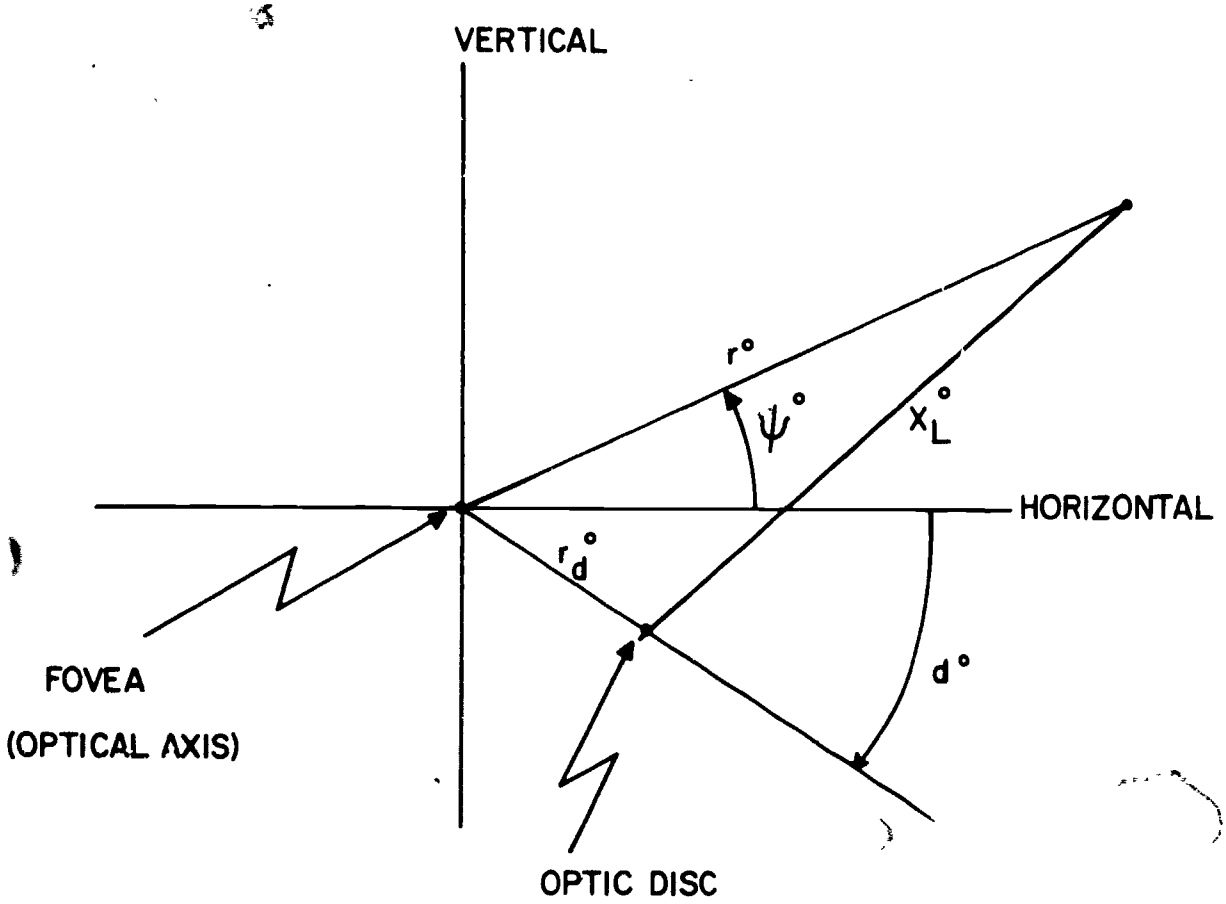

Figure 11. Right Eye Vision Field Under Acceleration

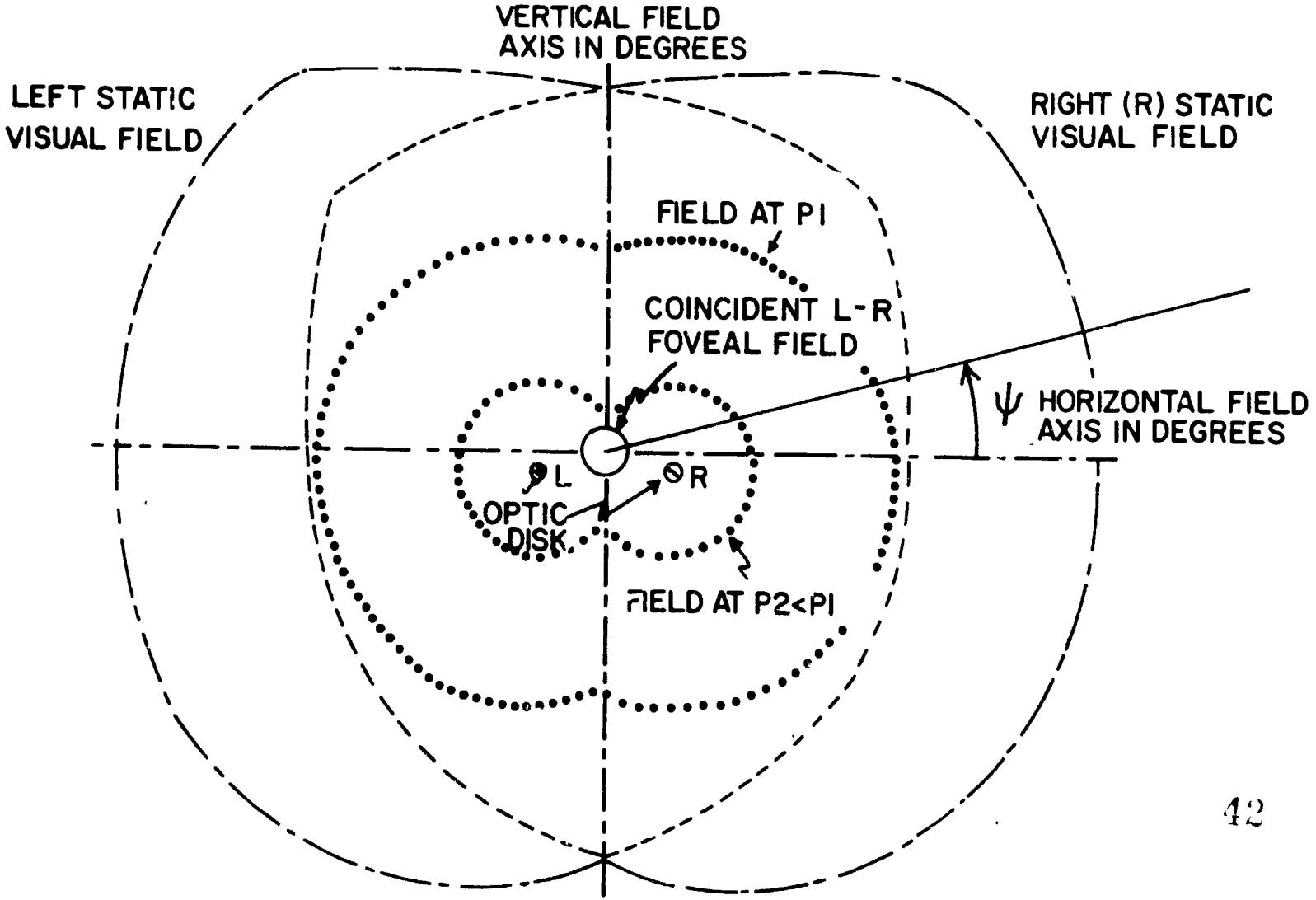

Figure 12. Binocular Visual Field Decay Due to Reduced Blood Supply Pressure

In the actual mechanization of the visual field model, the following data are used:

visual cone for foveal vision = 5^{o} (Gillingham, et al., 1972)

$r_d = 10^{o}$ (for both left and right eyes)
$= .175$ radians

$d = 10^{o}$ (right eye) measured clockwise from the right horizontal visual axis
$= .175$ radians

$d = 170^{o}$ (left eye) measured as for right eye
$= 2.967$ radians

$$x_L = \frac{110\,(P_{ae} - 37)}{P_{ae} - 20} \text{ degrees} \qquad \text{(Equation 9)}$$

$= 1.920\,(P_{ae} - 37)/P_{ae} - 20)$ radians

P_{ae} in this equation becomes PV, the generated protection value, which is equivalent to eye-level blood pressure under acceleration.

The above information is used in Equation 10 which is repeated below:

$$r^2 - 2r_d r \cos(d + \psi) + r_d^2 = x_L^2 \qquad (10)$$

All angles in degrees are converted to angles in radians and the equation is solved for "r", which is the visual limit at angle ψ about the visual axis.

In either field:

$$r = r_d \cos(d + \psi) \pm \sqrt{r_d^2 \cos^2(d + \psi) - (r_d^2 - x_L^2)} \qquad (11)$$

In the right field:

$$r_r = .175 \cos(.175 + \psi) \pm \sqrt{.031 \cos^2(.175 + \psi) - .031 + 3.686\left(\frac{PV-37}{PV-20}\right)^2} \qquad (12)$$

In the left field:

$$r_\ell = .175 \cos (2.967 + \Psi)$$

$$\pm \sqrt{.031 \cos^2 (2.967 + \Psi) - .031 + 3.686 \left(\frac{PV-37}{PV-20}\right)^2} \qquad (13)$$

Thus, using Equations 12 and 13, the sensed visual limit may be calculated for any angle Ψ and for any protection value PV. These equations are applied only to the point where all peripheral vision has collapsed and only the central (foveal) vision remains. The visual cone for foveal vision is selected as 5° (Gillingham, et al., 1972). In the software, the collapse point is reached at a value of PV which leaves the quantity under the radical in Equation 12 positive:

$$-.031 + 3.686 \left(\frac{PV-37}{PV-20}\right)^2 = 0 \qquad (14)$$

which gives,

$$PV = 38.72 \qquad (15)$$

The relationship between retinal blood perfusion, and the ability for contrast detection in a visual scene is apparently an oxygen transport phenomenon. The observed visual dimming and field collapse model could possibly be extended to include these effects. Chambers and Hitchcock, 1963, have documented the relationship between contrast detection threshold and the G field, and White (1958), has documented the effect of lowered visual acuity due to reduced oxygen content of blood in the retinal artery. Using the CV model for the response of eye level blood pressure to acceleration, the contrast and acuity results could be added to the visual dimming and field collapse model.

In the present simplified mechanization, it has been assumed that the brightness and contrast, at any given point in the visual field, are linearly related to PV, the eye level blood pressure as influenced by acceleration. When PV is known, the Visual Response Algorithm produces, in addition to the

visual field limit, signals appropriately scaled to be used for controlling both brightness and contrast at any point in the visual field.

The algorithm presently includes control of a center and two side visual TV screens with separate brightness and contrast signals. Collapse of the peripheral vision will result in the two side screens being dark while collapse of the foveal vision will result in all three screens being dark. Prior to collapse, the screens would exhibit a linear dimming.

2.5 THE EMG SUBSYSTEM

Figure 1 shows the EMG subsystem between the pilot and the straining model. The task of the EMG subsystem is to sense the raw EMG signal from the pilot's skin, amplify it, process it, and present it to the digital computer.

The expanded block diagram of the EMG subsystem is shown in Figure 13. Three electrodes (one is a reference ground) pick up the pilot's EMG signals. The bio-amplifiers add the two electrode voltages and provide a gain of 100. A hi-pass filter eliminates low frequency drift. Amplification up to 1000 then readies the signal for full-wave rectification. Finally, a two-stage low-pass filter provides a smooth usable signal for use in the simulator computer.

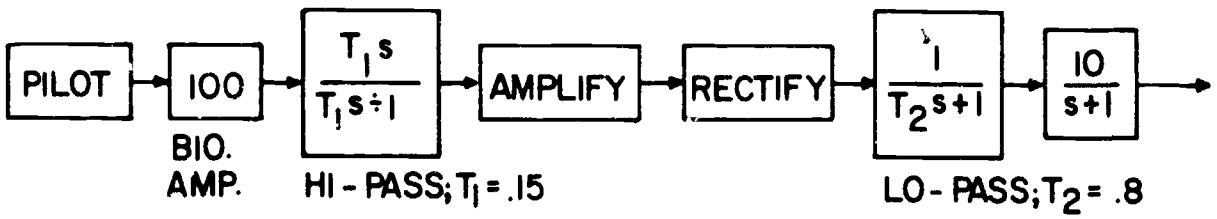

Figure 13. EMG Subsystem Block Diagram

Except for the electrodes and the bio-amplifiers, the EMG subsystem, as shown in Figure 13, was patched on an EAI TR-20 Analog Computer. The patchboard wiring diagram is shown in Figure 14.

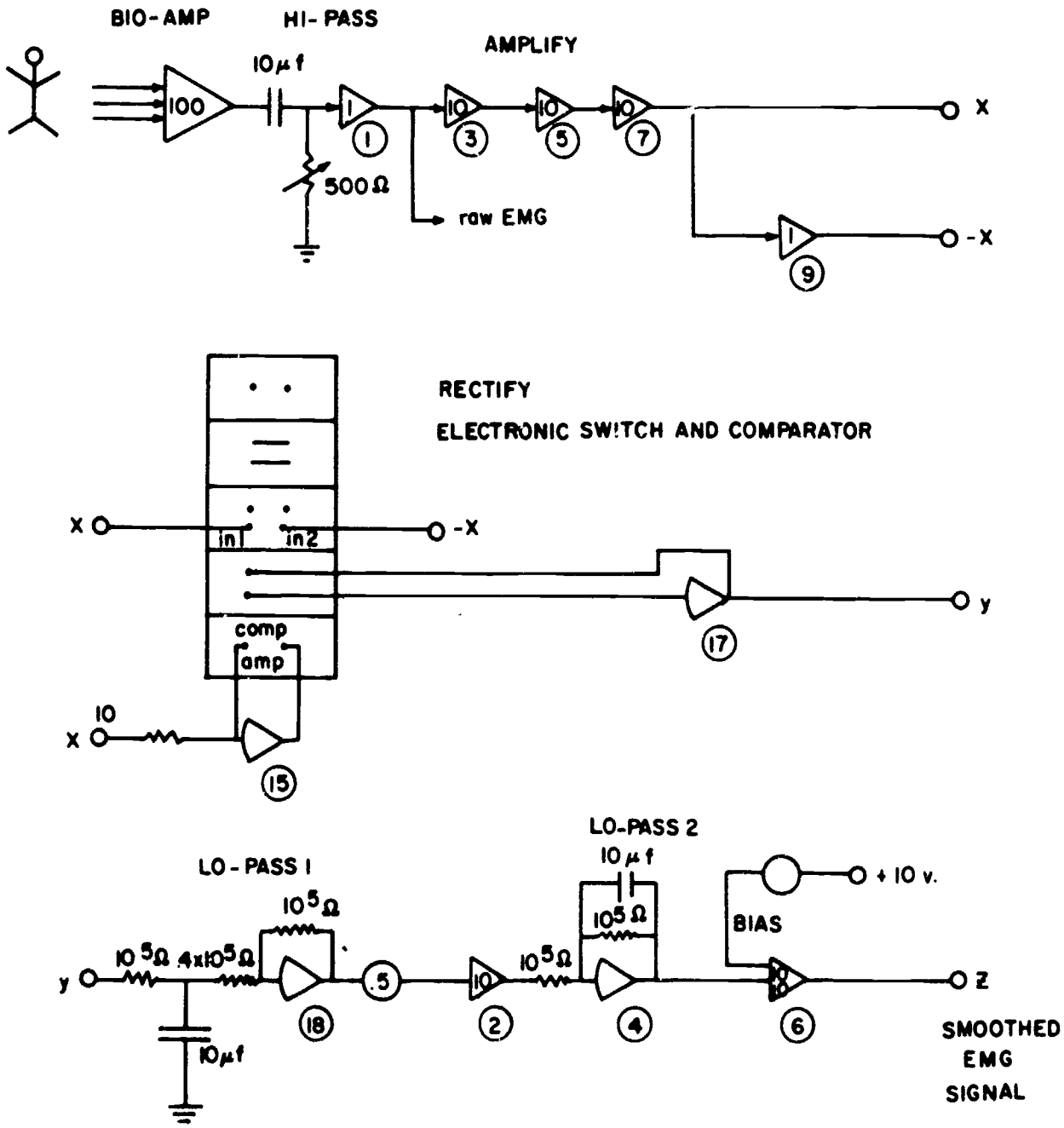

Figure 14. TR-20 Wiring Diagram - EMG Subsystem

2.6 SYSTEM INTEGRATION

The required dynamic model of pilot visual response to G_z can now be assembled as a summation of the separate models. The completed system algorithms provide the means for implementation in aircraft training simulators. The integrated system is shown in Figure 15.

Pilot commands (1)* enter the simulator aircraft dynamics (2) causing changes in the aircraft velocity vector. The resulting g-loading G(t), is used to drive the cardiovascular model (3). In addition the G(t) signal causes the pilots G-suit (4) to inflate according to a preselected schedule. The effect of the proper suit inflation is to increase the value of the protection variable within certain limits. The sum of these signals (5) is added with a computer generated random signal related to individual variations and with a set value representing the eye-level, nonaccelerating, blood pressure (120 mm Hg). The resulting PV signal drives the visual field model. The instrument panel and the view screen are then dimmed according to the output of the model (6). The pilot senses the size and brightness changes and has the option of reducing his aircraft maneuver intensity (g-loading) or increasing his g-tolerance level by performing a straining maneuver (M-1 or L-1). If he initiates such a maneuver, the EMG subsystem processes the myoelectric activity from his skin surface, providing a smoothed EMG signal (7) to the straining model. The straining model then generates a protection value, PV_s, (8), which is dependent on the straining level and on the straining interval. This PV_s is added with the other effects and thus serves to increase PV and to increase the visual field limits and brightness.

*Circled numbers refer to Figure 15.

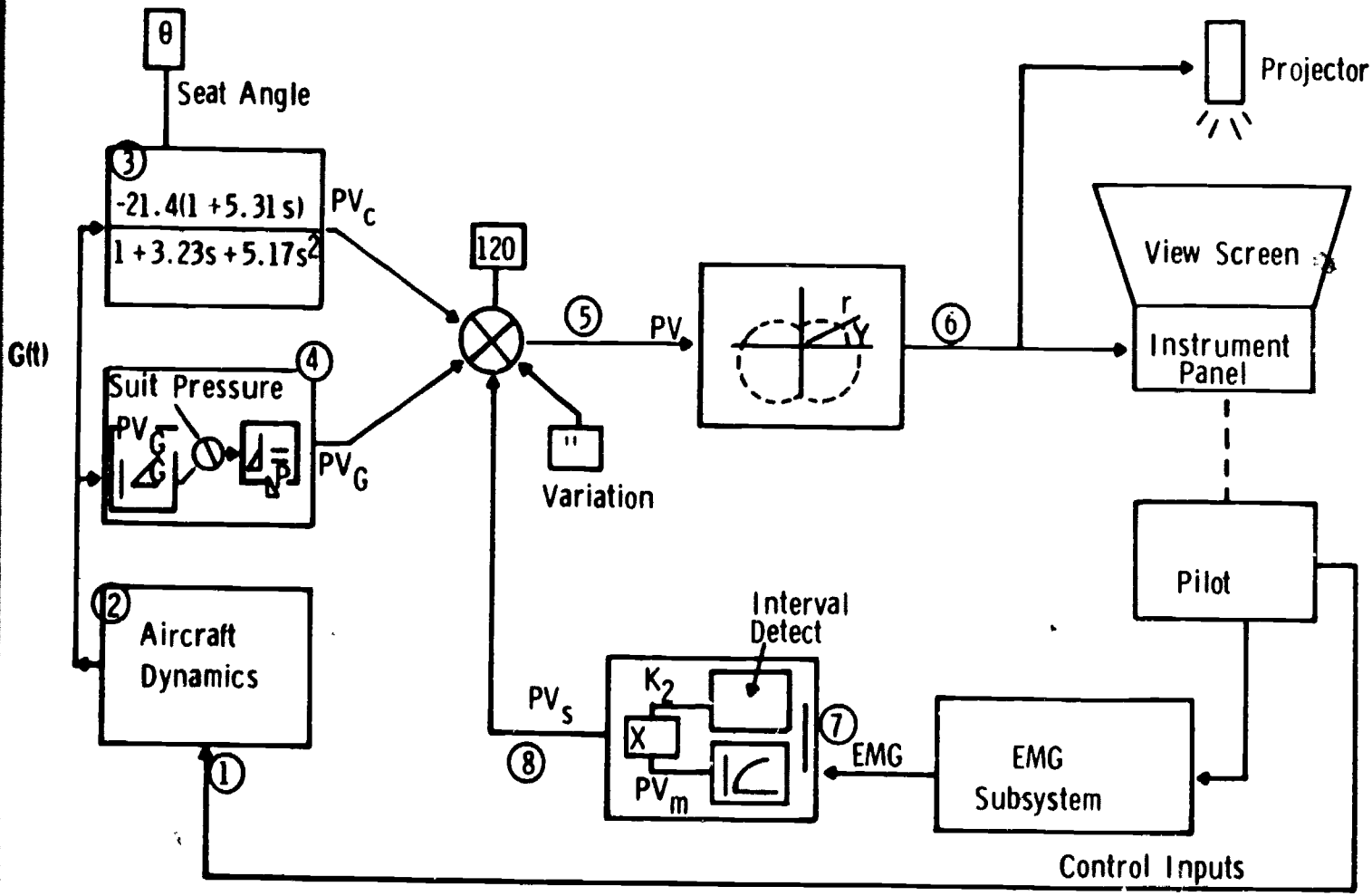

Figure 15. System Integration Diagram

SECTION 3

ALGORITHM DEVELOPMENT AND DOCUMENTATION

3.1 INTRODUCTION

Two FORTRAN algorithms have been developed from the physiological models presented in Section 2. These algorithms are:

1. The Dynamic Visual Response Algorithm
2. The EMG Algorithm

The Dynamic Visual Response Algorithm consists of a FORTRAN coded implementation of the Cardiovascular Response Model, the Protective Garment Model, and the Visual Response Model. The EMG Algorithm consists of a FORTRAN coded implementation of the EMG Straining Model. A description of each algorithm is presented along with its flow chart. In addition, a program listing combining the two algorithms, and the program results with several input profiles, are presented.

3.2 DYNAMIC VISUAL RESPONSE ALGORITHM

The flow chart for the Dynamic Visual Response Algorithm appears in Figure 16. The first input is simply the acceleration in units of G's (G = 9.81 m/sec [Rogers, 1978]). This input must be generated from the aircraft dynamics. This algorithm assumes that the acceleration is readily available. The acceleration is used to determine the cardiovascular protection variable contribution, PVC. The cardiovascular response model is represented by a linear transfer function which corresponds to the response of the pilot's blood pressure to acceleration. The calculations used in the transfer function are implemented with a recursion relation. As with all the various protection variable contributions a positive increasing value indicates an increased protection or tolerance level.

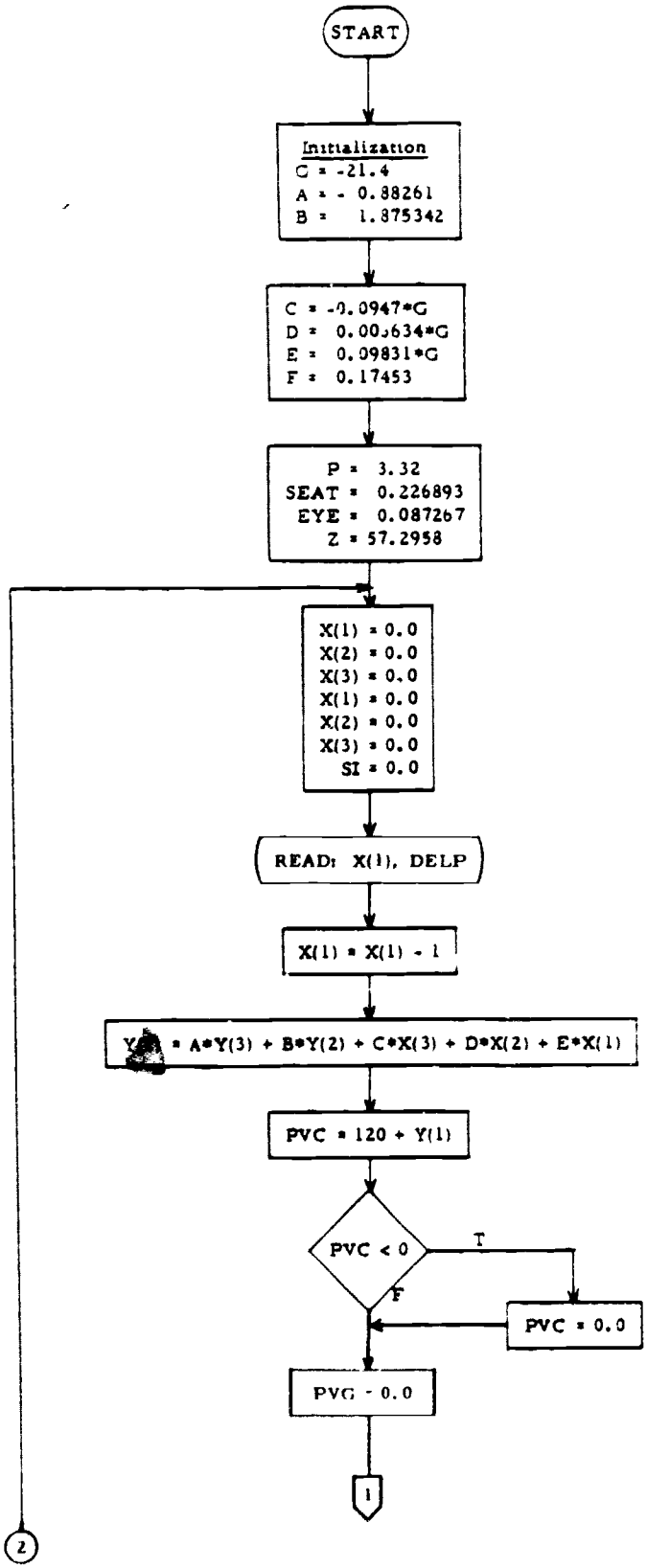

Figure 16. Dynamic Visual Response Algorithm

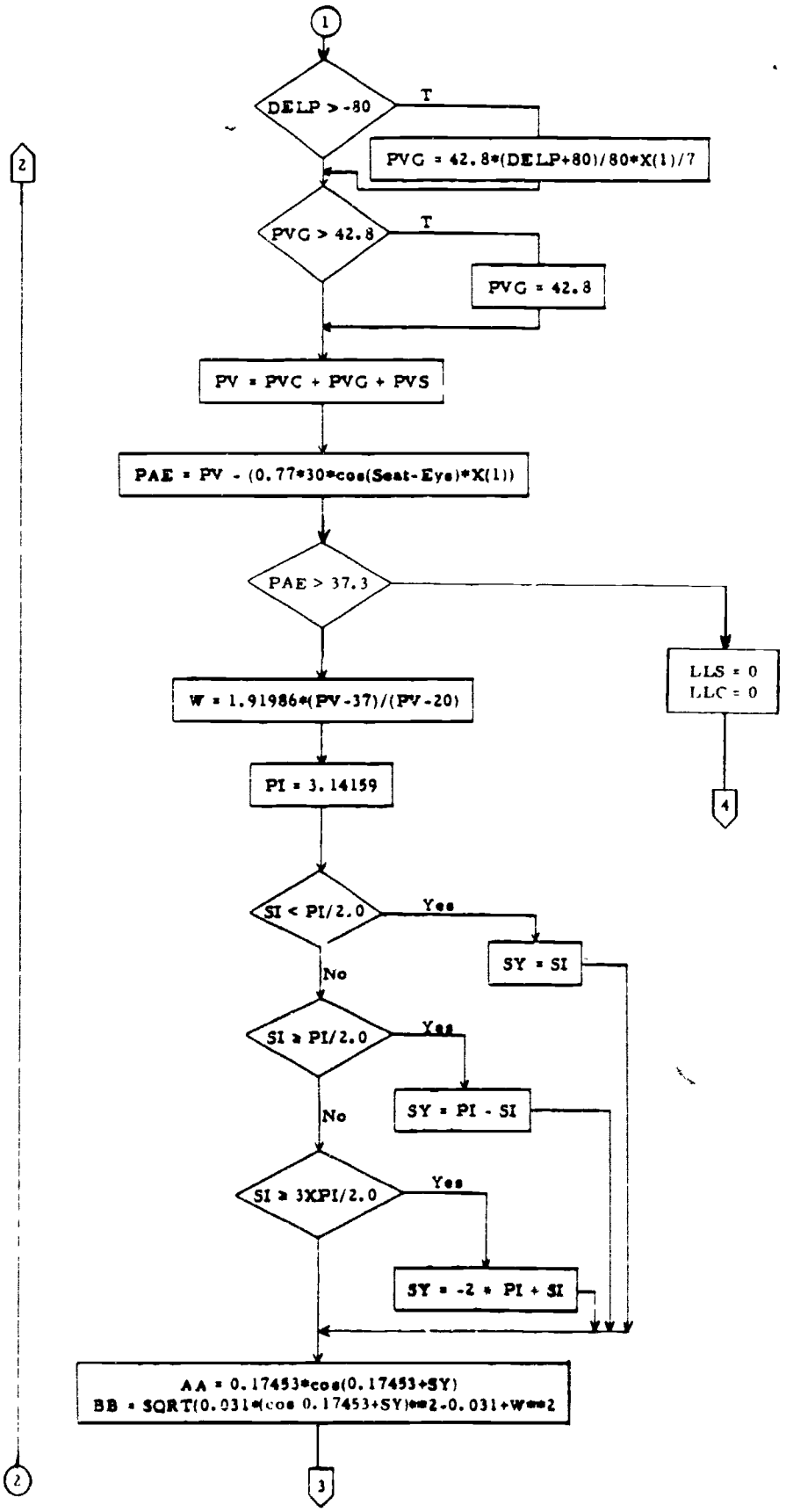

Figure 16. Dynamic Visual Response Algorithm (continued)

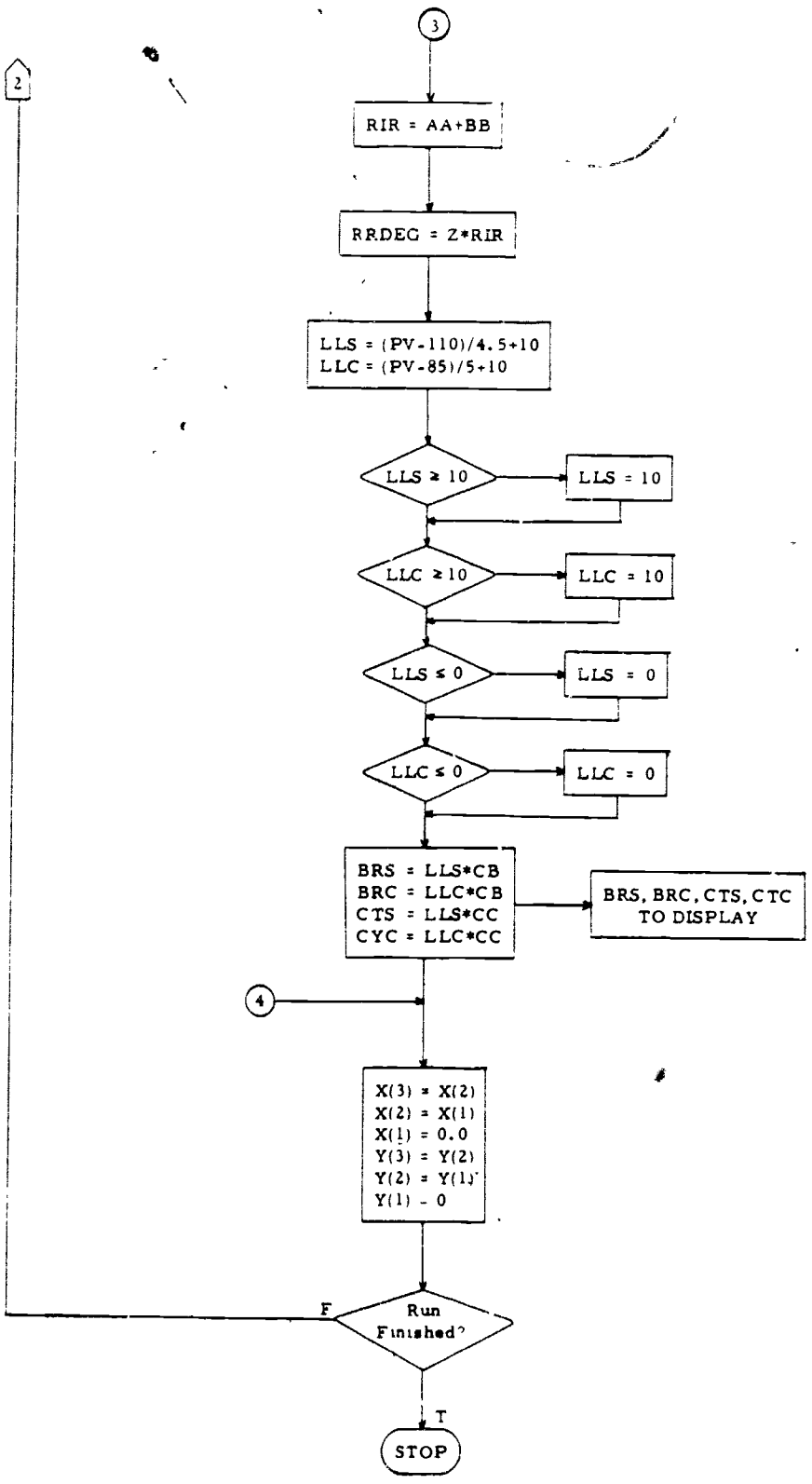

Figure 16. Dynamic Visual Response Algorithm (concluded)

The second input is the difference between the subject's actual G-suit pressure and the "standard curve pressure" (Rogers, 1978) (as calculated from the standard pressure suit valve fill schedule). This difference, which is labeled DELP, is used to calculate another protection variable contribution, PVG. The final input is from the EMG algorithm and consists of a single protection variable contribution, PVS. This input is explained more completely in the EMG algorithm section.

After all the protection variable contributions have been calculated, they are summed to form the protection variable, PV. This protection variable is then used to calculate the blood pressure at eye level, PAE. The variable PAE is then used to determine the size of the visual field.

The size of the visual field is then used to determine equivalent light levels for center and side CRT screens. Brightness and contrast signals for the center and side screens are then calculated by scaling these light levels.

This algorithm assumes that all three inputs are readily accessible, and the protection variables are positive. This algorithm was written in Fortran IV and was tested on both the University of Dayton Sperry-Univac 70/7 Computer and the Air Force Human Resources Laboratory (AFHRL) Simulation Training and Research System (STARS) Xerox Sigma 5 computer facility at Wright-Patterson Air Force Base.

3.3 EMG ALGORITHM

This algorithm is designed to take the rectified EMG signal from the subject's straining muscles and generate the protection variable contribution due to straining, PVS. The variable PVS in turn will be used in the main program as one of the protection variable contributions. In the process of calculating PVS, this program also calculates the EMG variable PVM, and the straining effectiveness value, K2. Both these variables, PVM and K2, are important because they are separate functions of time.

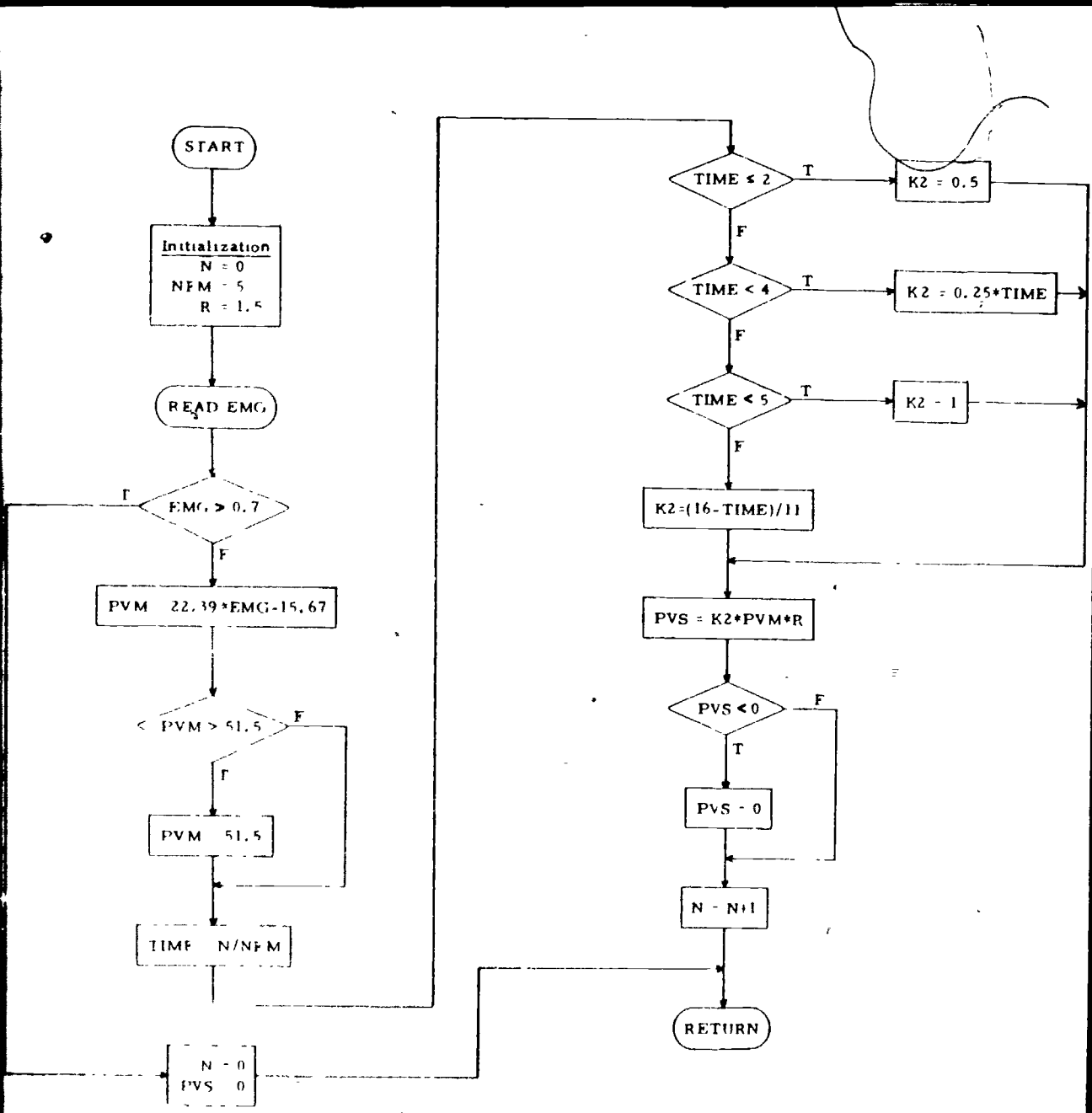

Figure 17. EMG Algorithm

Their product determines the straining protection variable contribution, PVS. The algorithm flow chart appears in Figure 17.

The single input of this algorithm is the rectified Electromyographic (EMG) signal from the subject's body. The EMG signal is used only in the determination of the EMG protection variable PVM. Upon the initiation of a desired level of straining the counter variable TIME is started. After TIME is initiated the straining effectiveness value K2 is calculated according to the current value of TIME.

The single output of this algorithm is the straining protection variable contribution, PVS. The variable PVS is calculated with the above mentioned variables K2 and PVM. Also a scaling variable, R, is used to keep the value of PVS between acceptable levels. Appropriate limiters have been written into the algorithm to keep the variable PVS positive.

This algorithm was written in Fortran IV and was tested on both the University of Dayton Sperry-Univac 70/7 Computer and the AFHRL STARS facility.

3.4 PROGRAM CHECK-OUT

These two algorithms have been combined together into a single program for use as software for the BIOCONAID system. The listing of this program, called BIO, is shown in Appendix B.

Six different computer generated input profiles were used for program check-out. Three of these had combined acceleration and straining inputs, while three contained acceleration inputs only. The results of these profiles, in terms of the protection variable, PV (calculated blood pressure at eye level), are presented in Figures 18 to 23. All of these results exhibit a delayed loss in PV due to acceleration and a delayed increase in P due to straining. In addition, these results agree with the models presented in Section 2.

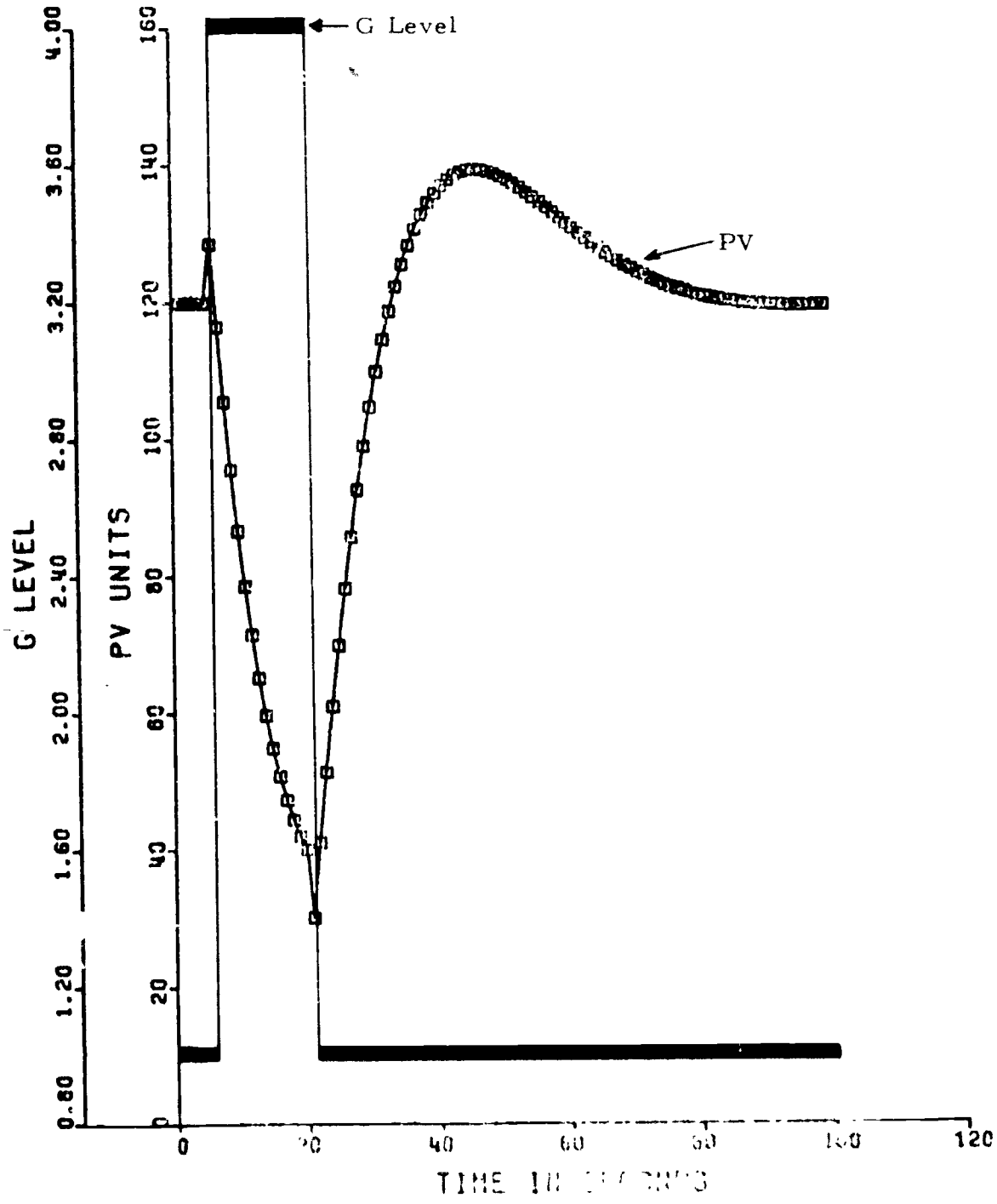

Figure 18. PV Response to Profile #1 (No EMG Input)

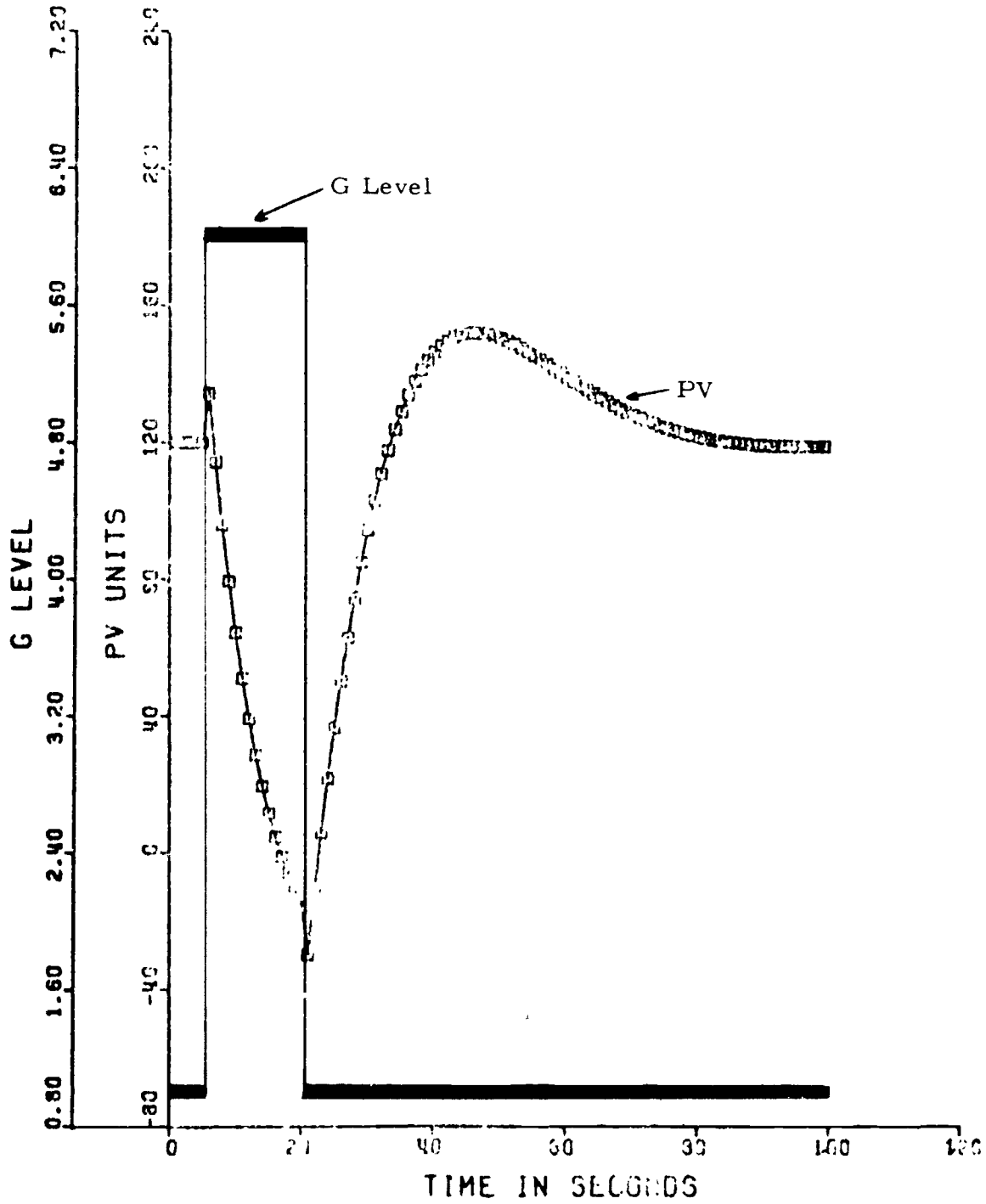

Figure 19. PV Response to Profile #2 (No EMG Input)

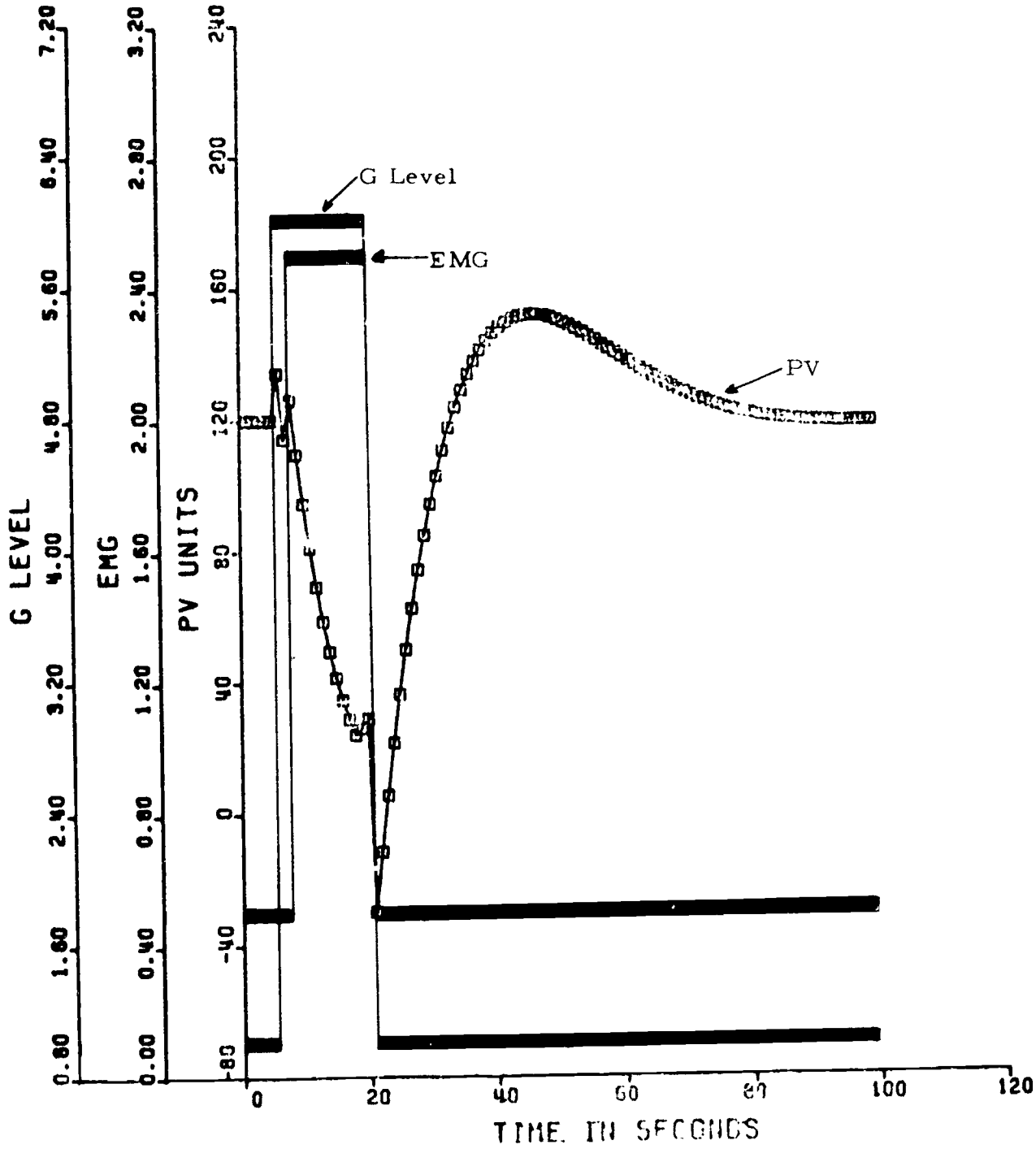

Figure 20. PV Response to Profile #3

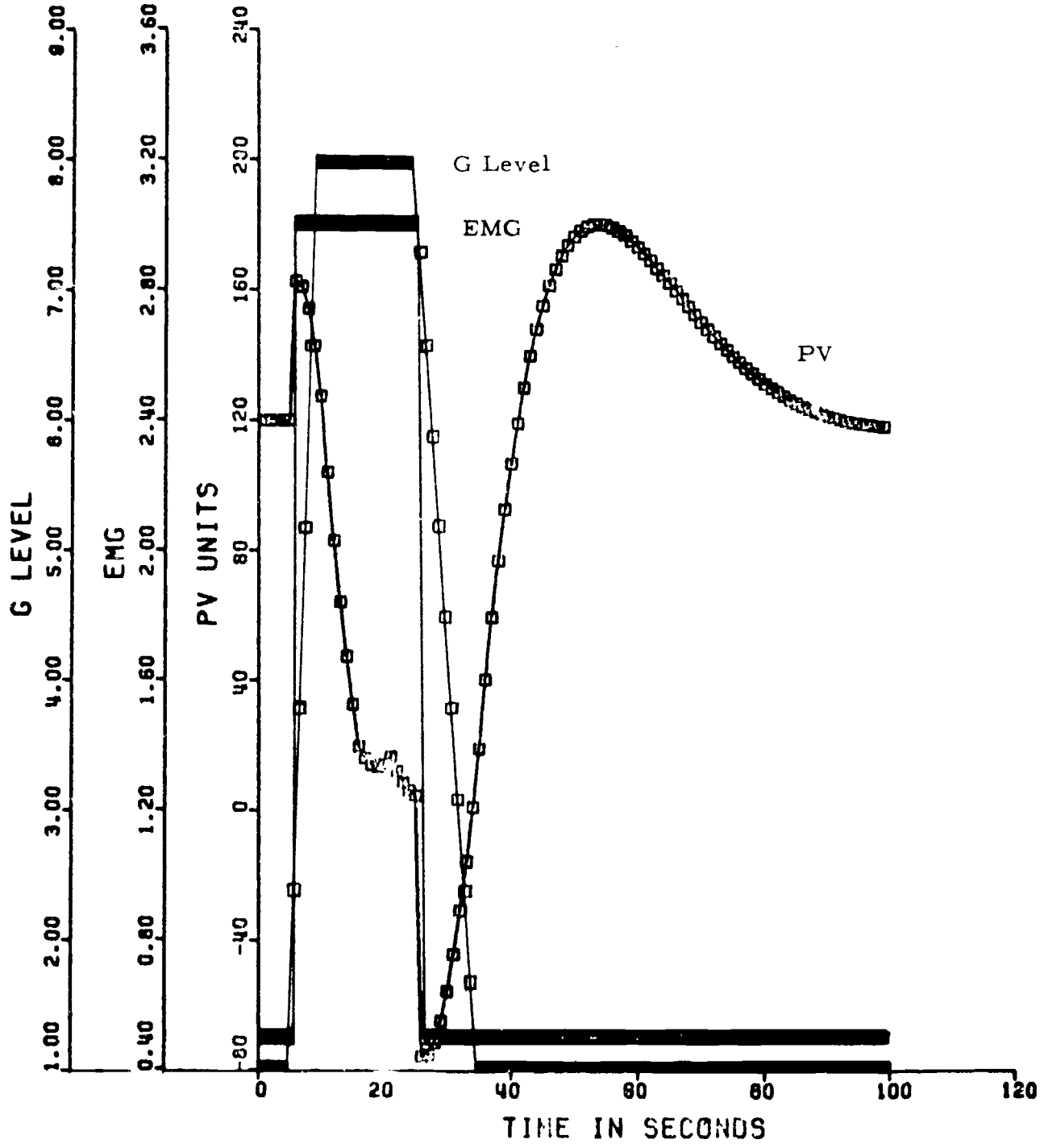

Figure 21. PV Response to Profile #4

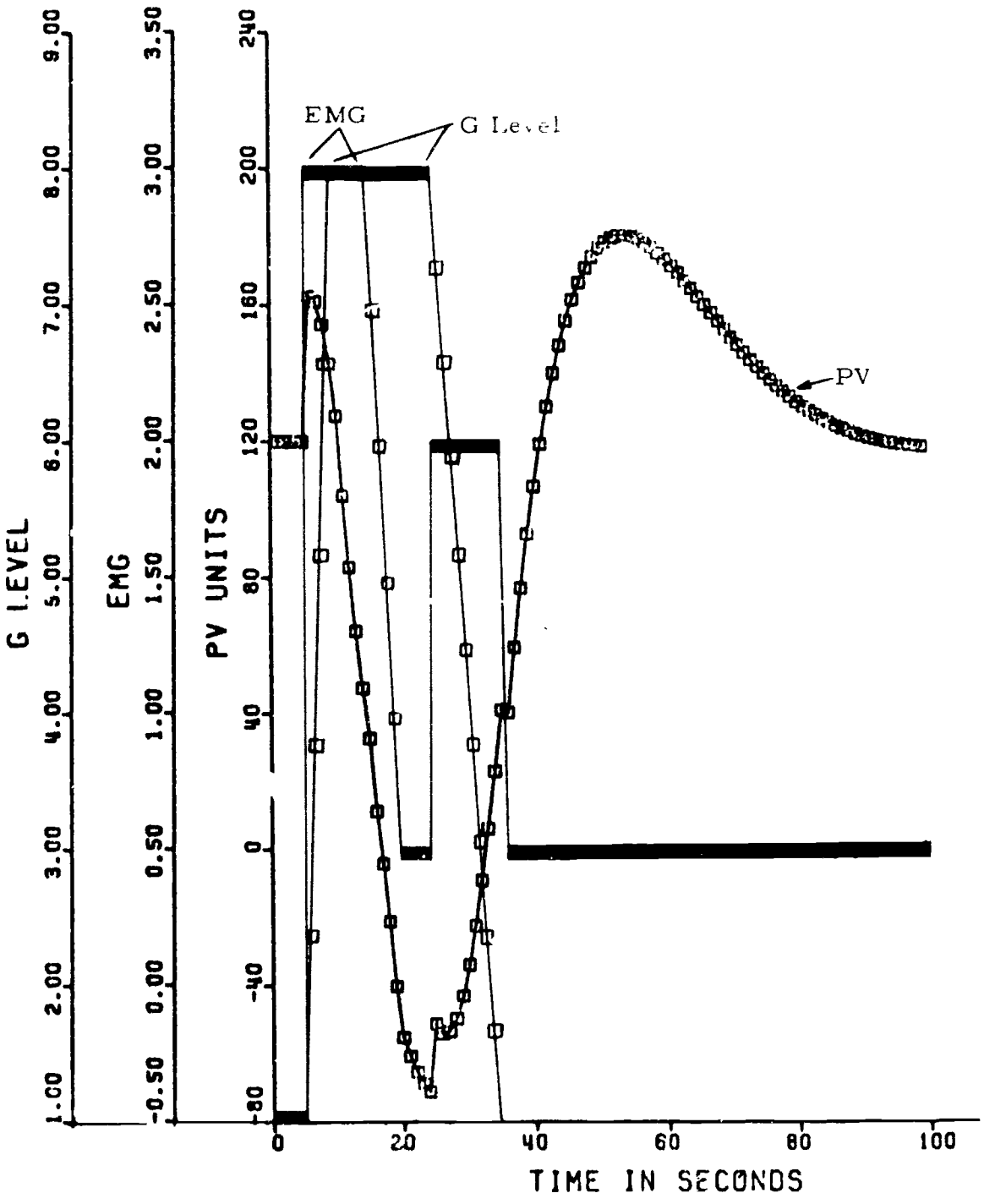

Figure 22. PV Response to Profile #5

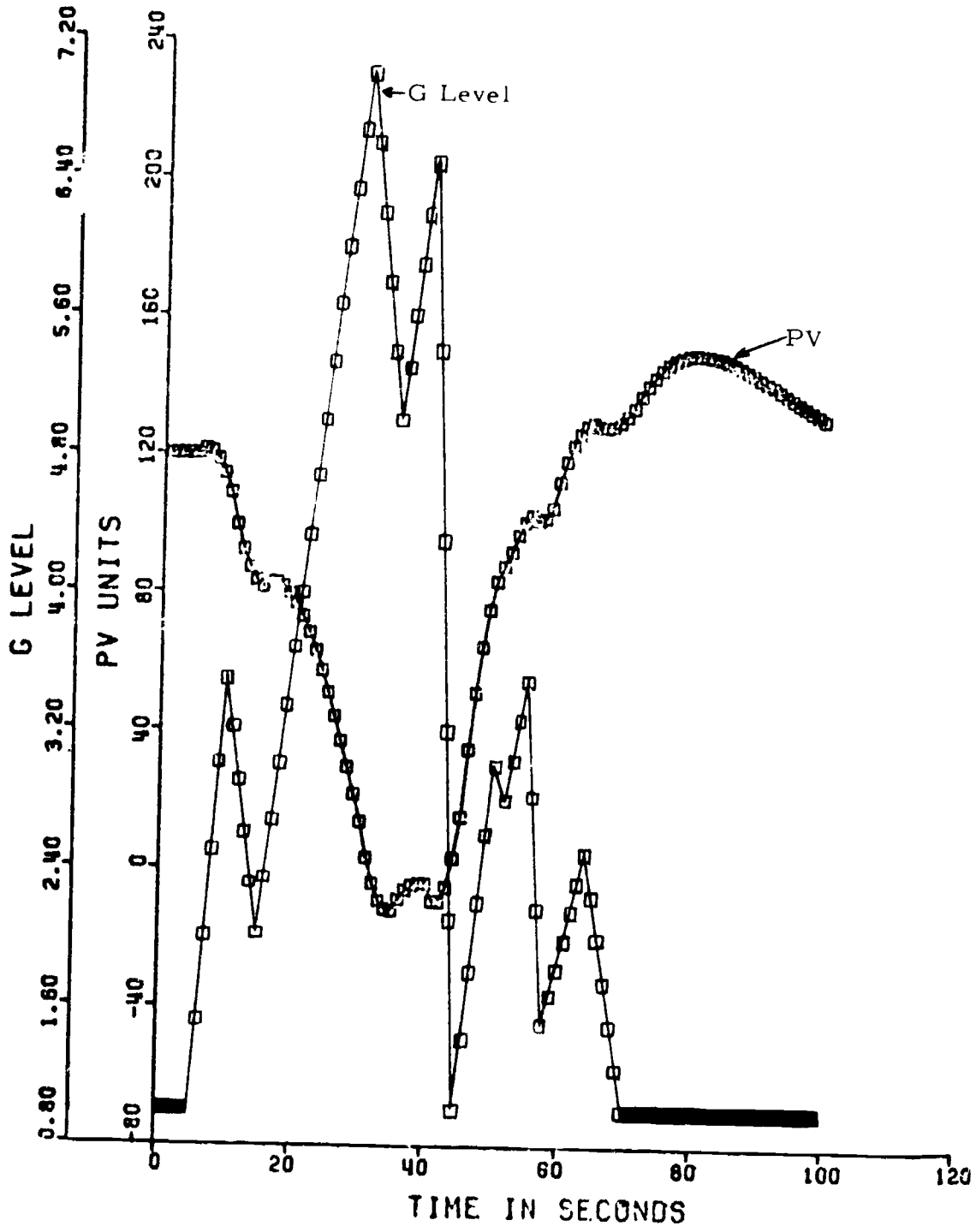

Figure 23. PV Response to Profile #6 (No EMG Input)

SECTION 4

STRAINING EXPERIMENTS WITH HUMAN SUBJECTS

4.1 INTRODUCTION

The experiments and equipment development described here pertain to the EMG subsystem which was described earlier in the report (Section 2.5). These experiments were done to accomplish the following goals:

1. To evaluate possible electrode sites on the pilot's body to pick up straining signals.
2. To show that a reliable, usable signal is produced.
3. To indicate tolerance of the EMG subsystem to extraneous body motions.
4. To aid in the development of electronic filters for the EMG subsystem.

The experiments involved recording the EMG signals produced as the subjects strained in response to visual commands. The seven subjects were faculty members and students. All faculty members were experienced pilots. The work was accomplished at the University of Dayton and at the Air Force Human Resources Laboratory, Wright-Patterson Air Force Base, during the period of November 1978 to February 1979.

4.2 EXPERIMENTAL SET-UP AND PROCEDURE

Figure 24 shows the experimental setup. The equipment used and the experimental procedure are described below.

Equipment:
1. Electrodes and wiring
2. Bio-signal amplifiers (Gain = 100)
3. TR-20 Analog (Hybrid) Computer (EAI) to provide:
   a. Hi-Pass Filter
   b. Amplification
   c. Signal Rectifier (full wave)
   d. Lo-Pass Filter for smoothing
   e. Voltmeter - used for visual feedback of error signal to subject
4. Strip Chart Recorder

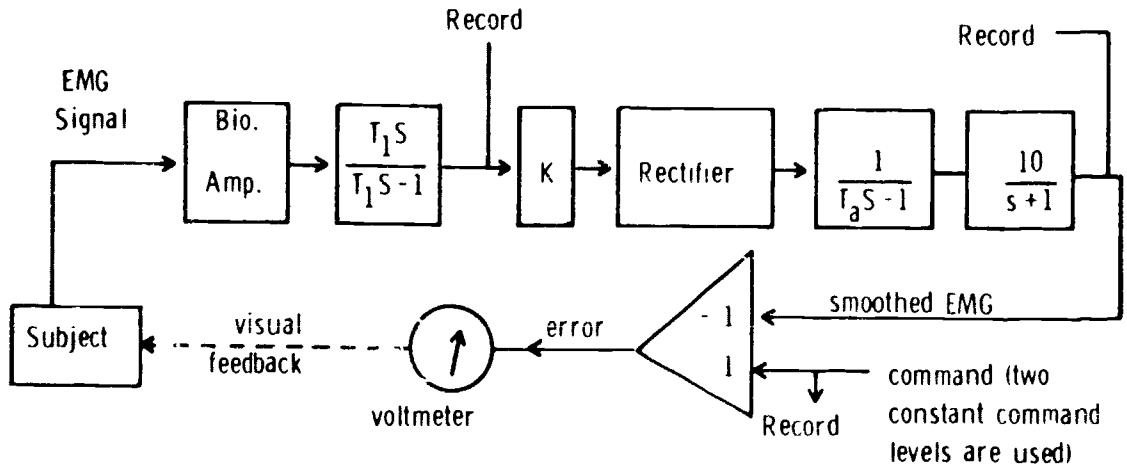

Figure 24. Experimental Setup

Procedure: (equipment "on" and checked out earlier)

(5 minutes) 1. Prepare subject. Strap-on electrodes. Use EMG Lotion. Explain M-1/L-1 straining maneuvers. Explain that his straining will make error needle move.

(3 minutes) 2. Subject practices straining and observes needle. Operator inserts practice commands and subject strains to bring needle back to zero.

(2 minutes) 3. First test period (Experiment No. 1). Electrodes on back. Subject relaxed and motionless. Command level one (3 volt) is inserted and subject strains to keep error zeroed. After about five seconds, command is removed and subject relaxes. Repeat, when subject ready, using command level two (6 volt).

(2 minutes) 4. Secont test period (Experiment No. 2). Repeat except subject periodically raises and lowers alternating feet (1-2 inches) during straining periods.

(5 minutes) Change electrodes to abdomen.

(2 minutes) 5. Third test period (Experiment No. 3). Repeat first.

(2 minutes) 6. Fourth test period (Experiment No. 4). Repeat second except subject raises and lower alternating arms (6-8 inches) during straining period instead of raising feet.

(5 minutes) Change electrodes to buttocks (seat).

(2 minutes) 7. Fifth test period (Experiment No. 5). Repeat first.

(2 minutes) 8. Sixth test period (Experiment No. 6). Repeat second except extraneous motion is turning head (about 45°) alternately each way during straining period.

(3 minutes) 9. Remove electrodes. Equipment off.

(33 minutes total time)

4.3 RESULTS

Preliminary results are presented in Figures 25-27 for three different subjects. This data was taken with an early technique of EMG signal processing. The upper trace is the commanded signal, which the subject attempts to match with his smoothed EMG signal (the middle trace). The bottom trace is the raw EMG signal.

Although these preliminary results gave useful raw EMG signals, the smoothed EMG signal suffered from a low frequency drift and excessive noise. In addition, the smoothed EMG signal exhibited an excessive time lag compared to the raw EMG signal.

Several changes in the EMG signal processing technique overcame these shortcomings and are discussed in Section 4.4. The results for experiments using five subjects conducted at the University of Dayton with the final signal processing technique are presented in Figures 28-33. These data show a well-behaved smoothed EMG signal, free of drift or extraneous noise.

In addition a number of runs were made with a different subject in the STARS simulator cockpit at AFHRL. The BIOCONAID EMG subsystem equipment was operated at the STARS facility to determine whether there would be an excessive amount of electronic noise interference in that environment. These results are presented in Figures 34-40, in terms of the raw EMG signal and an error signal (commanded signal minus

smoothed EMG output). The equipment operated satisfactorily without shielded-cables and amplifiers. All STARS equipment, including the TV view screens, was operating with the exception of the cockpit instruments (400 Hz).

4.4 DISCUSSION

Early in the experiments it became apparent that a more effective filter was needed for the EMG signal. The smoothed EMG signal had too much noise associated with it. The raw EMG signal included a low frequency, drift, which also affected the smoothed signal. The smoothed EMG signal also exhibited an excessive time lag.

Several changes were made to the EMG signal processing technique to improve the system. A high-pass filter was added to remove the DC drift from the incoming EMG signal. The low-pass filter (smoothing network) was converted to a two-stage filter. Time constants of all filters were adjusted for near-optimum response. The final configuration is that shown in Figures 13 and 24. Figures 28-40 show a smoothed EMG signal which is reliable, free from drift and free from excessive noise. This smoothed EMG signal shows very good correlation with the straining (raw EMG) signal from the pilot.

The Experimental Procedure lists Experiments 5 and 6 which were to be done with electrodes on the buttocks. Only Figures 25 and 26 show any such tests being accomplished. The reason Experiments 5 and 6 were discontinued is that consistently much better results were obtained with the lattisimus dorsi (back) muscles and with the external oblique (abdominal) muscles. Figure 26 shows a comparison between Experiments 4 and 5. The smoothed EMG response to the 3 volt command has roughly three times the magnitude in Experiment 4 (abdomen) than in Experiment 5 (buttocks). Similarly, the raw EMG traces showed a marked difference.

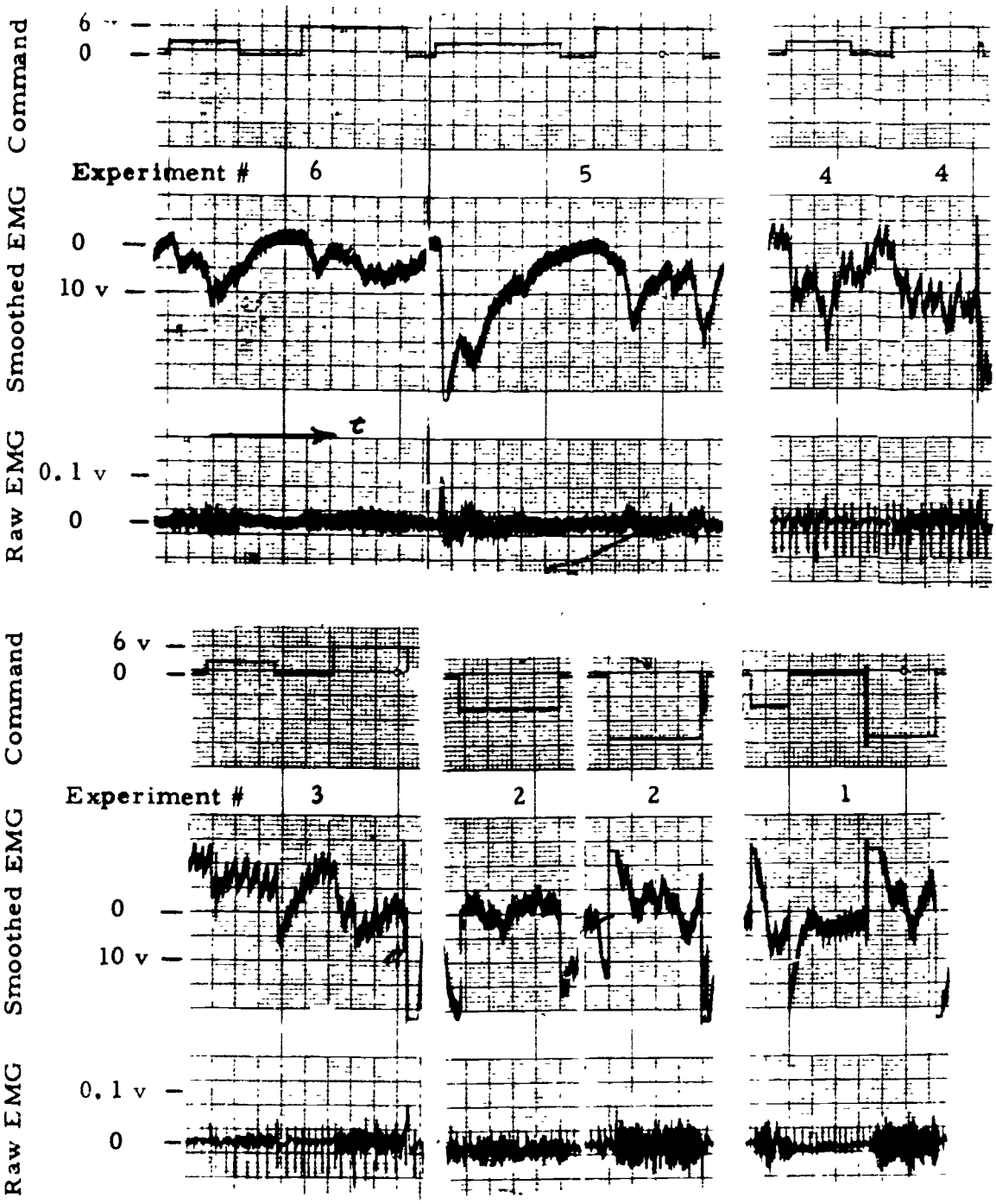

Figure 25. Subject #1 (Preliminary)

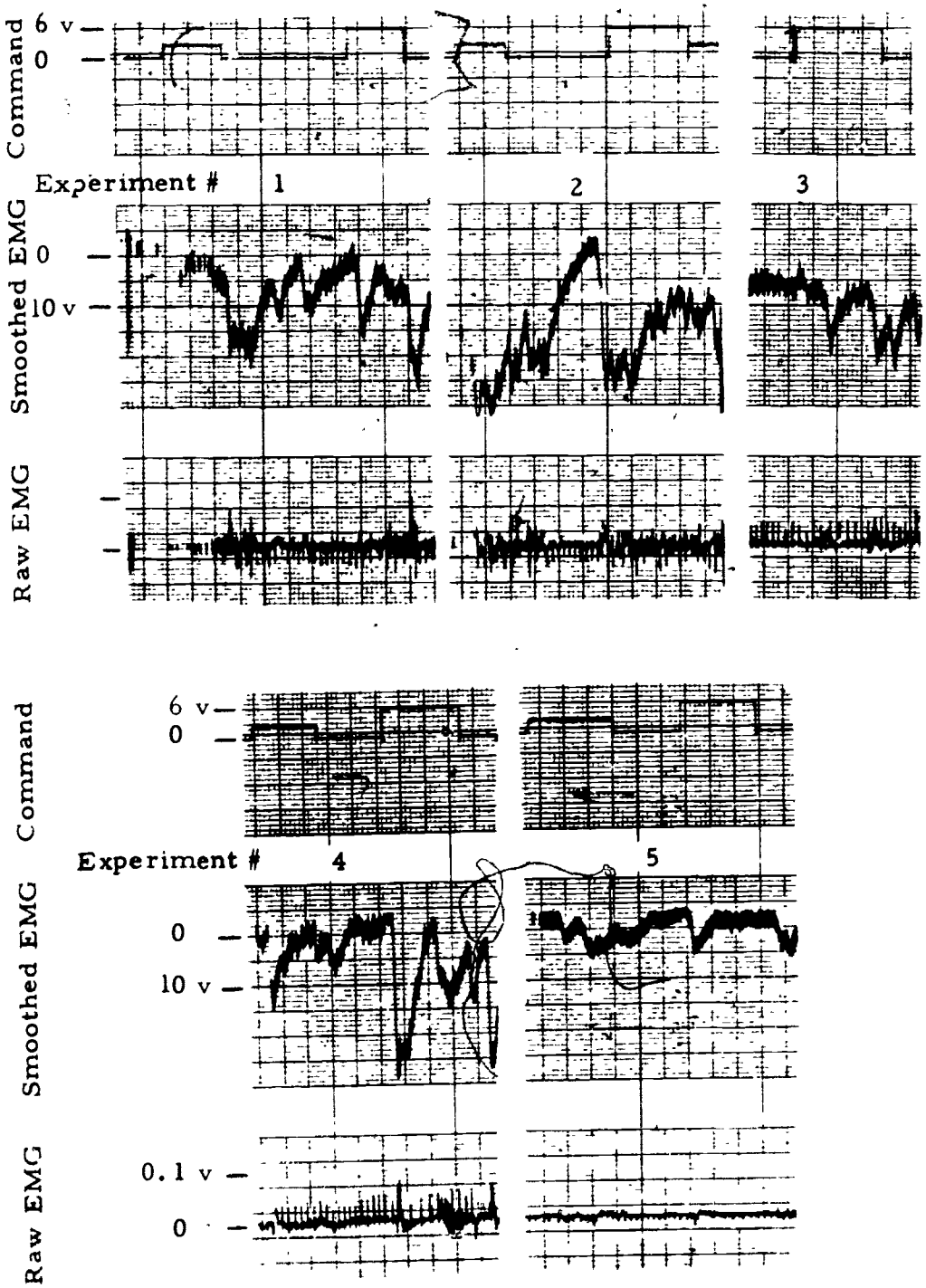

Figure 26. Subject #2 (Preliminary)

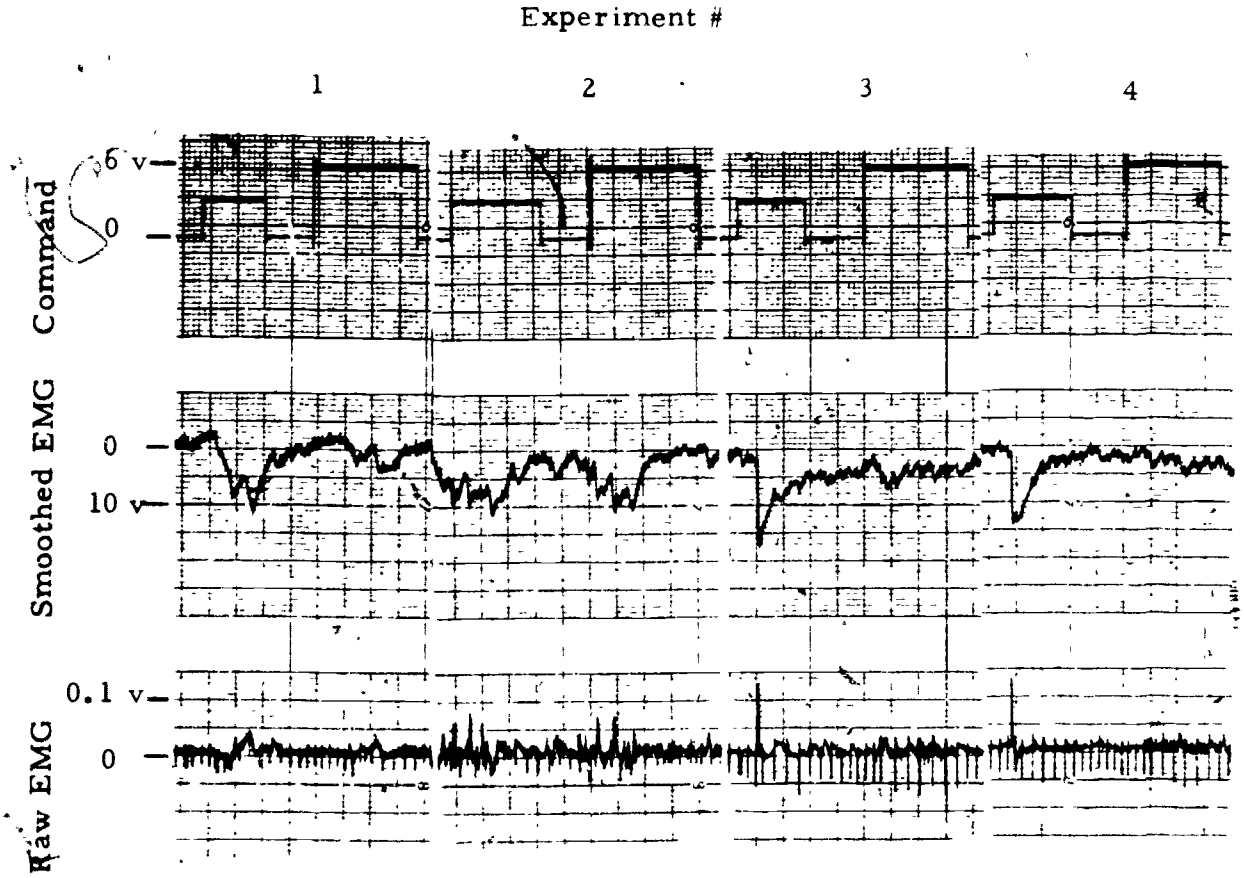

Figure 27. Subject #3 (Preliminary)

Another problem encountered with placing electrodes on the buttocks was the difficulty in strapping them on. This problem would be eliminated with the adhesive electrodes used in later tests.

It appears the great advantage of seat electrodes would be their possible use without the necessity of mounting electrodes on the pilot's skin. Efforts to develop "seat pan electrodes should be encouraged. If electrodes must be mounted on the pilot, then the abdomen or back gives a much stronger signal.

Experiments 1 and 2 had electrodes on the back while Experiments 3 and 4 had electrodes on the abdomen. Examination of the raw EMG traces in Figures 28 through 33 indicates either site is satisfactory but the abdomen usually gives a slightly stronger signal.

Experiments 2 and 4 involved having the subject do extraneous body motions while straining. Rhythmically raising and lowering feet (Experiment 2) and raising and lowering arms (Experiment 4) were the specific motions. Experiment 6 involved rhythmically turning the head from side to side. There was no noticeable effect on the smoothed EMG signal due to these motions. However, major motions (standing up or bending far forward) would saturate the signal processing equipment. Also touching or jostling the electrodes caused a large response. We feel that the normal motions of a pilot in the simulator cockpit will not adversely affect the BIOCONAID system.

Two input command levels (usually 3 and 6 volts) were used to show that the pilot can control his level of straining with reasonable accuracy. Figures 28 through 33 show the smoothed EMG signal approximating the command level.

Adhesive electrodes were obtained in time to be used in part of the University tests on one subject (Figure 33) and on all the tests in the STARS facility at AFHRL. As might be expected, these electrodes maintained a more constant skin contact then the strap-on type electrode. Also, they

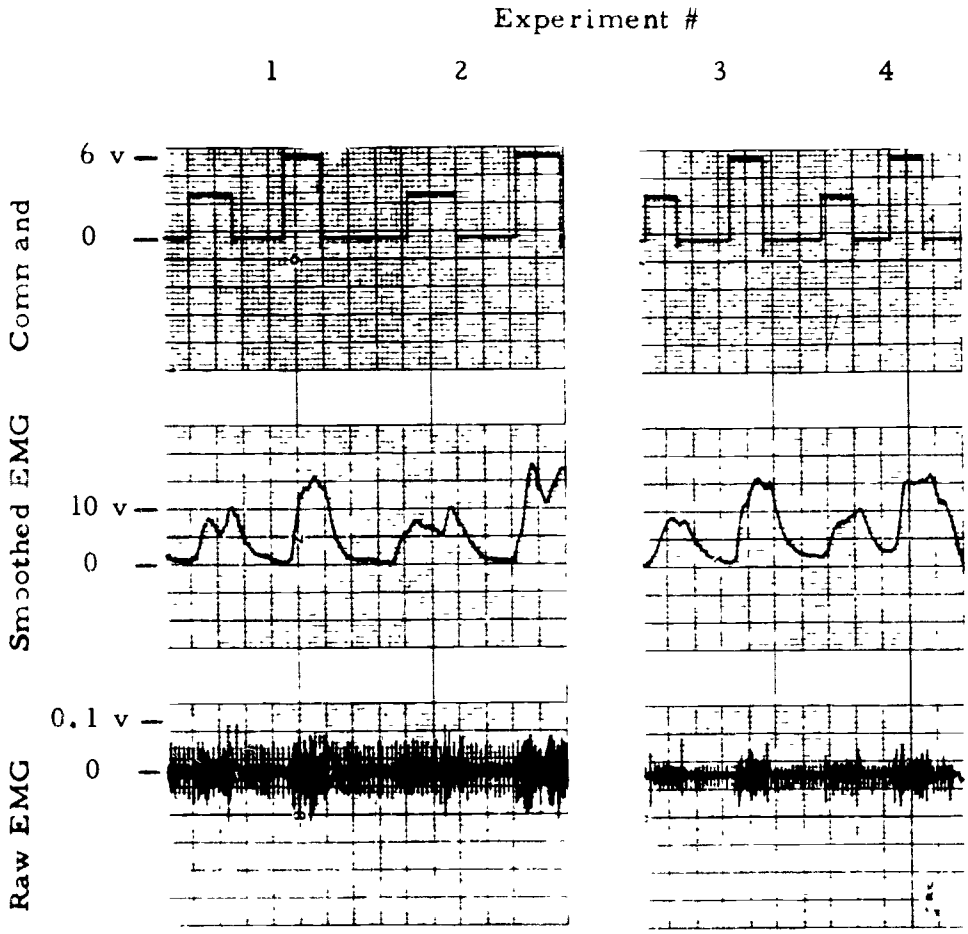

Figure 28. Subject #4

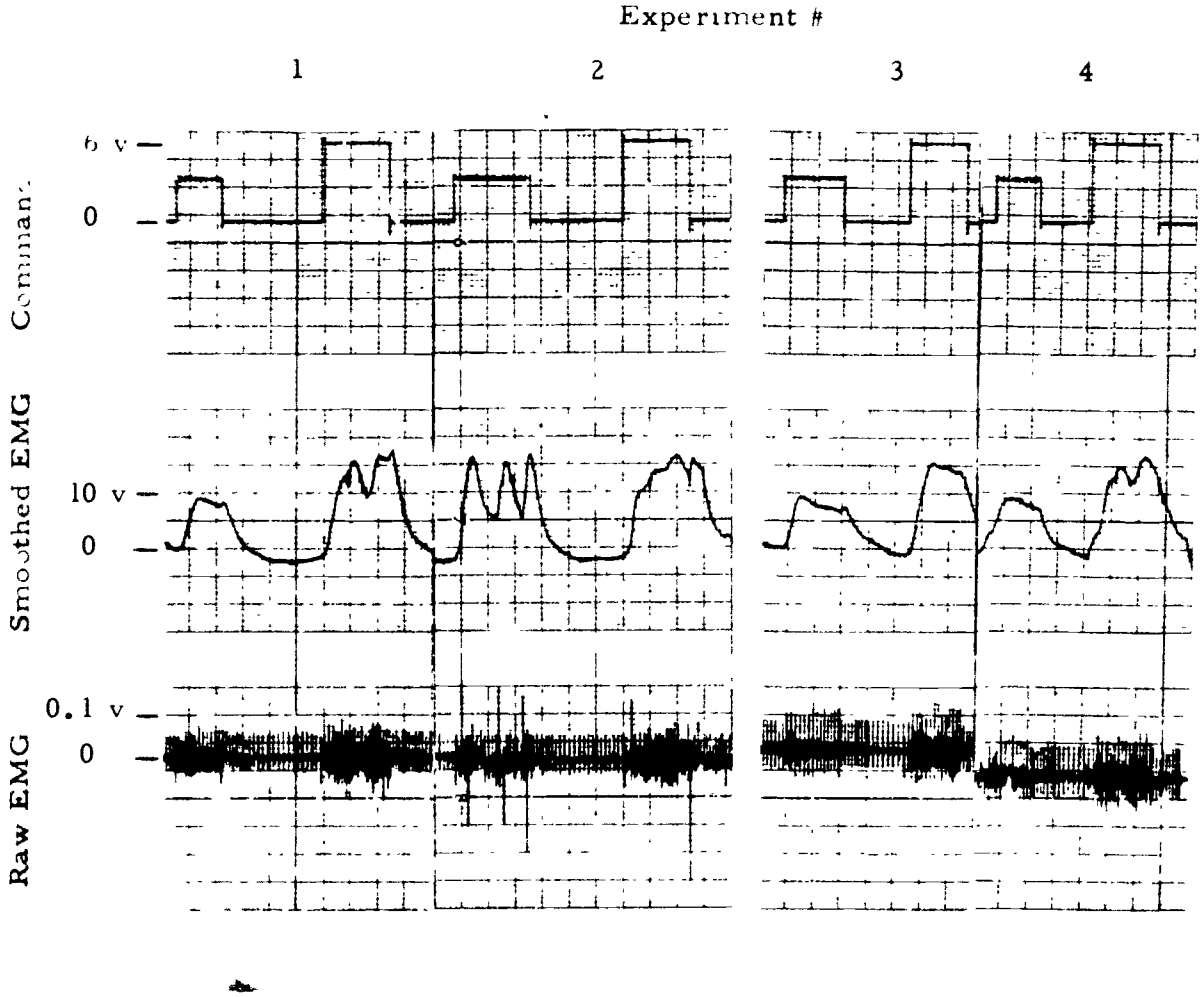

Figure 29. Subject #2

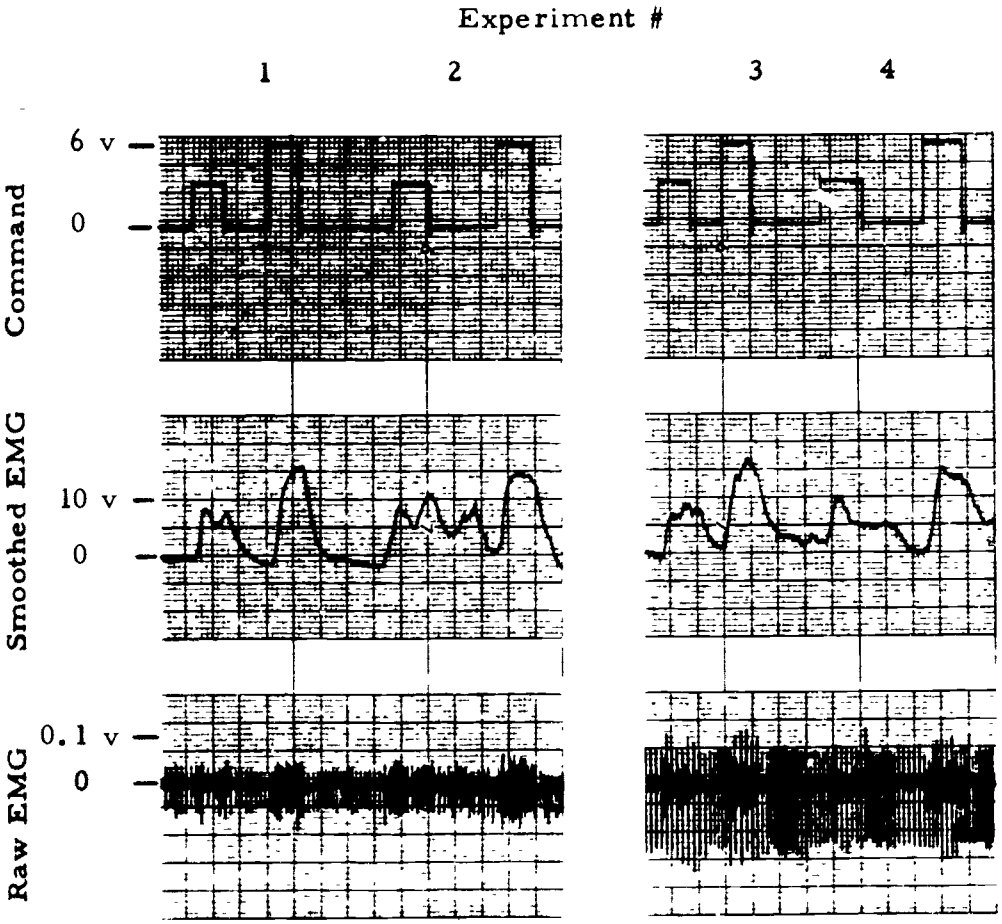

Figure 30. Subject #5

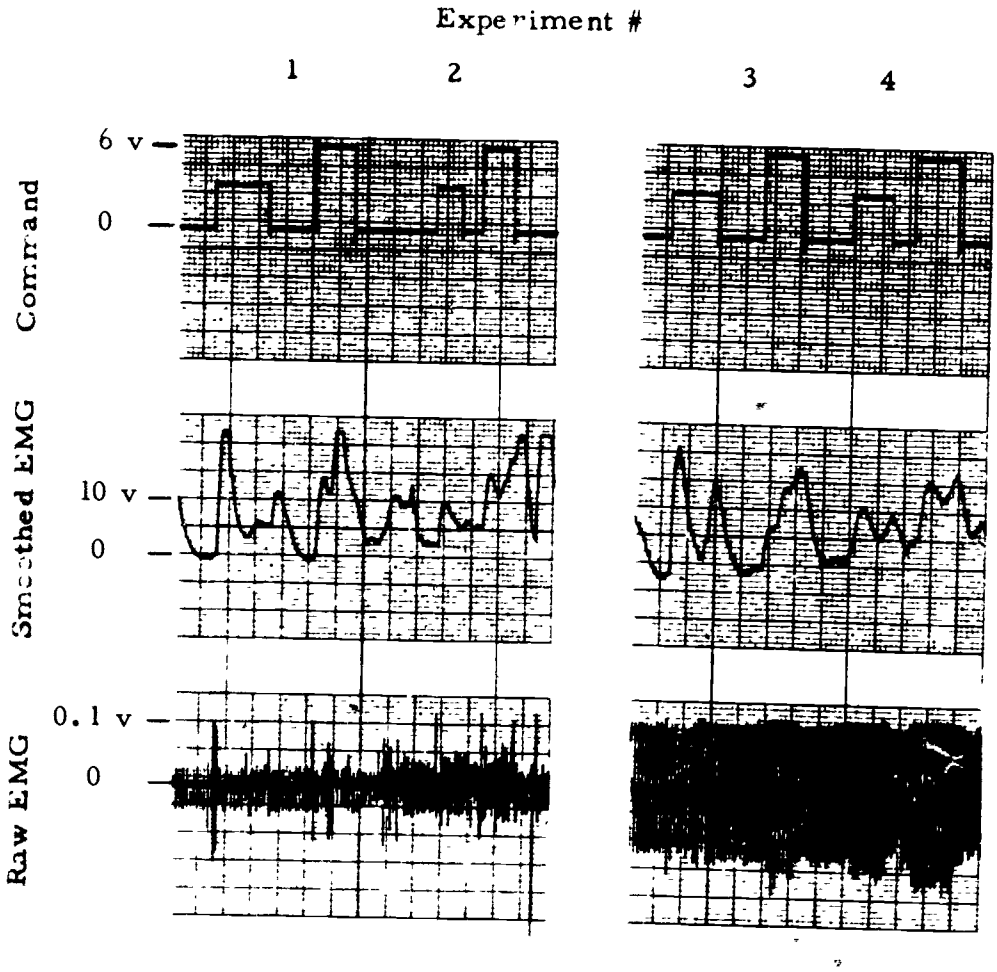

Figure 31. Subject #5

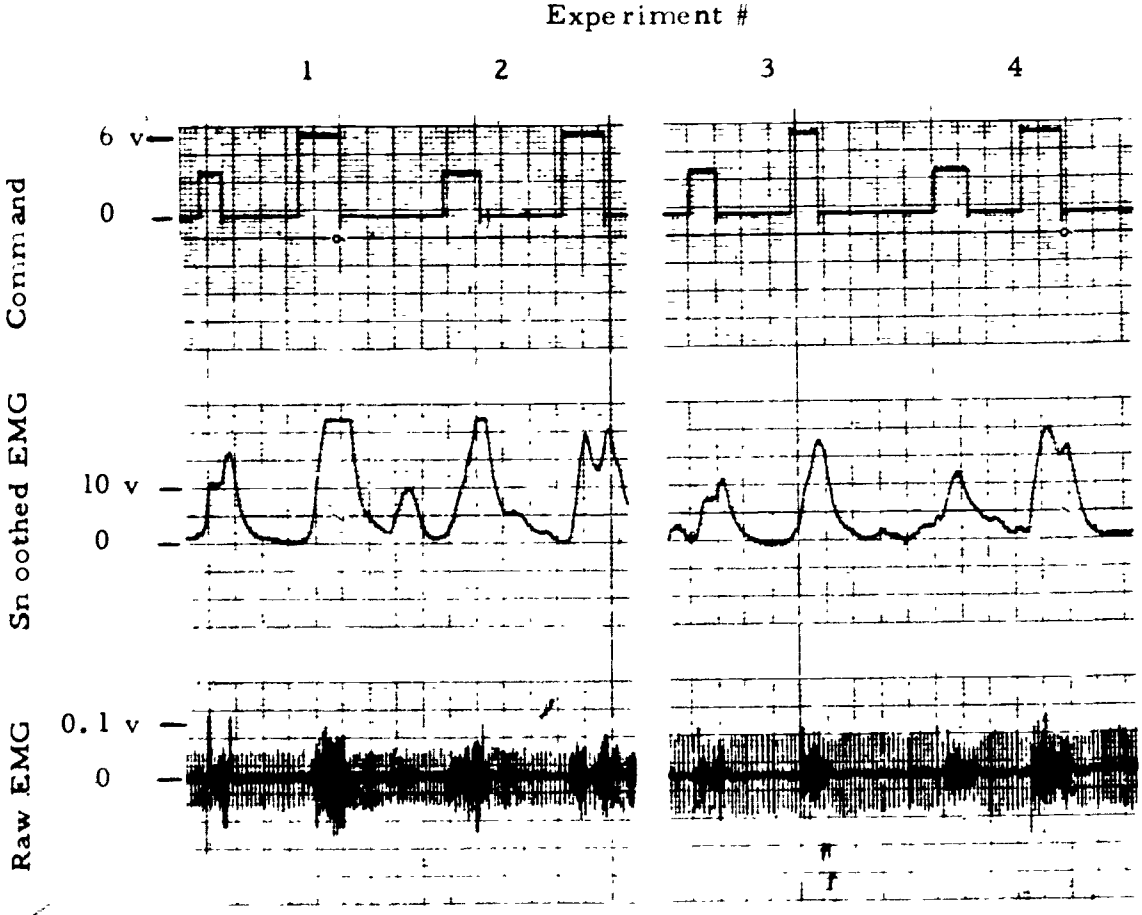

Figure 32. Subject #7

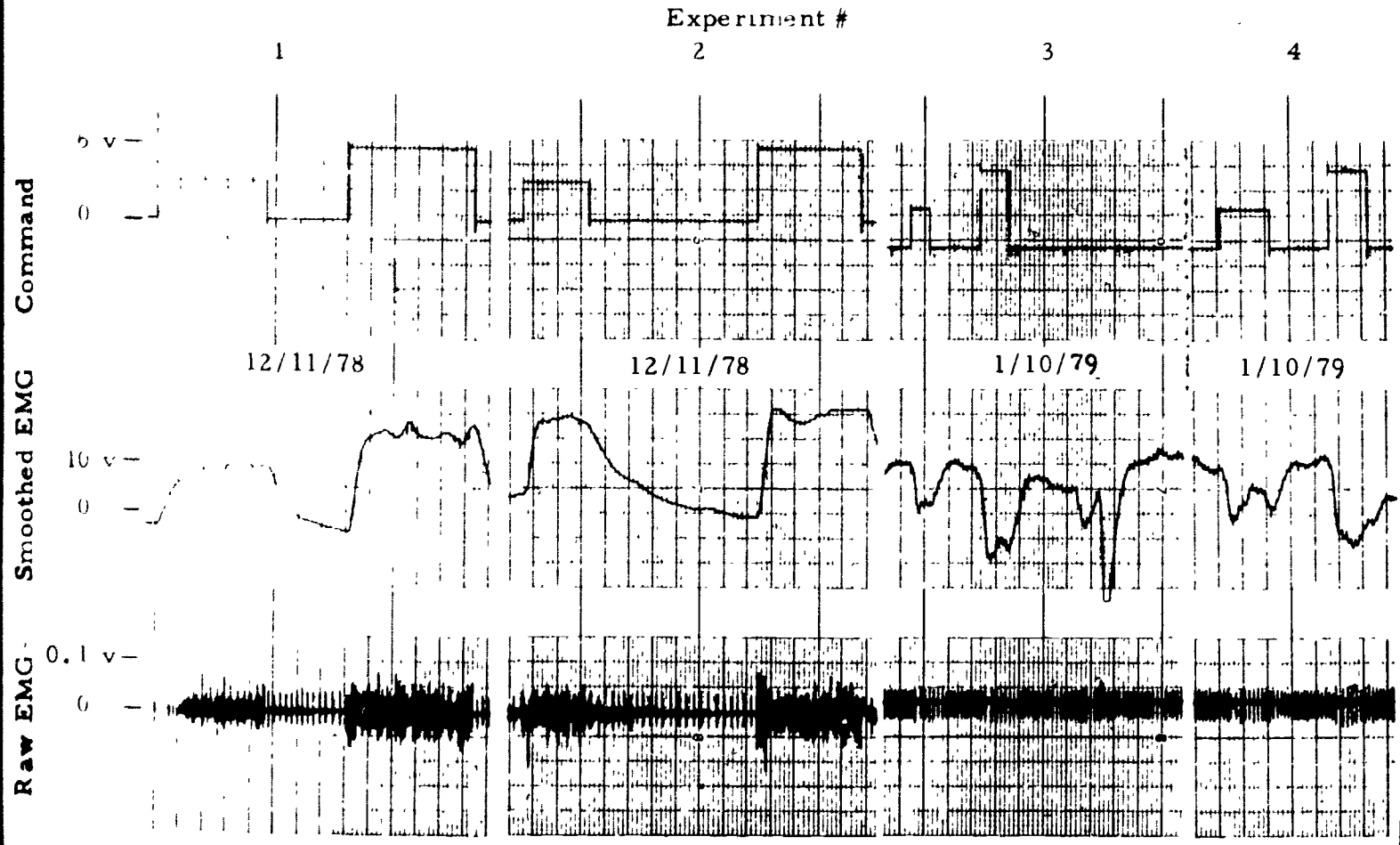

Figure 33. Subject #1

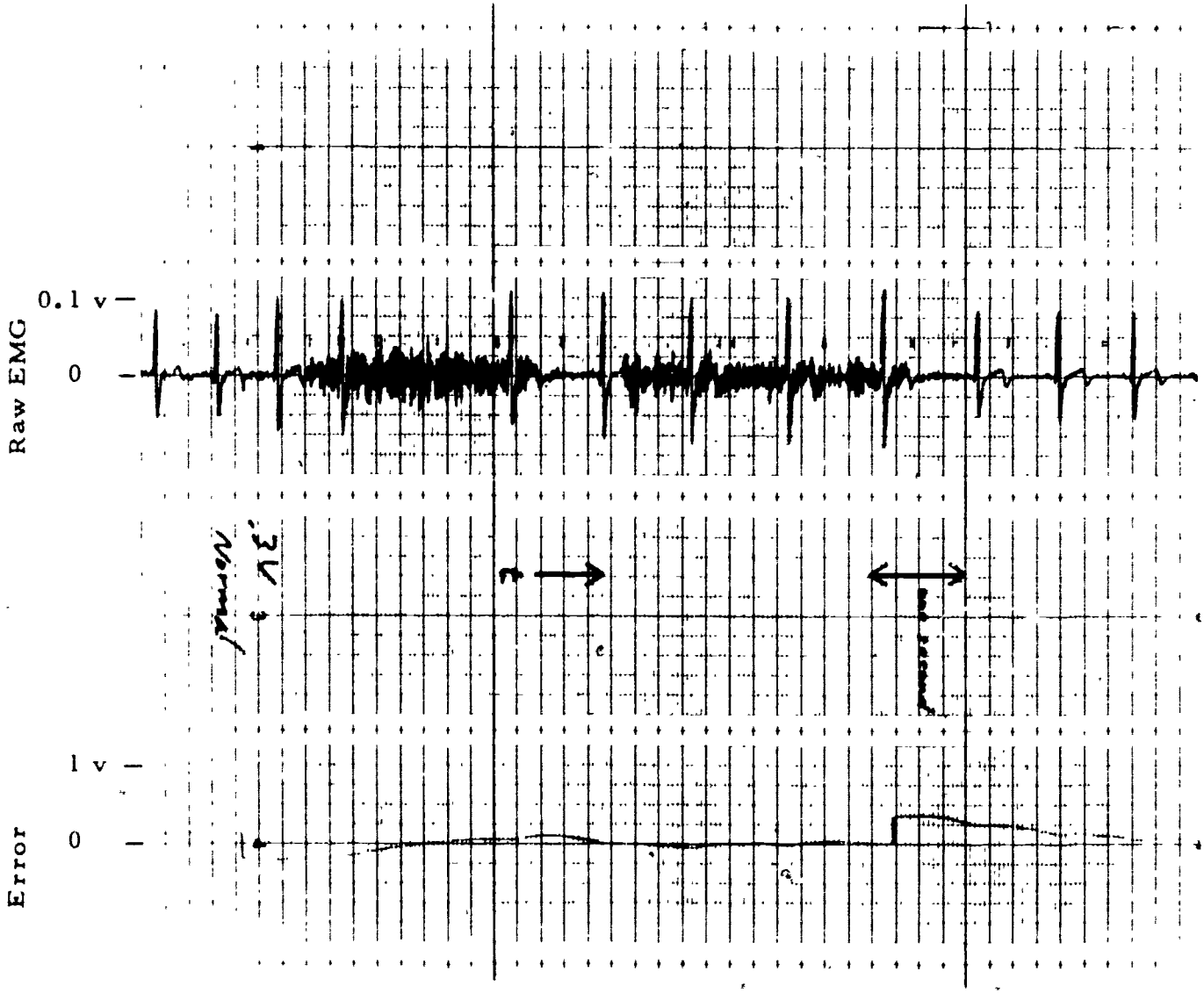

Figure 34. Subject #8, STARS

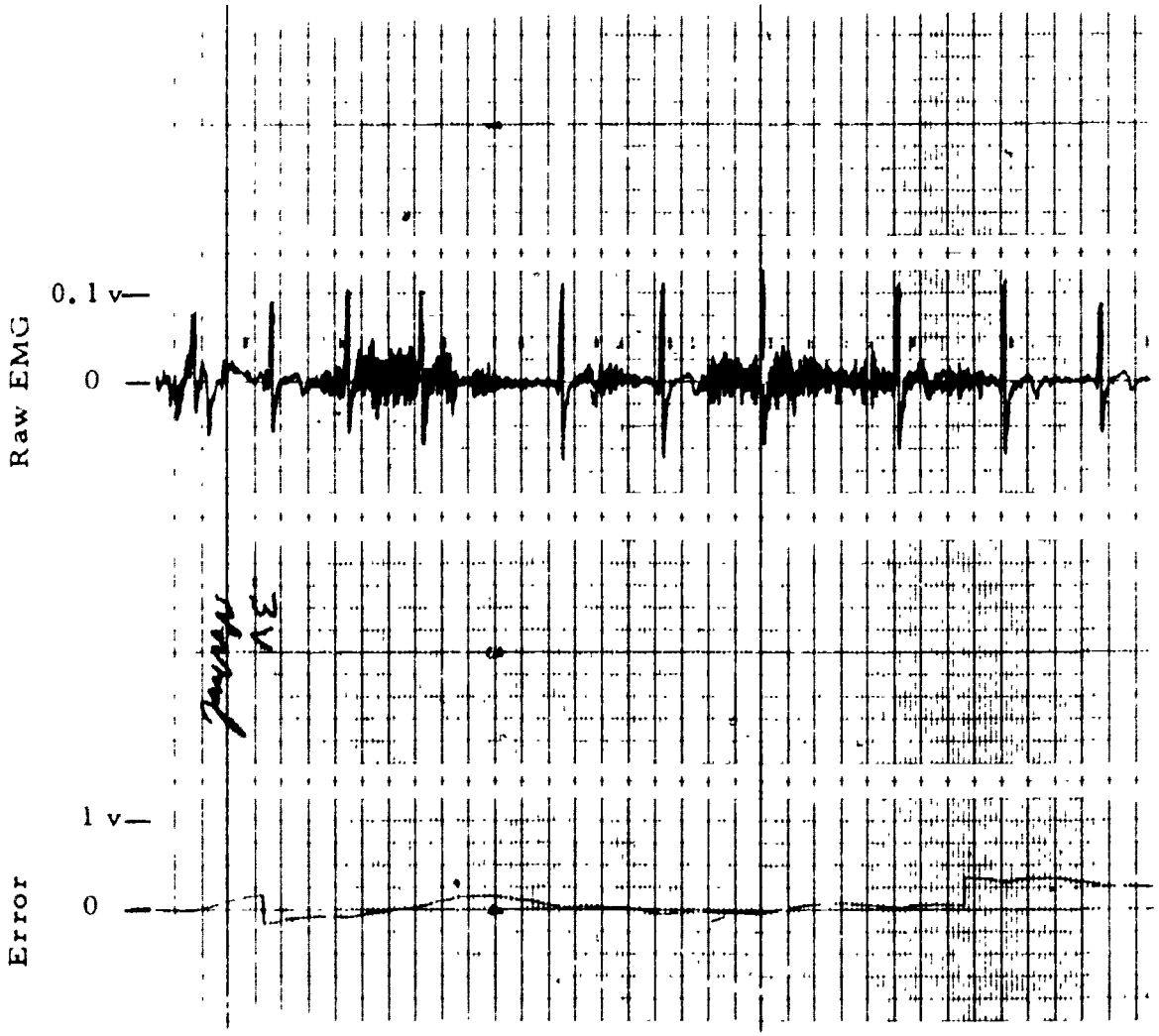

Figure 35. Subject #8, STARS

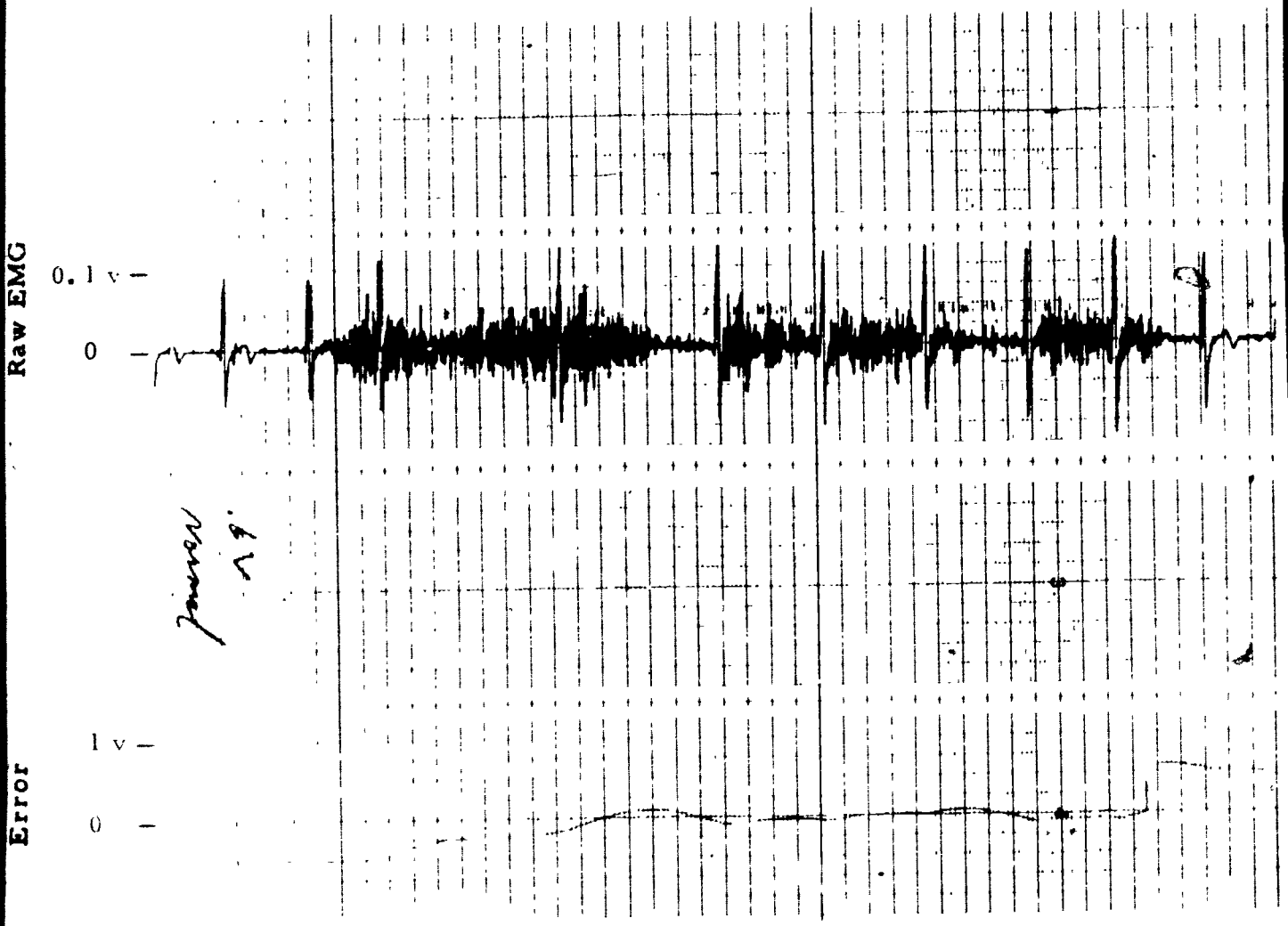

Figure 36. Subject #8, STARS

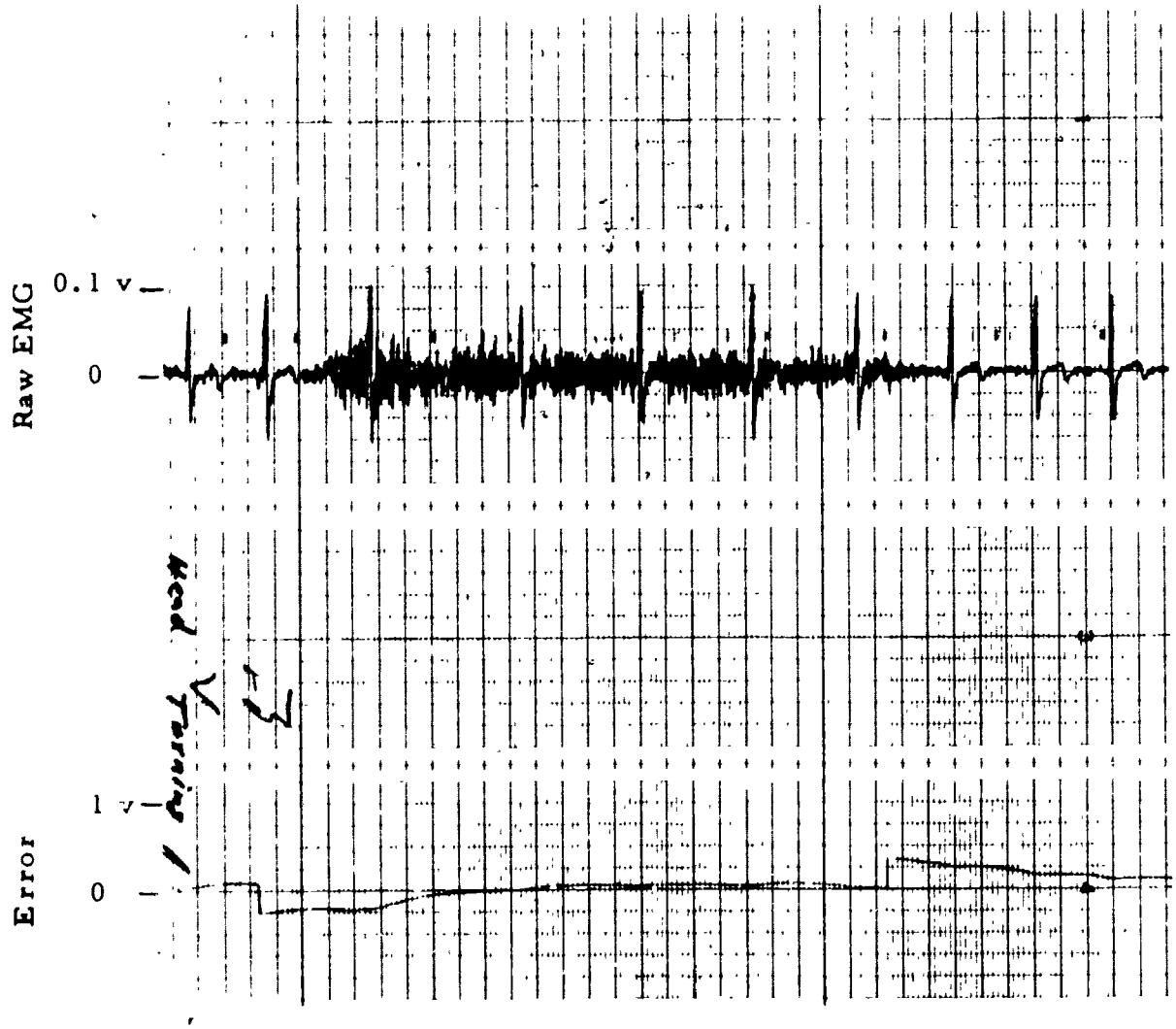

Figure 37. Subject #8, STARS

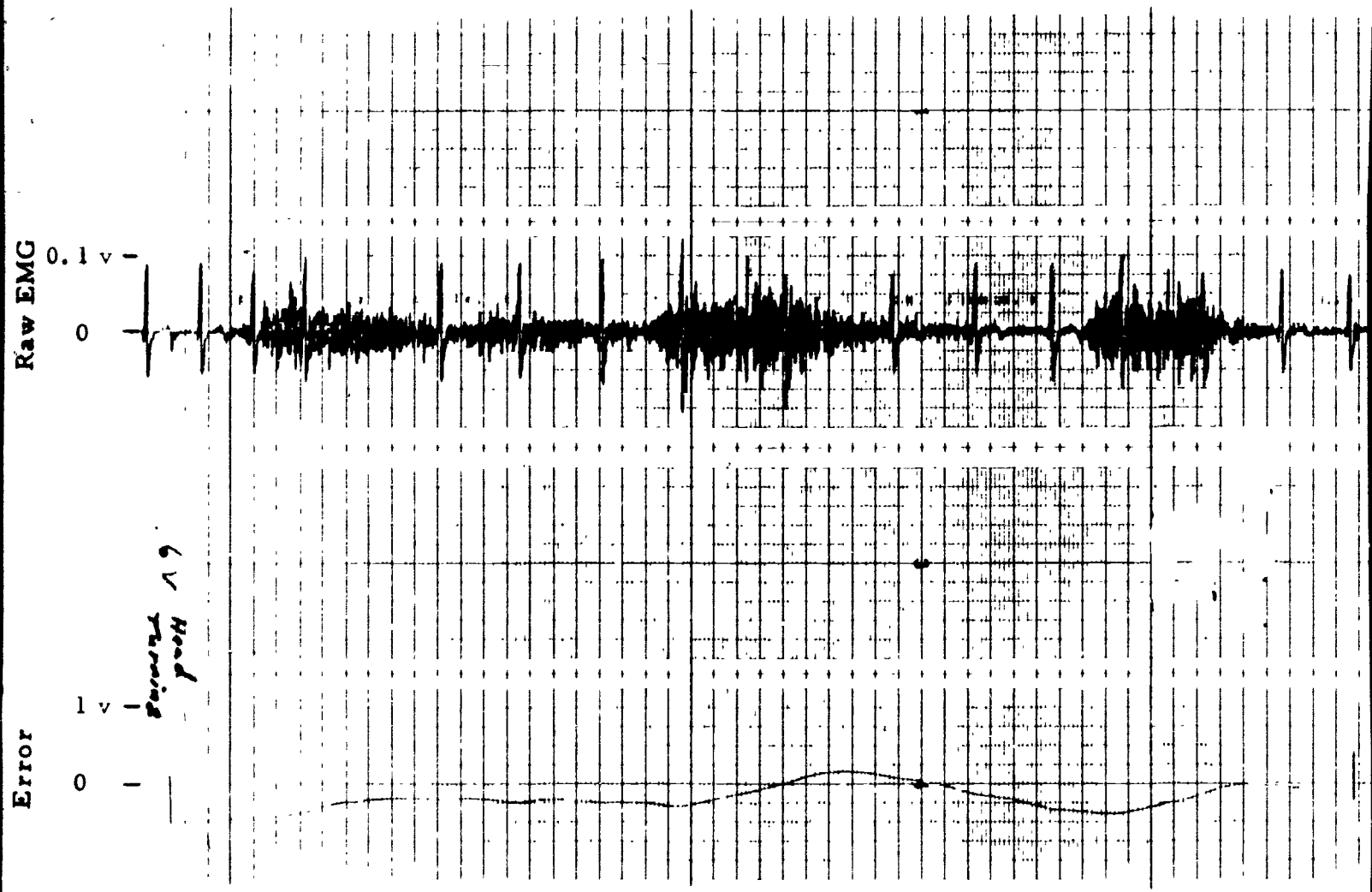

Figure 38. Subject #8, STARS

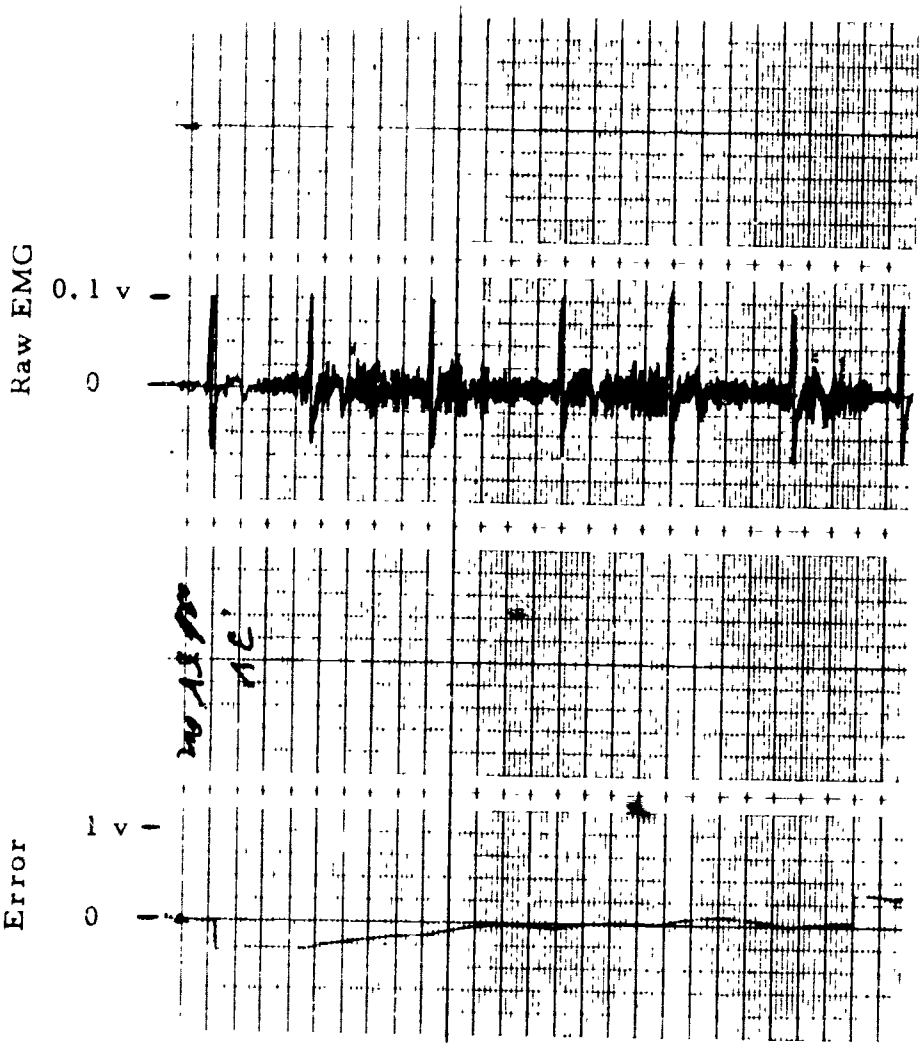

Figure 39. Subject #8, STARS

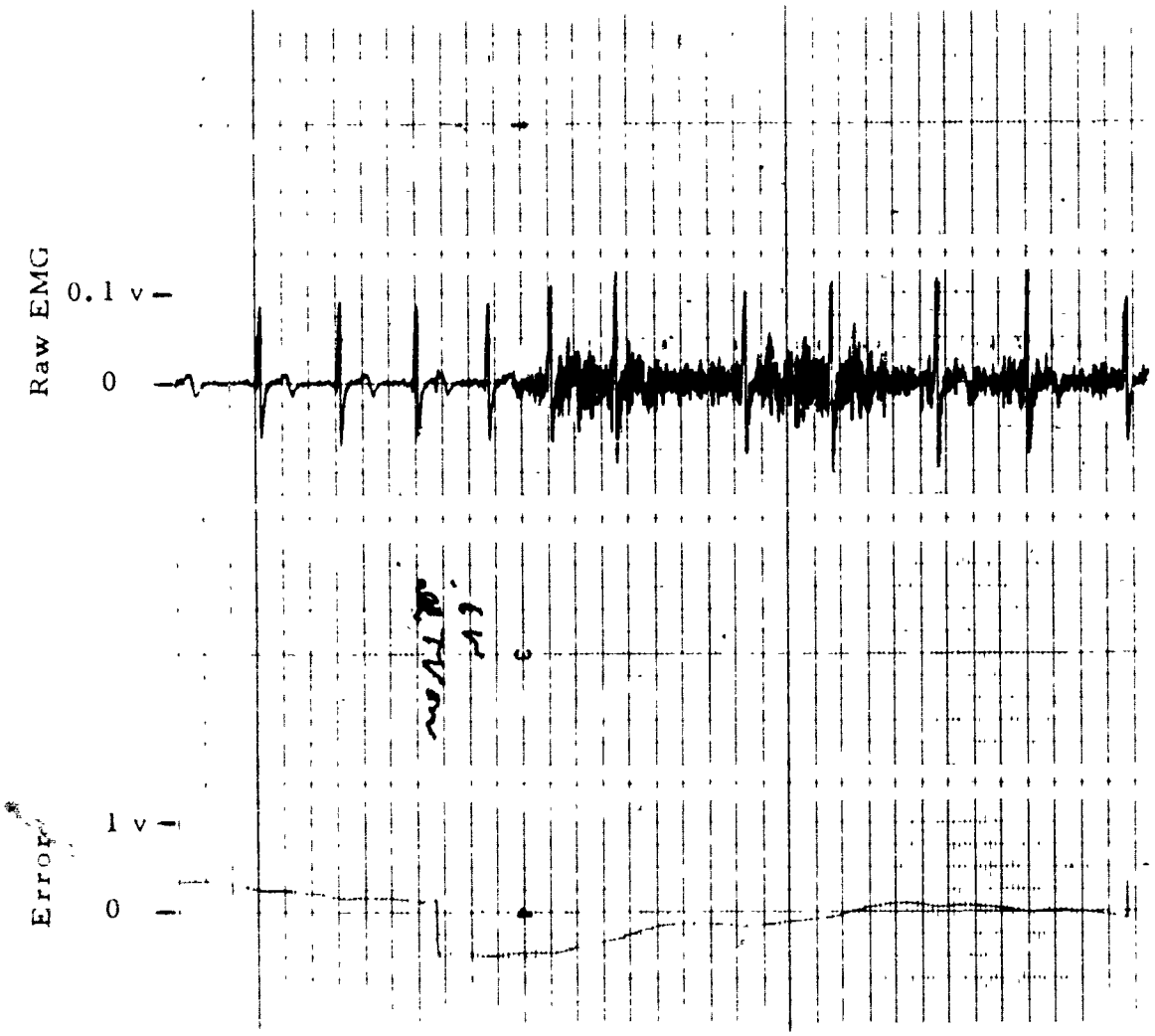

Figure 40. Subject #8, STARS

are easier to mount, may be used several times, and the lotion in them may be replenished if dry. However, removal of the adhesive electrodes is not pleasant since they pull hairs out.

A difficulty with amplifier saturation in the TR-20 was initially encountered at the STARS facility. However, when the gain was reduced by a factor of 10, everything operated normally. To compensate for the reduced gain, command signal levels were also reduced to 0.3 and 0.6 volts.

Some very high frequency (2 MHz), low amplitude, noise pick-up was observed on an oscilloscope connected to the raw EMG signal. This may have been due to the TV. Since it did not interfere with the BIOCONAID system operation, it was concluded that electronic noise pick-up at the STARS facility would not be too severe.

SECTION 5
CONCLUSIONS AND RECOMMENDATIONS

5.1 CONCLUSIONS

The BIOCONAID System offers the potential to provide a very realistic simulation of visual dimming with straining during large accelerations. The Dynamic Visual Response Algorithm provides a simulated visual response in agreement with experimental observations and known physiology. The EMG Algorithm provides an input to the visual response which is also in agreement with experimental observations of straining during large accelerations.

The EMG subsystem provides a smoothed, reliable straining signal, not adversely affected by extraneous limb movements. Either abdomen (external oblique) or the back (latissimus dorsi) muscles are suitable as electrode sites.

All parts of the BIOCONAID System have been carefully checked-out with the exception of the Visual Field Model. Equipment limitations at the STARS facility prevented the full implementation of the Visual Field Model during the contract period. Thus final determination of system effectiveness must await complete system implementation and evaluation in an appropriate simulator. A test plan for such implementation and evaluation is contained in Appendix A.

5.2 RECOMMENDATION

It is strongly recommended that the BIOCONAID System be implemented, demonstrated and evaluated in an appropriate Air Force simulator with experienced pilots. Although the system appears to provide a realistic simulation of visual dimming while straining, human pilot evaluations are necessary to determine system effectiveness. It is expected that such

implementation would involve fine adjustment of some algorithm gains, thereby enhancing the system.

It is also recommended that some medical research be conducted into the physiological effects of sustained straining in a 1-G environment. It would be extremely useful to identify the level of straining which causes significant detrimental cardiovascular effects, as well as the level of straining which causes negligible detrimental effects. This medical research should begin with a literature review of experimental and historical data. If this review does not yield definitive answers on the above straining levels, new experiments on human subjects or animals should be conducted to yield the desired results. This information is necessary for the safe implementation of the BIOCONAID System in a training environment.

SECTION 6

REFERENCES

1. Berne, Robert M. and Levy, M. N., Cardiovascular Physiology, 2nd Ed., St. Louis, Missouri: The C. V. Mosby Company, 1972.

2. Bigland, B. and Lippold, O. C. J., "The Relation Between Force, Velocity and Integrated Electrical Activity in Human Muscles," J. Physiol., Vol. 123, pp. 214-224, 1954.

3. Brody, G., Scott, R. N., and Balasubiramanian, R., "A Model for Myoelectric Signal Generation," Medical and Biological Engineering, pp. 29-41, January 1974.

4. Burton, R. R., Leverett, S. D., and Michaelson, E. D., "Man at High Sustained $+G_z$ Acceleration: A Review," Aerospace Med., Vol. 45, No. 10, pp. 1115 1136, 1974.

5. Chambers, R. M. and Hitchcock, Lloyd, Effects of Acceleration on Pilot Performance, Johnsville, Penn.: U.S. Naval Air Development Center, NADC-MA-6219, March 1963.

6. Davenport, Wilbur B., Jr. and Root, William L., Random Signals and Noise, N. Y.: McGraw Hill Book Co., 1958.

7. Davson, H., editor, The Eye, 2nd Ed., N. Y.: Academic Press, 1969.

8. Fraser, T. M., Human Responses to Sustained Acceleration, NASA SP-103, 1966.

9. Gaur, O. H. and Zuidema, G. D., Gravitational Stress in Aerospace Medicine, Boston, Mass.: Little, Brown & Co., 1961.

10. Gillingham, K. K. and McNaughton, G. B., "Visual Field Contraction During G Stress at 13°, 45° and 65° Seatback Angles," Aviation Space and Environmental Med., Vol. 48, No. 2, pp. 91-96, 1972.

11. Gillingham, K. K., Freeman, J. J., and McNee, R. C., "Transfer Functions for Eye Level Blood Pressure During $+G_z$ Stress," Aviation Space and Environmental Med., Vol. 48, No. 11, pp. 1026-1034, 1972.

12. Gillingham, K. K. and Krutz, R. W., Brooks AFB, Texas, USAFSAM AR10-74, 1974.

13. Howard, P., "The Physiology of Positive Acceleration," Chapter 23 in A Textbook of Aviation Physiology, Edited by J. A. Gilles, Pergamon Press, 1965.

14. Knapp, C., Randall, D., Evans, J. and Marquis, J., "Frequency Response of Cardiovascular Regulation in Canines to Sinusoidal Acceleration at Frequencies Below 1.5 Hz," paper presented at the Review of Air Force Sponsored Basic Research in Environmental and Acceleration Physiology, Wright-Patterson AFB, Ohio, October 13-15, 1978.

15. Koushanpour, E. and Spickler, J., "Effect of Mean Pressure Levels on the Dynamic Response Characteristics of the Carotid Sinus Baroreceptor Process in a Dog," IEEE Trans. Biomed. Engineering, BME, Vol. 22, No. 3, pp. 502-507, 1975.

16. Leverett, S. D., Whitney, R. U., and Zuidema, G. C., "Protective Devices Against Acceleration," in Gravitational Stress in Aerospace Medicine, Edited by O. H. Gauer and G. D. Zuidema, Boston, Mass.: Little, Brown & Co., 1961.

17. Lewis, D. H. and Duane, T. D., "Electroretinogram in Man During Blackout," J. Appl. Physiol., Vol. 9, pp. 105, 1956.

18. Lindberg, E. F. and Wood, E. H., "Acceleration," in Physiology of Man in Space, Edited by J. H. U. Brown, N. Y.,: Academic Press, 1963.

19. Lindberg, E. F., Sutterer, W. F., Marshall, H. W., Headley, R. N., and Wood, E. H., "Measurement of Cardiac Output During Headward Acceleration Using the Dye-Dilution Technique," Aerospace Med., Vol. 31, No. 8, pp. 817, 1960.

20. Miller, N. C. and Green, J. F., "A Model Describing Acceleration-Induced Blackout," Annals of Biomedical Engineering, Vol. 2, 1973.

21. McCally, M., "The Effect of Sustained Muscular Contraction on Tolerance to $+G_z$ Acceleration," Ph. D. Dissertation, The Ohio State University, 1970.

22. Newsom, W. A., Leverett, S. D., and Kirkland, V. E., "Retinal Circulation in Man During Centrifugal Acceleration," Trans. Amer. Acad. Ophthal. and Otalaryn., Vol. 72, pp. 39, 1968.

23. Rogers, Dana B., Myoelectric Feedback Control of Acceleration Induced Visual Scene Dimming in Aircraft Training Simulators, the University of Dayton, Ph. D. Dissertation (copyrighted), July 1978.

24. Rushmer, R. F., "Circulatory Effects of Three Modifications of the Valsalva Experiment: An Experimental Survey," Amer. Heart J., 1946.

25. Shannon, R. E., Systems Simulation: The Art and Science, Englewood Cliffs, N. J.: Prentice Hall, 1975.

26. White, William J., Acceleration and Vision, Wright-Patterson AFB Ohio: Wright Air Development Center, WADC TR-58-333, November 1958.

SECTION 7

BIBLIOGRAPHY

1. Barton, R. F., A Primer on Simulation and Gaming, Englewood Cliffs, N. J.: Prentice Hall, 1970.

2. Cadzow, J. A. and Martens, H. R., Discrete-Time and Computer Control Systems, Edited by F. F. Kuo, Englewood Cliffs, N. J.: Prentice Hall, 1970.

3. Chambers, R. M., "Acceleration," Chapter 3, Bioastronautics Data Book, NASA SP-3006, 1964.

4. Clark, W. G. and Jorgenson, H., Studies of Self-Protective Anti-Blackout Maneuvers, Washington, D.C.: National Research Council, Committee on Aviation Medicine, Report No. 488, 1945.

5. Coggshall, J. C. and Bekey, G. A., "EMG-FORCE Dynamics in Human Skeletal Muscle," Medical and Biological Engineering, Vol. 8, No. 3, pp. 265-270, May 1970.

6. Cole, D. F., "Comparative Aspects of Intraocular Fluids," Chapter 2 in The Eye, Vol. 5, Davison, H. and Graham, L. T., Jr., N. Y.: Academic Press, 1974.

7. Forrester, J. W., World Dynamics, Cambridge, Mass.: Wright Allen Press, Inc., 1973.

8. Gauer, O. H., "The Physiological Effects of Prolonged Acceleration," in German Aviation Medicine, World War II, Vol. I, Washington, D. C.: Superintendent of Documents, U.S. Government Printing Office, 1950.

9. Glaister, D. H., The Effects of Gravity and Acceleration on the Lung, England: Technivision Services, AGARDograph 133, 1970.

10. Gray, H., Anatomy, Descriptive and Surgical, Philadelphia, Penn.: Running Press, 1974.

11. Gray, S., III., Shaver, J. A., Kroetz, F. W., and Leonard, J. J., "Acute and Prolonged Effects of G Suit Inflation on Cardiovascular Dynamics," AMA Proceedings, Bal Harbor, Florida, 1968.

12. Greer, B. Y., Smedal, H. A., and Wingrove, R. C., Centrifuge Study of Pilot Tolerance to Acceleration and the Effects of Acceleration on Pilot Performance, NASA TN D-337, 1960.

13. Ham, G. C., "Effects of Centrifugal Acceleration on Living Organisms," War Med., Vol. 30, No. 3, 1943.

14. Harrison, L., III., "A Study to Investigate the Feasibility of Utilizing Electrical Potentials on the Surface on the Skin for Control Functions," Blue Bell, Penn.: Philco Corp., Report No. 2386, AD-619311, July 1964.

15. Kron, G., Young, L., and Alberry, W., "High-G Simulation - The Tactical Aircraft Simulator Problem," Proceedings of the 10th NTEC/Industry Conference, Orlando, Florida, pp. 49-59, November 1977.

16. Lambert, E. H., "The Physiologic Basis of 'Blackout' as it Occurs in Aviators," Fed. Proc., Vol. 4, pp. 43, 1945.

17. Lambert, E. H., "Physiologic Studies of Man's G Tolerance in Aircraft," Fed. Proc., Vol. 5, pp. 59, 1946.

18. Lambert, E. H., Wood, E. H., and Baldes, E. J., The Protection Against the Effects of Acceleration Afforded by Pulling Against a Weighted Control Stick and the Influence of this on the Effectiveness of Pneumatic Anti-Blackout Suits, Washington, D. C.: National Research Council, Committee on Aviation Medicine, Report No. 265, 1944.

19. Levison, W., Barnett, G., and Jackson, W., "Nonlinear Analysis of the Baroreceptor Reflex System," Circulation Research, Vol. 18, pp. 673-682, 1966.

20. Lewis, D. H., "An Analysis of Some Current Methods of G Protection," J. Aviat. Med., Vol. 26, pp. 479, 1955.

21. Lind, A. R., Taylor, S. H., Humphreys, P. W., Kennelly, B. M., and Donald, K. W., "The Circulatory Effects of Sustained Voluntary Muscle Contraction," Clin. Sci., Vol. 27, pp. 229, 1964.

22. Lind, A. R., McNicol, G. W., and Donald, K. W., "Circulatory Adjustments to Sustained (Static) Muscular Activity," Proc. Symp. Physical Activity in Health and Disease, Oslo: Universitetsforlaget, pp. 38-63, 1966.

23. McRuer, D. T., Magdaleno, R. E., and Moore, G. P., "A Neuromuscular Actuation System Model: IEE Transactions on Man Machine Systems," MMS-0, No. 3, September 1968.

24. Scher, A. and Young, A., "Acceleration," in Physiology of Man in Space, Edited by J. Brown, N. Y.: Academic Press, 1963.

25. Shwedyk, E., Balasubramanian, R., and Scott, R. N., "A Nonstationary Model for the Electromyogram," IEEE Transactions on Biomedical Engineering, Vol. BME-24, No. 5, pp. 417-424, 1977.

26. Stoll, Alice M., "Human Tolerance to Positive G as Determined by the Physiological End Points," Aviation Medicine, August 1956.

27. Wani, Ali M. and Guha, S. K., "Summation of Fibre Potentials and the e.m.g.-Force Relationship During the Voluntary Movement of a Forearm," Medical and Biological Engineering, pp. 174-180, March 1974.

28. Wiley, R. L. and Lind, A. R., "Respiratory Response to Sustained Muscle Contractions in Man," Fed. Proc., Vol. 29, pp. 265, 1970.

29. Wirta, R. W., Cody, K. A., and Finley, F. R., "Myopotential Patterns and External Control: Effects of Practice and Fatigue," Willow Grove, Penn.: Philco Ford Corp., Report AD-655140, 1967.

30. Wood, E. H. and Lambert, E. H., "Some Factors Which Influence the Protections Afforded by Penumatic Anti-G Suits," J. Aviat. Med., Vol. 23, pp. 218, 1952.

31. Zarriello, J. J., Seale, L. M., and Norsworthy, M. E., "The Relationship Between Cardiovascular Response and Positive G Tolerance," Aviation Medicine, November 1958.

32. Bioastronautics Data Book, Edited by Paul Webb, NASA SP-3006, 1964.

APPENDIX A

TEST PLAN
BIOCONAID
(Bionic Control of Acceleration Induced Dimming)
SYSTEM TEST AND EVALUATION

A.1 INTRODUCTION

This test plan pertains to the performance evaluation of the final design of a system for bionic control of acceleration induced dimming (BIOCONAID). Present advanced flight simulators provide a system for dimming the pilot's visual scene to simulate partial blackout when the aircraft normal acceleration exceeds an appropriate level. The new system goes one step beyond and provides for control of the dimming through the pilot's muscular straining action (M-1 or L-1 maneuver). The BIOCONAID system has been designed by the University of Dayton under Contract F33615-77-C-0080 with the Air Force Human Resources Laboratory. This test plan has been prepared to fulfill a contractual requirement.

The plan involves installing the BIOCONAID system in the SAAC F-4 Simulator at Luke AFB, conducting the tests using experienced Air Force pilots, removing the BIOCONAID system and writing a report. The intention is to minimize interference with normal training use of the simulator during the evaluation. A seven week period is provided for installation, interfacing and check-out followed by a one-week test period. Disassembly and removal will be accomplished in one day.

The specific time schedule for the tests is dependent upon the date Air Force go-ahead is given and upon other Air Force instructions. The University of Dayton anticipates this evaluation will be conducted under an additional contractual arrangement. The following section contains the test objectives.

A.2 TEST OBJECTIVES

A.2.1 Objective A

To evaluate the performance of the final design, specifically, is the visual scene dimming reliably and realistically controlled by pilot straining? To answer this question, the system must be observed during long-term, high-acceleration turns. In addition, however, observations must be made during rapidly changing maneuvering accelerations as well as during periods of low dynamic acceleration. These latter observations will be for the purpose of determining whether the final design is free from inappropriate responses. All tests will be done with and without the electromyographic feedback to allow comparisons to be made.

A.2.2 Objective B

To conduct other tests on the final system. These "other tests" include further evaluation of several EMG electrode types and electrode sites and further evaluation of system tolerance to extraneous motion. These tests can be done with minimal increase in test time beyond the Objective A_2 tests and they should be very significant since they will involve Air Force pilots in actual simulated flight. Pilot tolerance for the electrodes is the most important question to be answered. Electrodes to be included in these tests are:

- strap-on, reusable many times
- adhesive, disposable
- electrode belt
- seat pan electrodes (if available)

Electrode sites included are:

- abdomen (external oblique)
- back (latissimus dorsi)
- buttock (with seat pan electrodes)

A.3 TEST PROCEDURE

A.3.1 General

During a one-week test period a number of experienced Air Force pilots will act as test subjects to perform simulator flights aimed at accomplishing the test objectives. The planned number participating is ten (10), although more would be welcome. Each pilot will be briefed, electrodes will be installed and a short practice period with the BIOCONAID system will be provided. Next, the actual test maneuvers will be accomplished. These maneuvers consist of long-term, high acceleration turns in both directions, short-term, rapidly changing acceleration turns or aerobatics and normal operations near one-G, such as landing pattern. Details of the test protocol are given below. Finally, after the flight, the electrodes will be removed and the pilot will be debriefed. Each pilot will provide a brief written observation report which will be included in the final test report.

The actual time-in-simulator for each pilot is estimated as 30-45 minutes and the total time per pilot is estimated as 1—1-1/2 hours. The time of day for the tests will be such as to minimize interfering with the normal simulator training schedule. Once the BIOCONAID equipment is installed, it can be used or not used as desired. Merely placing a switch in the OFF position returns the simulator to its original configuration.

A.3.2 Specific Test Protocol

Time (min)/Cum.	Activity
13/13	Pilot Briefing: - Review blackout phenomena - Review M-1/L-1 maneuver - Explain BIOCONAID system - Explain test objectives - Describe test procedure - The need for electrodes

2/15 Install electrodes according to the following table:

No. Pilots	Type	Location
1	Strap-on	back
1	Strap-on	abdomen
2	Belt	waist
3	Paste-on	back
3	Paste-on	abdomen

If seat pan electrodes are available, they will be used with all pilots (i.e. for part of each pilot-test period).

10/25 Pilot enters and starts simulator, climbs to 5000 ft altitude and practices turns to familiarize himself with BIOCONAID.

20/45 Test Period. Pilot does the following maneuvers at 5000 ft, Mach .8 on instruction from controller (roll level after each turn):

- A 360° turn right with 60° bank angle (2G)
- Repeat to left without EMG feedback
- A 360° turn right with 70° bank angle (2.92 G) twist body and head to look over right shoulder
- Repeat to left without EMG feedback, twist body and head to look over left shoulder
- A 360° turn right with 80° bank angle (5.76G)
- Repeat to left without EMG feedback
- A series of alternating right and left turns of 45° with bank angle 70°, rolling directly from one turn into the next. Eight turns will be done (last four without EMG).
- A Chandelle right followed by a Chandelle left (no EMG)
- A Lazy-Eight (no EMG when turning left)
- A rectangular landing pattern

5/50 Pilot shuts down simulator, deplanes, and electrodes are removed.

20/70 Pilot is debriefed and gives written observations:

- Tolerance for electrodes.
- Was energy expenditure to avoid blackout realistic?
- Compare with and without EMG as regards realism of simulated flight.
- Was the onset of blackout and the recovery through straining realistic?
- Was the beneficial effect of the G-suit realistically simulated?
- Tolerance of system to body twisting.
- Further comments or recommendations.

A.3.3 Recordings

Figure 41 shows a block diagram of the integrated system including pilot, aircraft, G-suit, cardiovascular model, straining model, and visual scene model. The numbers and names used below for recorded variables refer to Figure 41.

Both digital and analog signals will be recorded. It is anticipated that digital variables will be transferred to tape and printed off-line. The analog recorder will be turned on and off by one of the operators as the test progresses.

Teletype input to the simulator computer will result in appropriate printed identification of data pertaining to each maneuver. When a new maneuver is due, the teletype input is changed by the operator.

Table A-1 lists variables to be recorded together with type (digital or analog) and frequency of observation.

A.4 TIME SCHEDULE

(Note: T = First test day, designated by AF)

TIME	EVENT
T-49	UD personnel (3) visit Luke AFB for test planning
T-39	UD ship or transport equipment to Luke AFB

TABLE A-1

TABLE OF RECORDINGS

	Type	Once	Each Maneuver	Each Second	Continuous
Date, hour, subject	D	X			
Electrode Location	D	X			
Electrode Type	D	X			
Maneuver	D		X		
Time	D			X	
Roll Angle (ϕ)	D			X	
Heading Angle (ψ)	D			X	
G-level (N_Z)	D			X	
Raw Straining Signal	A				X
Processed Strain Signal (EMG)	A				X
G-Suit Protection Value PV_G	D			X	
Cardiovascular Model Output, PV_C	D			X	
Straining Protection Value, PV_S	D			X	
Net Protection Value, PV	D			X	
Dimming Signal (Output of Visual Scene Model)	A				X
Visual Scene Light Intensity	A				X

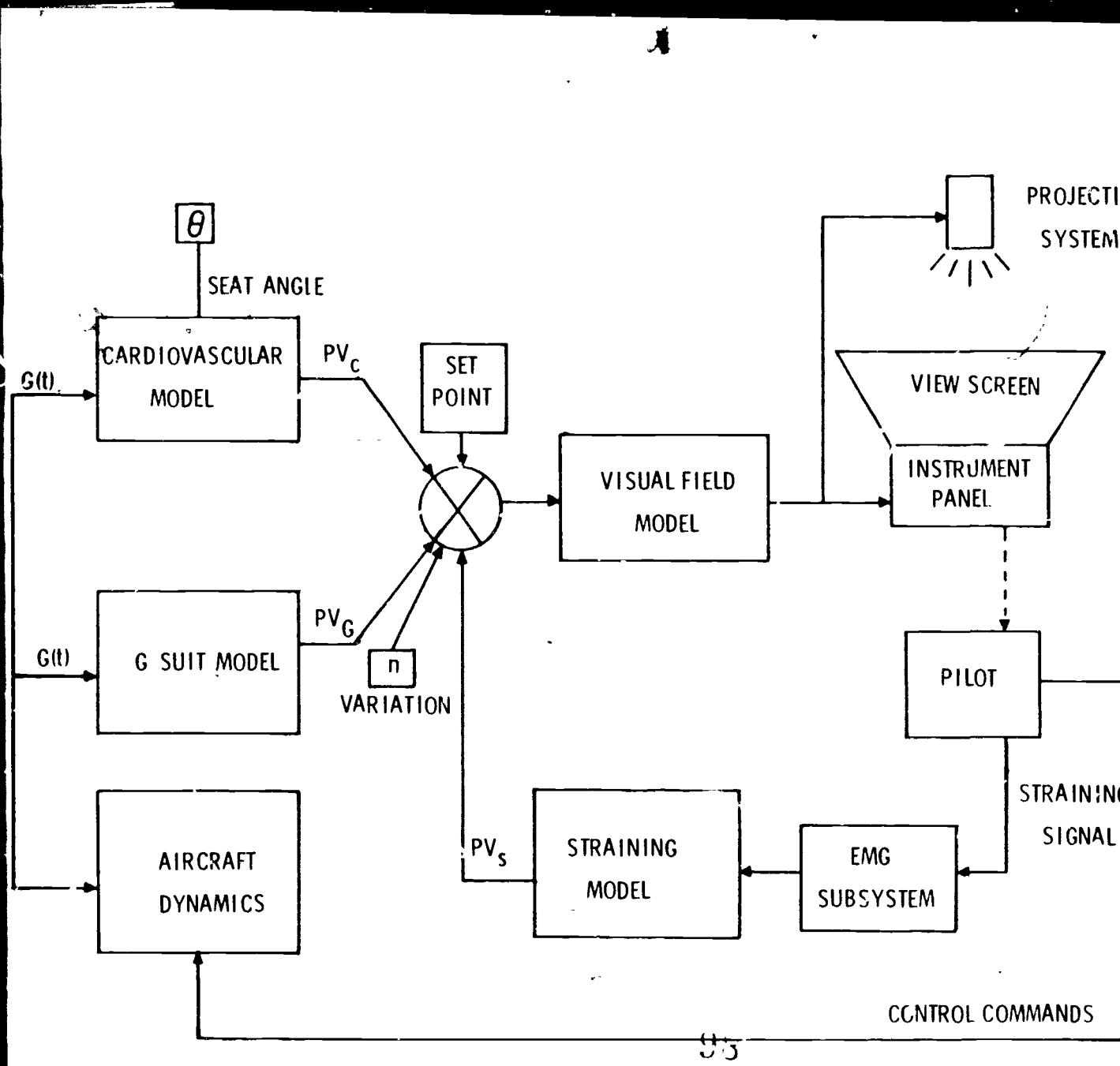

Figure A-1 System Integration Diagram

T-37	UD engineer/programmer arrives Luke AFB, begin interfacing equipment and software
T-27	Interfacing complete
T-17	Piloted system checkout starts (one AF pilot needed)
T-10	BIOCONAID system check-out complete
T-5	Formal demonstration of system and AF approval to proceed with test
T	Testing starts
T+6	Testing ends
T+7	Equipment removed, simulator restored to original configuration
T+67	Draft copy of final test report to AFHRC

A.5 IMPACT ON SAAC SIMULATOR SCHEDULE

It is expected that the simulator designated for these tests will be already fully utilized during normal duty hours for training activities. Consequently, the training usage should retain first priority and the test program activities would proceed on a "time available" basis. Hopefully, evening and weekend hours would be available regularly during the 44 day set-up and test period. It is estimated that an average of two hours operating time per day would be required.

Care will be taken to insure that installation of the test equipment and software is done in such a way that it does not affect the normal training use of the simulator. This means that simple switches and teletype entries will disarm all test provisions and leave the simulator in its original operating mode.

Also, the test provisions will be installed so that they may be rapidly removed leaving the simulator in its original configuration. Complete removal of test provisions from the site will require less than one day.

A.6 AIR FORCE SUPPORT REQUIREMENTS

A.6.1 Equipment

SAAC (F-4) Simulator (80 operating hours)

Includes:
- digital computer capable of handling software
- one analog/digital port
- light dimming capability

Four channel strip chart recorder.

A.6.2 Personnel

1 Project Officer - liaison with base (part-time)

1 Simulator operator/maintenance technician - to operate simulator (if required), monitor test installation (part-time), answer questions

10 (or more) voluntary pilot subjects (1-1/2 hrs each)

1 pilot for "piloted system check-out" prior to tests (4 hrs)

A.6.3 Work Space

Combination office/workroom near simulator.

Access to simulator.

A.6.4 Security

Secure area for UD equipment (table top analog computer, meters, oscilloscope, oscillator, bio-amplifiers, cables, tools).

Security passes for four UD project workers.

Car pass for rental car.

A.7 UNIVERSITY OF DAYTON SUPPORT

A.7.1 Equipment and Supplies

Oscillator

Bio-Amplifiers (6)

Cables and wiring

EMG electrodes

A.7.2 Personnel

2 engineers (one visit per week)

2 technicians or students (full-time on site)

A.7.3 Transportation, Housing and Food

The University will furnish transportation for its personnel and equipment as well as housing and meals for its personnel.

A.8 REPORT REQUIREMENTS

A report will be prepared as prescribed by Air Force instructions. A draft copy will be furnished to AFHRL 60 days after completion of the tests. The report will include the recorded data, the data analysis, the pilot comments, conclusions and recommendations, and a discussion.

APPENDIX B

ALGORITHM LISTINGS

```
00010 C      TFORSRC.BIO  .........DAVID QUAM
00020        COMMON/INPUTS/X(6),DELP,PVS
00030        COMMON/OUTPUT/BPS,BRC,CTS,CTC
00040        DIMENSION Y(3)
00050        REAL N,NFM,K2,LLS,LLC
00060        CB = 1.0
00070        CC = 1.0
00080 C
00090 C
00100 C      INITIALIZATION
00110 C
00120 C
00130 C    G = GAIN OF CARDIOVASCULAR TRANSFER FUNCTION.
00140 C    A,B,C,D,E = TUSTIN CO-EFFICIENTS OF TRANSFER FUNCTION.
00150 C    F = OFFSET DISTANCE OF THE OPTIC DISC FROM THE CENTRAL
00160 C        VISUAL AXIS(10 DEGREES FOR RIGHT EYE)
00170 C    P = OFFSET DISTANCE OF THE OPTIC DISC FROM THE CENTRAL
00180 C        VISUAL AXIS(110 DEGREES FOR THE LEFT EYE)
00190 C    SEAT = SEAT ANGLE (STANDARD IS 13 DEGREES)
00200 C    EYE = OFFSET ANGLE OF EYE FROM PHYSIOLOGIC Z-AXIS
00210 C                  (TYPICALLY, EYE = 5 DEGREES)
00220 C    Z = CONVERSION FACTOR FOR DEGREES TO RADIANS CONVERSION.
00230 C    X(N) = G => DIMENSIONLESS MULTIPLE OF GRAVITY CONSTANT.
00240 C    Y(1) = OUTPUT OF CARDIOVASCULAR TRANSFER FUNCTION.
00250 C    DELP = DIFFERENCE BETWEEN STANDARD PRESSURE SUIT VALVE
00260 C           FILL SCHEDULE AND THE ACTUAL SUIT PRESSURE.
00270 C    PV = TOTAL PROTECTION VALUE.
00280 C    PVC = CARDIOVASCULAR PROTECTION VALUE.
00290 C    PVS = ELECTROMYOGRAPHIC PROTECTION VALUE.
00300 C    PVG = G-SUIT PROTECTION VALUE.
00310 C    PAE = CALCULATED BLOOD PRESSURE AT EYE LEVEL.
00320 C    SI = POLAR POSITION ANGLE IN VISUALFIELD MEASURED
00330 C         COUNTERCLOCKWISE ABOUT VISUAL AXIS FROM RIGHT
00340 C         HORIZONTAL AXIS. (0.LE.SI.LT.2*PI RADIANS.)
00350 C
00360 C    INITIALIZATION FOR DYNAMIC VISUAL RESPONSE ALGORITHM
00370 C
00380 C
00390        G = -21.4
00400        A = -0.882609
```

```
00410         R = 1.875342
00420         C = -0.0947   *G
00430         D = 0.003634 *G
00440         E = 0.09831   *G
00450         F = 0.17453
00460         P = 3.32
00470         IEAT = 0.226893
00480         EYE = 0.0872665
00490         I = 57.2958
00500         X(1) = 0.0
00510         X(2) = 0.0
00520         X(3) = 0.0
00530         Y(1) = 0.0
00540         Y(2) = 0.0
00550         Y(3) = 0.0
00560         II = 0.0
00570 C
00580 C   ********************************************************
00590 C
00600 C    INITIALIZATION FOR EMG ALGORITHM
00610 C
00620         N = 0
00630         NNM = 0
00640         NFM = 5
00650         P = 1.5
00660 C   ********************************************************
00670 C
00680 1       READ(99,101)X(1),EMG,DELP
00690 101     FORMAT(3F14.5)
00700         X(1) = X(1) - 1
00710 C   ********************************************************
00720 C
00730         NNM = NNM + 1
00740 C   ********************************************************
00750 C
00760 C       EMG ALGORITHM
00770 C
00780 C   ********************************************************
00790 C
00800 C       DETECT ITRAINING
00810 C
00820         IF(EMG.GT.0.7) GO TO 15
00830 C
00840 C       NO ITRAINING SO LET PVS = 0.0
00850 C
00860         N = 0
00870         PVS = 0.0
00880         GO TO 21
00890 C
00900 C       ITRAINING DETECTED == ITART COUNTER
00910 C
00920 C       CALCULATE AND LIMIT PVM
00930 C
```

```
00940 15     PVM = (22.39*EMG)-15.67
00950        IF(PVM.GT.51.5)  PVM = 51.5
00960 C
00970 C      DETERMINE EFFECTIVENESS OF STRAINING DUE TO TIME
00980 C        FACTOR (K2)
00990 C
01000        TIME =N/NFM
01010        IF(TIME.LE.2.0) GO TO 10
01020        IF(TIME.LT.4.0) GO TO 11
01030        IF(TIME.LT.5.0) GO TO 12
01040        K2 = (16.0 - TIME)/11.0
01050        GO TO 20
01060 10     K2 = 0.5
01070        GO TO 20
01080 11     K2=.25*TIME
01090        GO TO 20
01100 12     K2 = 1.0
01110 C      DETERMINE AND LIMIT PVS
01120 C
01130 20     PVS = K2 * PVM * R
01140        IF(PVS.LT.0.0)PVS = 0.0
01150        N = N + 1.0
01160 21     CONTINUE
01170 C  ************************************************************
01180 C
01190 C      END OF EMG ALGORITHM
01200 C
01210 C  ************************************************************
01220 C
01230 C
01240 C  ************************************************************
01250 C
01260 C      CARDIOVASCULAR RESPONSE ALGORITHM
01270 C
01280 C  ************************************************************
01290 C
01300 C
01310 C      CALCULATE PVC FROM CARDIOVASCULAR TRANSFER FUNCTION
01320 C
01330 C  ************************************************************
01340 C
01350        Y(1) = A*Y(3) + B*Y(2) + C*X(3) + D*X(2) + E*X(1)
01360        PVC = 120 + Y(1)
01370 C
01380 C  ************************************************************
01390 C
01400 C      LIMIT PVC ==> NOT TO BE LESS THAN 0
01410 C
01420 C  ************************************************************
01430 C
01440 C      IF( PVC. LT. 0.0 ) PVC = 0.0
01450 C
```

```
C     ************************************************************
C
C        G-SUIT MODEL
C
C     ************************************************************
C
C        CALCULATE PVG ==>NOT TO EXCEED 42.8
C
C
         PVG=0.
         IF(DELP.GT.-80) PVG = (42.8*(DELP + 30) /80)*X(1) /7
         IF(PVG.GT.42.8) PVG = 42.8
C
C     ************************************************************
C
C        CALCULATE PV -- TOTAL PROTECTION VALUE
C
C     ************************************************************
C
         PV = PVC + PVG + PVS
C
C     ************************************************************
C
C        CALCULATE PAE
C
C     ************************************************************
C
         PAE = PV - (0.77*30.48*COS(SEAT - EYE)*X(1))
C
C        IF PAE IS LESS THAN 37.3, VISION COLLAPSES
C
         IF (PV.GT.37.3) GO TO 7
         LLS = 0.0
         LLC = 0.0
         WRITE(1,88)
         WRITE(98,87) NNM,X(6),EMG,PV
88       FORMAT(5X,'VISION COLLAPSE')
         GO TO 32
C
C     ************************************************************
C
C        CALCULATE SENSED VISUAL ANGLE (RRDEG,RLDEG)
C        WE CALCULATE THE VISUAL LIMIT,RRDEG,AT ANY
C        ANGLE,SI,USING ONLY THE RIGHT EYE.
C
C     ************************************************************
C
7        W=1.91986*(PV-37)/(PV-20)
         PI = 3.14159
         IF (SI.LT.PI/2.0) SY = SI
         IF (SI.GE.PI/2.0) SY = PI-SI
         IF (SI.GE.3.*PI/2.0) SY = -2.*PI+SI
```

```
01980 C
01990 C      NOW -PI/2..LE.CY.LE.+PI/2.
02000 C
02010        AA=F*COS(.17453+CY)
02020        BB=SQRT(.031*(COS(.17453+CY))**2-.031+W**2)
02030        P1P = AA + BB
02040 C
02050 C  ******************************************************
02060 C
02070 C      CHOOSE CORRECT SENSED VISUAL ANGLE AND CONVERT
02080 C           TO DEGREES
02090 C
02100 C  ******************************************************
02110 C
02120        PPDEG = 2 * P1P
02130        LLS = (PV-110.) *4.5+10.
02140        LLC = (PV-85.) 5.0+10.
02150        IF(LLS.GE.10.) LLS = 10.
02160        IF(LLC.GE.10.) LLC = 10.
02170        IF(LLS.LE.0.) LLS = 0.
02180        IF(LLC.LE.0.) LLC=0.
02190 32     BRS=LLS*CB
02200        BRC = LLC * CB
02210        CTS = LLS * CC
02220        CTC = LLC * CC
02230        IF(LLC.LE.0.) LLC = 0.
02240 C
02250 C  ******************************************************
02260 C
02270 C      OUTPUT SENSED VISUAL ANGLE AND UPDATE ARRAYS
02280 C
02290 C  ******************************************************
02300 C
02310 8      X(6) = X(1) + 1
02320        PRINT X(6),EMG,PV,LLS,LLC
02330        WRITE(98,87)NNM,X(6),EMG,PV
02340 87     FORMAT(I2,3F3.3)
02350 33     X(3) = X(2)
02360        X(2) = X(1)
02370        X(1) = 0.0
02380        Y(3) = Y(2)
02390        Y(2) = Y(1)
02400        Y(1) = 0.0
02410 C
02420 C      RUN FINISHED ?
02430 C
02440        IF(NNM.NE.99)GO TO 1
02450        STOP
02460        END
```

APPENDIX C

THE M-1 AND L-1 STRAINING MANEUVERS

C.1 M-1 MANEUVER

"Pilots commonly refer to the M-1 Maneuver as the 'grunt' maneuver since it approximates the physical effort required to lift a heavy weight. The M-1 maneuver consists of pulling the head down between the shoulders, slowly and forcefully exhaling through a partially closed glottis, and simultaneously tensing all skeletal muscles. Pulling the head downward gives some degree of postural protection (shortens the vertical head-heart distance): intrathoracic pressure is increased by strong muscular expiratory efforts against a partially closed glottis: and the contraction of abdominal and peripheral muscles raises the diaphragm and externally compresses capacitance vessels. For long-duration G exposures, the maneuver must be repeated every 4 or 5 seconds. When properly executed, the exhalation phase of the M-1 results in an intrathoracic pressure of 50 to 100 mm Hg which raises the arterial blood pressure at head level and thereby increases +G tolerance at least 1.5 G. The inspiratory phase of the M-1 maneuver must (be done as rapidly as possible, sic.)."

C.2 L-1 MANEUVER

"The L-1 maneuver is similar to the M-1 maneuver except the aircrew member forcefully attempts to exhale against a completely closed glottis while tensing all skeletal muscles. Using either maneuver the pilot obtains equal protection, i.e. 1.5 G greater than relaxed blackout level with or without the anti-G suit. In a 1972 study, subjects wearing anti-G suits and performing either the M-1 or L-1 straining maneuver were able to maintain adequate vision during centrifuge exposure of +9G for 45 seconds. Higher and longer runs have not been attempted. However, it is important to note (a word of caution) that forcefully exhaling against a closed glottis

without vigorous skeletal muscular tensing (Valsalva maneuver) can reduce +G tolerance and lead to an episode of unconsciousness at extremely low G_z levels. Therefore, instruction and training on the proper method of performing these straining maneuvers is essential."

(Source: Gillingham, K. K. and Krutz, USAFSAM AR 10-74, Brooks Air Force Base, Texas.)

APPENDIX D

THE SOLUTION ALGORITHM FOR THE CARDIOVASCULAR MODEL

A digital algorithm is used to represent the cardiovascular transfer function.

$$\frac{21.4 \cos \theta (1 + 5.31s)}{1 + 3.23s + 5.17s^2} \qquad (D.1)$$

This algorithm employs Tustin's method[6] for computational efficiency. For a given recursion period T, determined by the simulation computer frame rate, the output y(k) is given by the following equation.

$$y(k) = -y(k-2)\frac{T^2 - 6.46T + 20.68}{T^2 + 6.46T + 20.68} - y(k-1)\frac{2T^2 - 41.36}{T^2 + 6.46T + 20.68}$$

$$+ x(k-2)\frac{T^2 - 10.62T}{T^2 + 6.46T + 20.68} + x(k-1)\frac{2T^2}{T^2 + 6.46T + 20.68}$$

$$+ x(k)\frac{T^2 + 10.26T}{T^2 + 6.46T + 20.68} \qquad (D.2)$$

Here, y(k) represents the output PV_c at time t_k, y(k-1) is PV_c at $t_{k-1} = t_k - T$ and x(k) is $G(t_k)$. A complete listing of coefficients for different values of T is given in Table D-1. The coefficients are derived with a transfer function gain equal to 1.

A hypothetical aircraft maneuvering profile is shown in Figure D-1. The predicted eye level protection value (PV) due to the cardiovascular response model is shown in Figure D-2. The PV values are derived using T = .02 and the hypothetical profile as a driving function.

TABLE D-1

Listing of Coefficients for PV_c Simulation

T	A	B	C	D	E
0.02	0.9876	-1.9875	-0.0102	0.0000	0.0102
0.04	0.9753	-1.9750	-0.0202	0.0002	0.0204
0.06	0.9632	-1.9625	-0.0301	0.0003	0.0304
0.08	0.9513	-1.9501	-0.0398	0.0006	0.0404
0.10	0.9394	-1.9376	-0.0493	0.0009	0.0502
0.12	0.9278	-1.9251	-0.0587	0.0013	0.0600
0.14	0.9163	-1.9127	-0.0679	0.0018	0.0697
0.16	0.9049	-1.9002	-0.0770	0.0024	0.0793
0.18	0.8937	-1.8878	-0.0859	0.0030	0.0889
0.20	0.8826	-1.8753	-0.0947	0.0036	0.0983
0.22	0.8717	-1.8629	-0.1033	0.0044	0.1077
0.24	0.8609	-1.8505	-0.1118	0.0052	0.1169
0.26	0.8502	-1.8382	-0.1201	0.0060	0.1261
0.28	0.8397	-1.8258	-0.1283	0.0069	0.1352
0.30	0.8293	-1.8135	-0.1363	0.0079	0.1443
0.32	0.8191	-1.8011	-0.1442	0.0090	0.1532
0.34	0.8089	-1.7888	-0.1520	0.0101	0.1621
0.36	0.7990	-1.7766	-0.1597	0.0112	0.1709
0.38	0.7891	-1.7643	-0.1672	0.0124	0.1796
0.40	0.7794	-1.7521	-0.1745	0.0137	0.1882
0.	0.7698	-1.7398	-0.1818	0.0150	0.1967
0.	0.7603	-1.7276	-0.1889	0.0163	0.2052
0.46	0.7509	-1.7155	-0.1959	0.0177	0.2136
0.48	0.7417	-1.7033	-0.2027	0.0192	0.2219
0.50	0.7326	-1.6912	-0.2094	0.0207	0.2301

$$y(k) = -y(k-2)A - y(k-1)B + x(k-2)C + x(k-1)D + x(k)E$$

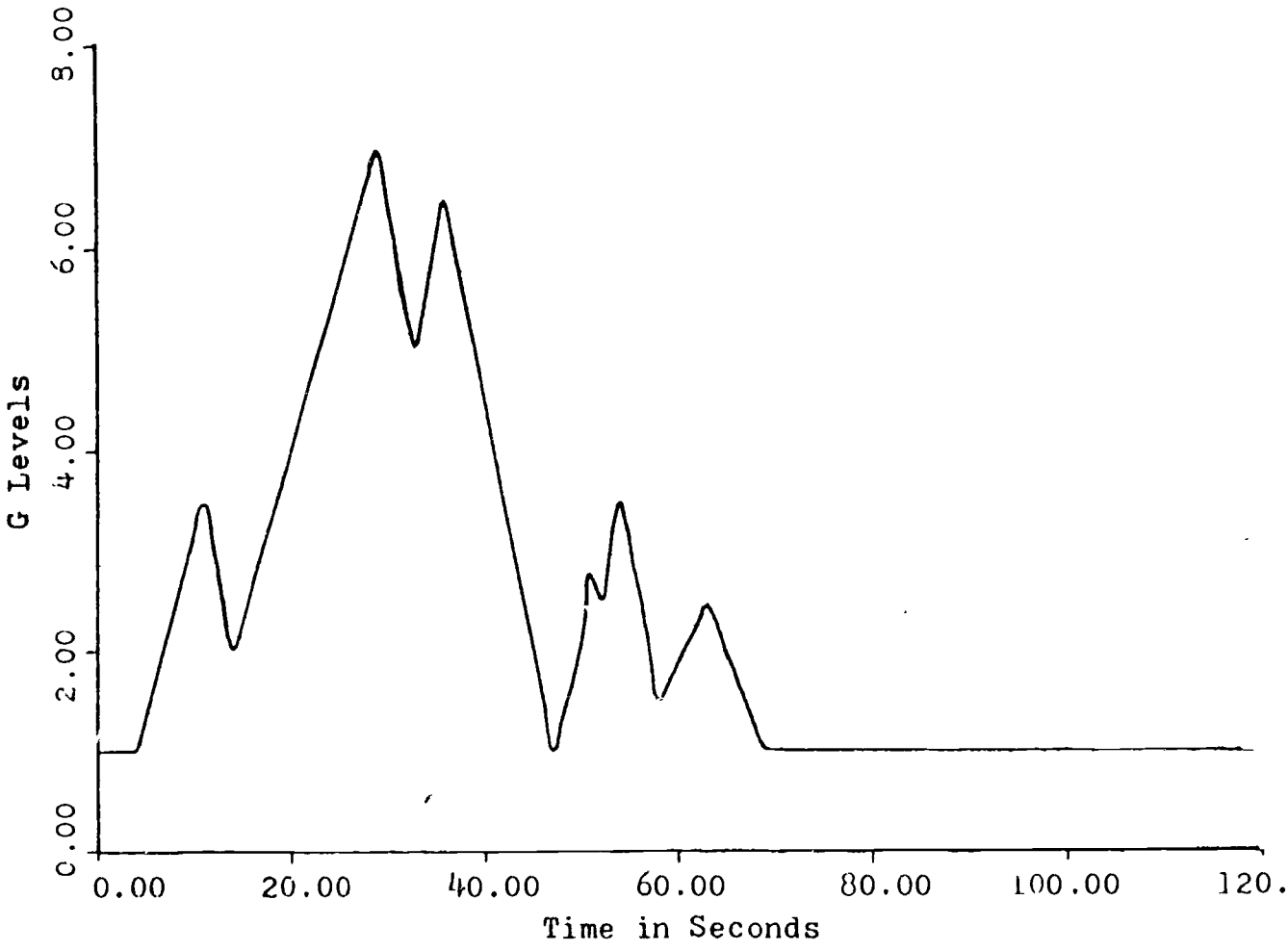

Figure D-1 Hypothetical Aircraft Maneuvering Profile

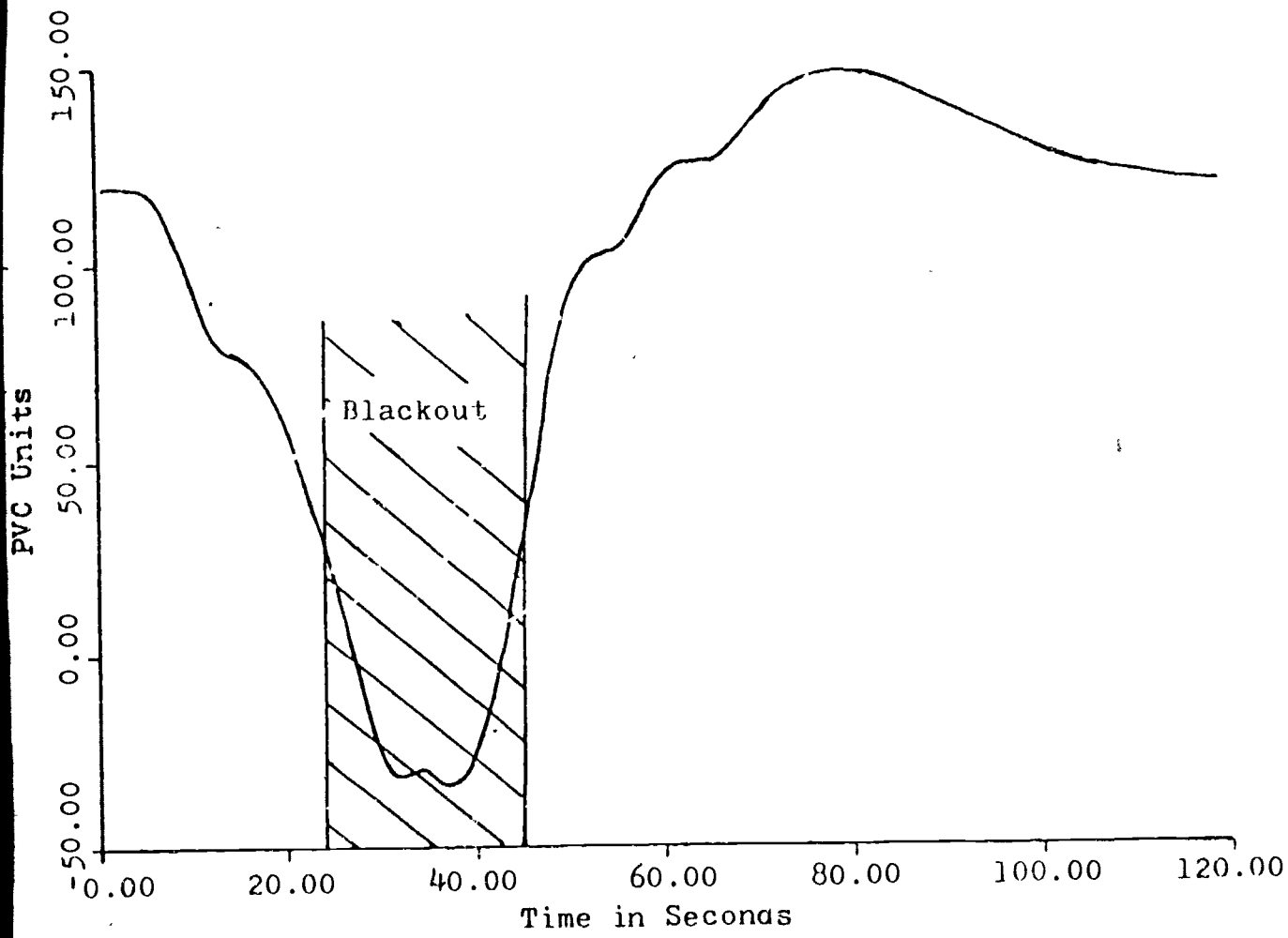

Figure D-2 PV_c (Eye Level Blood Pressure) Response to Maneuvering Profile